NOVEL SWITCHABLE SYSTEMS AND APPLICATIONS

A Thesis
Presented to
The Academic Faculty

By

Ejae A. John

In Partial Fulfillment
Of the Requirements for the Degree
Doctor of Philosophy in Chemistry

Georgia Institute of Technology

December, 2007

Novel Switchable Systems and Applications

Approved by:

Dr. Charles Liotta, Advisor
School of Chemistry and Biochemistry
Georgia Institute of Technology

Dr. Charles Eckert, Co-Advisor
School of Chemical and Bimolecular
Engineering
Georgia Institute of Technology

Dr. David Collard
School of Chemistry and Biochemistry
Georgia Institute of Technology

Dr. Facundo Fernandez
School of Chemistry and Biochemistry
Georgia Institute of Technology

Dr. Leslie Gelbaum
School of Chemistry and Biochemistry
Georgia Institute of Technology

Date Approved: 22 August 2007

This work is dedicated to Mum, Auntie Gail (my other Mum), Grandmummy, and Ma.

ACKNOWLEDGEMENTS

First and foremost, I would like to acknowledge God for His help throughout my tenure at Georgia Tech. I would next like to thank my advisor Dr. Charles Liotta for all of his guidance and direction, and my co-advisor Dr. Charles Eckert for his assistance. I am also truly grateful to the rest of my committee (past and present members) for their guidance and mentorship. I would also like to acknowledge GT and NSF for funding. I would next like to thank all of the members of the Eckert-Liotta group (past and present) and its collaborators for their assistance and friendship. I am especially grateful to Dr. Phillip Jessop, Dr. Wenjian Li, Dr. Daniele Vinci, and Hillary Huttenhower for their assistance with the switchable ionic liquids project. I am also thankful to all of the people that reviewed various parts of my thesis for me. Finally, I would like to thank my family and friends (who have become my family) for their support and love (Everyone who knows me knows that my family is far too large to list each person). I want to most especially thank my friend and mentor Dr. Pamela Pollet for all of her advice, assistance, and support. "I no doubt deserved my enemies, but I don't believe I deserved my friends." (Walt Whitman) Lastly, I want to thank my sisters Ejima and Shari for being my sisters (and all that such an important job entails).

TABLE OF CONTENTS

LIST OF TABLES

LIST OF FIGURES

LIST OF SYMBOLS AND ABBREVIATIONS

Room temperature ionic liquid (RTIL)

1,8-Diazabicyclo[5.4.0]undec-7-ene (DBU)

n-butylimidazolium chloride ([bmim][Cl])

2-butyl-1,1,3,3-tetramethylguanidinium methylcarbonate (TMBG MC IL)

2-butyl-1,1,3,3-tetramethylguanidine (TMBG)

λ_{max} is the wavelength of maximum absorbance

bmim is1-butyl-3-methylimidazonium

eim is ethylimidazonium

microSiemens (uS)

Differential Scanning Calorimetry and Thermogravimetric Analysis (DSC-TGA)

2-butyl-1,1,3,3-tetramethylguanidinium methylsulfite (TMBG MS IL)

Piperylene sulfone (PS)

π^* is a quantitative index of solvent dipolarity and polarizability

α is a measure of the solvents strength as a hydrogen bond donor

$E_T(30)$ indicates solvent strength

β is the solvent's hydrogen bond acidity

ε is dielectric constant

Gas-Expanded Liquids (GXLs)

Fluorous Biphasic Catalysis (FBC)

Perfluoropolyether (PFPE)

Inductively Coupled Plasma/Atomic Absorption (ICP/AA)

High value-added chemicals (HVAC)

(9,14-bis[tris(3,3,4,4,5,5,6,6,7,7,8,8,8-trideca-fluorodecyl)silyl]-(R)-(3,5-dioxa-4-phospha-cyclohepta[2,1-a;3,4-a']dinapthalen-4-yl)-dimethyl amine (F-MonoPhos)

(R)-6,6'-bis[tris(1H,1H,2H,2H-perfluorooctyl)silyl]-1,1'-bi-2-napthol (F-BINOL)

Low-molecular mass organic gelator (LMOG)

polyallylamine (PAA)

Polyethyleneimine (PEI)

Methyl ethyl ketone (MEK)

High resolution scanning electron microscope (HRSEM)

Small angle neutron scattering (SANS)

SUMMARY

This work showcases the utility of switchable materials. Included are a switchable room-temperature ionic liquid, a switchable solvent, a switchable heterogeneous catalyst system, and a switchable gel. First, the switchable ionic liquid 2-butyl-1,1,3,3-tetramethylguanidium methylcarbonate is fully investigated. Its use in a complete chemical process (including reaction, separation, reformation, and recycle) is demonstrated with several reactions. Furthermore, its potential use for bitumen separation and purification and SO_2 capture/isolation are discussed, and preliminary data is presented. Next, piperylene sulfone (PS), a switchable solvent, is synthesized and fully characterized. Anionic nucleophilic substitution reactions were performed in PS, the products were isolated in high yields, and then the PS was reformed for reuse. Then, we designed an immobilized fluorous microphase system that uses F-MonoPhos to induce high enantioselectivities as a switchable heterogeneous catalyst system. Finally, stable reversible polyethyleneimine-CO_2 gels have been synthesized with 1-octanol. Our findings indicate that PEI-1200/octanol/CO_2 gels have potential as a possible drug carrier matrix for transdermal delivery applications.

CHAPTER 1
SWITCHABLE ROOM TEMPERATURE IONIC LIQUIDS

1.1 Introduction

Solvents have fixed properties: for example, polar solvents are always polar and non-polar always non-polar. Although moderate changes in pressure and temperature can cause some changes to overall chemical and physical properties, these are usually only minor. We depend upon the static nature of solvents for different processes; however, it is this static nature of solvents that is also a limitation. For instance, multi-step syntheses normally require very different solvent conditions for reaction and separation in each step. A solvent system that could dramatically change its properties with a moderate stimulus, or a "switchable solvent," would be a benefit. Of late, switchable materials have become quite popular in the literature.[1, 2] The Liotta-Eckert and Jessop groups were the first to publish a switchable solvent system, specifically a switchable room temperature ionic liquid (RTIL).[3] In the 1,8-Diazabicyclo[5.4.0]undec-7-ene (DBU)/hexanol system, the addition of CO_2 in the presence of an alcohol was used to switch from a molecular liquid to a room temperature ionic liquid. This is akin to going from chloroform to DMF in polarity. Moreover, the system was easily reversed by bubbling N_2 or Ar, or by heating at 50-60°C (**Fig 1.1**).
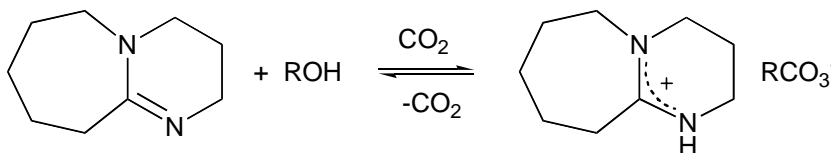
Fig 1.1: DBU-based switchable RTIL

A switchable RTIL would then be a system where one can use some switch to first do a reaction in very polar media and then simply "switch" to generate a non-polar (or much less polar) environment to carry out a separation or another reaction—or vice-versa.

1.2 Background

1.2.1 Room temperature Ionic Liquids

Room temperature ionic liquids (molten salts; RTIL) have been extensively investigated in the literature as novel solvents. They generally are conductive, have high solvating properties, low vapor pressure, and are very viscous. Because of their low vapor pressure, they have been recognized as green solvents. Recent literature, however, has indicated that many RTILs are toxic and not very environmentally friendly because of possible bioaccumulation since they often are not biodegradable, have low volatility, and can be made water soluble by ligand exchange with water-soluble anions/cations.[4-6]

1.2.2 Guanidine-based ILs

Ionic liquids based on guanidines are relatively new to the literature. In 2003, Mateus *et al.* published a series of hexa-alkyl guanidinium salts (**Fig 1.2**).[7]
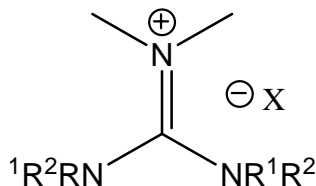
$$R^1, R^2 = Me, Et, n\text{-}Bu, n\text{-}Hex, n\text{-}Oct$$
$$X = PF_6, BF_4, Tf_2N$$

Fig 1.2: Hexa-alkyl guanidinium salts

Of fifteen combinations tested, ten proved to be RTILs. Furthermore, these RTILs presented high stability under thermal (25-150°C for 24-48h), basic, acidic, nucleophilic and oxidative conditions, and low-temperature glass transition phases (-79 to –55.3^{o}C). When compared to the common RTIL n-butylimidazolium chloride ([bmim][Cl]), the hexa-alkyl guanidinium salts showed comparable stability. However, the hexa-alkyl guanidinium salts were stable in the presence of neat base, whereas [bmim][Cl] was not. Also, neat [bmim][Cl] was stable in the presence of the reducing agent NaBH$_4$ whereas neat hexa-alkyl guanidinium salts were not. Since the physical and solubility properties of hexa-alkyl guanidinium salts do not completely parallel those of the more common imidazolium RTIL, the authors suggested that there may be greater opportunities for the guanidinium systems with a wider range of properties. Three other papers based on hexa-alkyl guanidinium RTILs were published thereafter,[8] presenting the possibility of using these novel RTILs for dye-sensitized solar cells[9] and oxidations.[10]

1,1,3,3-tetramethylguanidine-based RTILs have been reported in the literature by neutralizing tetramethylguanidine with a series of acids (**Fig 1.3**).
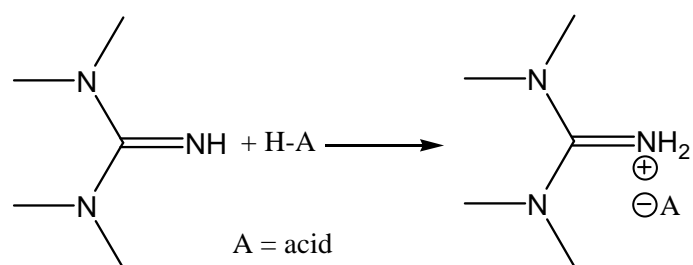
Fig 1.3: Tetramethyl guanidinium salts

These RTILs have been used as basic catalysts in Henry reactions[11] (**Fig 1.4A**) and aldol condensation reactions[12, 13] (**Fig 1.4B**), and in the preparation of immobilized catalysts for olefin hydrogenation[14] (**Fig 1.4C**).
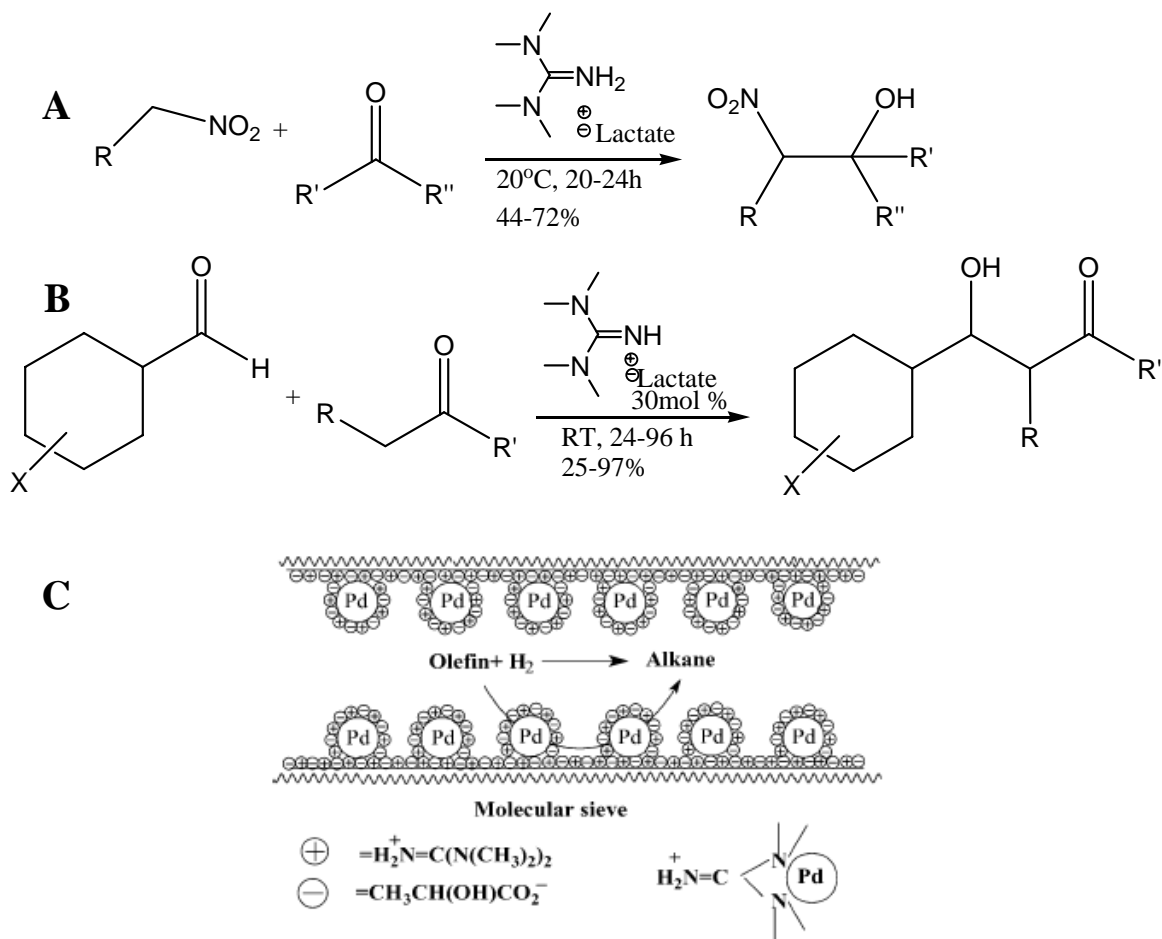
Fig 1.4: 1,1,3,3-tetramethylguanidinium salts as basic catalysts in A- Henry reaction; B- Aldol reaction; and C- Part of an immobilized catalyst

These RTILs were recycled and reused after the Henry and aldol condensation reactions by extracting them in water, and then evaporating the water. Upon reuse, the authors report no significant change in the yields of the Henry and aldol condensation products. However, they do not discuss the energy costs associated with their strategy.

Li *et al*. recently published a palladium catalyzed Heck reaction in 2-butyl-1,1,3,3-tetramethylguanidinium acetate ionic liquid (**Fig 1.5**).[15]
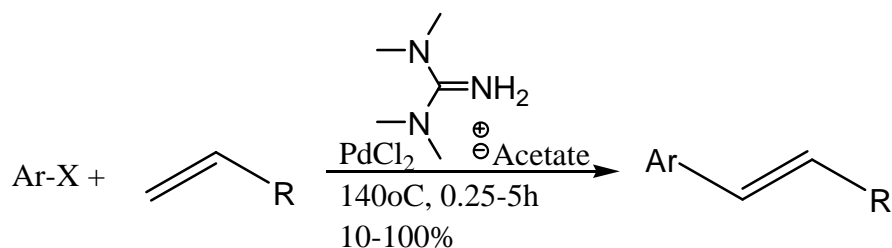
Fig 1.5: Heck reaction with 1,1,3,3-tetramethylguanidinium acetate

In this work, a number of substituted aryl halides underwent Heck couplings with olefins.

Li *et al.* also demonstrated recycling in this sequence with bromobenzene and styrene.

After completion of the first reaction cycle, the products are extracted into a polar solvent

mixture (1:1 toluene/hexane), while the palladium catalyst remains in the ionic liquid. At

this point, some of the 2-butyl-1,1,3,3-tetramethylguanidinium acetate ionic liquid is

converted to guanidinium bromide (**Fig 1.6**).
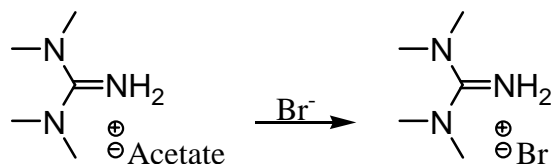
Fig 1.6: Conversion of 2-butyl-1,1,3,3-tetramethylguanidinium acetate to 2-butyl-1,1,3,3-tetramethylguanidinium bromide

The authors state that 2-butyl-1,1,3,3-tetramethylguanidinium bromide cannot be used as

a solvent for Heck coupling. Catalytic activity is maintained, however, until all of the

guanidinium acetate is converted to the unreactive guanidinium bromide: the authors are

able to recycle the guanidinium acetate IL and palladium catalyst five times with similar

yields.

The Liotta-Eckert group recently discovered that guanidines in the presence of

alcohols can reversibly react with CO_2. In particular, we found that exposure of an

equimolar mixture of methanol and 2-butyl-1,1,3,3-tetramethylguanidine[16] to gaseous

CO_2 at one atmosphere causes the formation of a RTIL: 2-butyl-1,1,3,3-tetramethylguanidinium methylcarbonate (TMBG MC IL) (**Fig 1.7**).
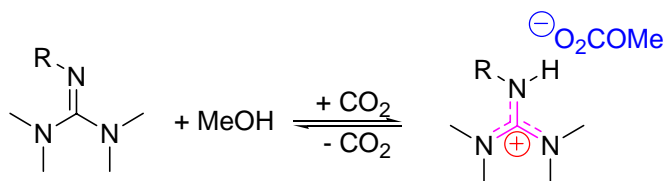
Fig 1.7: Reversible formation of 2-butyl-1,1,3,3-tetramethylguanidinium methylcarbonate

In contrast with previously published guanidine ionic liquid systems, TMBG MC is easily reversible by bubbling N_2(g), or by heating at 80^oC.

1.3 Results and Discussion

1.3.1 Synthesis of 2-butyl-1,1,3,3-tetramethylguanidine (TMBG)

The synthesis of 2-butyl-1,1,3,3-tetramethylguanidine was not straightforward. Initially, the protocol of U. Schuchardt *et al*,[17] which was reported for the synthesis of 1,1,2,3,3-pentamethylguanidine, was used to prepare 2-butyl-1,1,3,3-tetramethylguanidine (**Fig 1.8**).
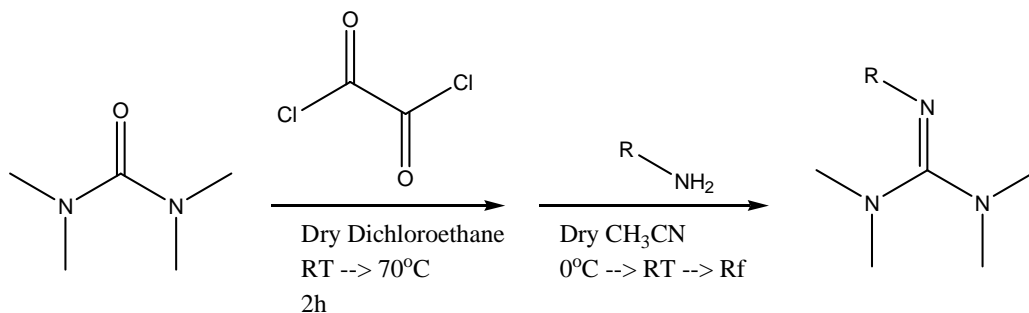
Fig 1.8: Synthesis of 2-alkyl-1,1,3,3-tetramethylguanidine from 1,1,3,3-tetramethylurea

This protocol required rigorously anhydrous conditions because of the instability of the dichloride intermediate (**Fig 1.9**).
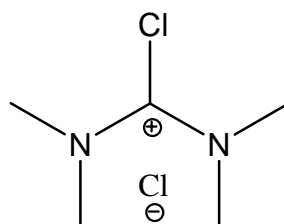
Fig 1.9: Dichloride intermediate

Unfortunately, Schuchardt's procedure did not consistently yield product; more often than not, starting material or some degradation product was isolated from the reaction mixture. Thus, the Costa *et al* protocol was adopted.[18] This procedure was essentially an improvement of Schuchardt's method with longer reaction times (24h vs. 8h), slower additions, and different stoichiometries (1/1.6/1.025 vs. 1/2/1.9 urea/oxalyl chloride/amine). Even though strict anhydrous conditions still had to be observed, the yields of the liquid 2-butyl-1,1,3,3-tetramethylguanidine product were optimized from 30-40% to >80%. High yields were not consistent, however. Even under the most scrupulous conditions, we sometimes produced none of the expected product. This could often be traced to the oxalyl chloride, even though NMR (^{1}H, ^{13}C) of the oxalyl chloride was consistent with Aldrich's specifications (~ 98% pure). We found that using a fresh bottle of oxalyl chloride restored high yields, but we cannot explain what minor impurity so detrimentally affects the synthesis of 2-butyl-1,1,3,3-tetramethylguanidine. Once 2-butyl-1,1,3,3-tetramethylguanidine was synthesized and isolated, it was stored in the glove box because of instability towards moisture. Furthermore, all reactions utilizing 2-butyl-1,1,3,3-tetramethylguanidine were done in the glove box to prevent water contamination.

1.3.2 Synthesis and Characterization of 2-butyl-1,1,3,3-tetramethylguanidinium methylcarbonate

To 2-butyl-1,1,3,3-tetramethylguanidine, an equimolar amount of methanol was added. Then, CO_2 was bubbled into the solution to yield 2-butyl-1,1,3,3-tetramethylguanidinium methylcarbonate. This compound was characterized using NMR (^{1}H, [13]C & DEPT-135), IR, elemental analysis, and melting point. All NMR data were run neat and were consistent with the proposed structure. Furthermore, the elemental analysis was consistent with methyl carbonate and 2-butyl-1,1,3,3-tetramethylguanidinium in a 1:1 ratio. IR data indicates the formation of methyl carbonate (1780 cm^{-1}), consistent with the IR data for dimethyl carbonate (1758cm^{-1}). The melting point of 2-butyl-1,1,3,3-tetramethylguanidinium methylcarbonate is –24 +/- 1°C.

Once 2-butyl-1,1,3,3-tetramethylguanidinium methylcarbonate was completely characterized, its solvatochromic properties were investigated. Kamlet-Taft parameters and dielectric constants were not accessible since the Reichardt's Dye appeared to be bleached when it was added to our guanidine system. In addition, TMBG absorbs at the exact same wavelength as the other dyes that are commonly used for these measurements. Furthermore, dielectric constants are often not reliable for RTILs.[19] To overcome these limitations polarities of ILs are generally measured using Nile red as a probe.[20] The polarity of our 2-butyl-1,1,3,3-tetramethylguanidinium methylcarbonate IL was evaluated with the solvatochromic dye Nile Red, where λ_{max} is the wavelength of maximum absorbance, and a comparative indication of polarity (**Table 1.1**). Equimolar mixtures of

methanol and TMBG become significantly more polar when exposed to CO_2, as shown by the shift of the λ_{max} from 538nm to the longer wavelength 554nm. Commonly the addition of CO_2 to liquid induces a decrease in polarity (*i.*e. GXL). The unusual increase in polarity was a clear indication that the reaction taking place was forming a more polar product, the 2-butyl-1,1,3,3-tetramethylguanidinium methylcarbonate (TMBG MC). In fact, such a shift in λ_{max} quantifies a polarity switch akin to going from chloroform (537.6nm) to acetic acid (557.2nm).

Table 1.1: Comparison of common λ_{max} values with TMBG and TMBG MC IL

Solvent	λ_{max}, nm, Nile Red
Ether	504.4
CH_2Cl_2	535.2
$CHCl_3$	537.6
TMBG + MeOH	538.0
DMF	541.2
Propanoic acid	542.4
[bmim][PF$_6$][1]	547.5
DMSO	549.2
[bmim][BF$_4$][1]	550.8
TMBGH$^+$ + MeOCO$_2^-$	554.0
Acetic Acid	557.2

1. bmim = 1-butyl-3-methylimidazonium

Upon comparison with λ_{max} values reported in the literature,[21, 22] the solvent 2-butyl-1,1,3,3-tetramethylguanidinium methyl carbonate is comparable to the

hexylmethylimidazole tetrafluoroborate ionic liquid ($[C_6mim][BF_4]$, λ_{max} (Nile Red)=

551.9) and to liquid ammonia (λ_{max} (Nile Red)= 555.0).

1.3.3 Synthesis and Characterization of 2-butyl-1,1,3,3-tetramethylguanidinium

alkylcarbonates

1-butanol, 1-hexanol, 1-octanol, and 1-dodecanol were tested to potentially form

reversible RTILs (**Fig 1.10**).
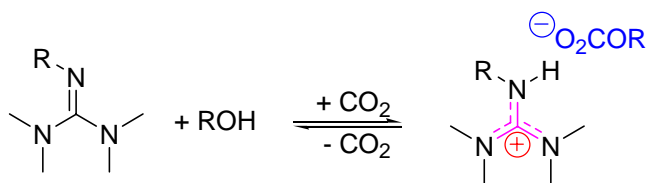
**Fig 1.10: Reversible formation of 2-butyl-1,1,3,3-tetramethylguanidinium
alkylcarbonate**

To 2-butyl-1,1,3,3-tetramethylguanidine, an equimolar amount of alcohol was added.

Then, CO_2 was bubbled into the solution to yield 2-butyl-1,1,3,3-tetramethylguanidinium

alkylcarbonate. These compounds were characterized using NMR (^1H, ^{13}C), melting

point, and polarity studies. All NMR data were run neat and were consistent with the

proposed structures. Figure **1.11** shows the melting points of the 2-butyl-1,1,3,3-

tetramethylguanidinium alkylcarbonate RTILs as a function of the length of the alkyl

chain in the alcohol.
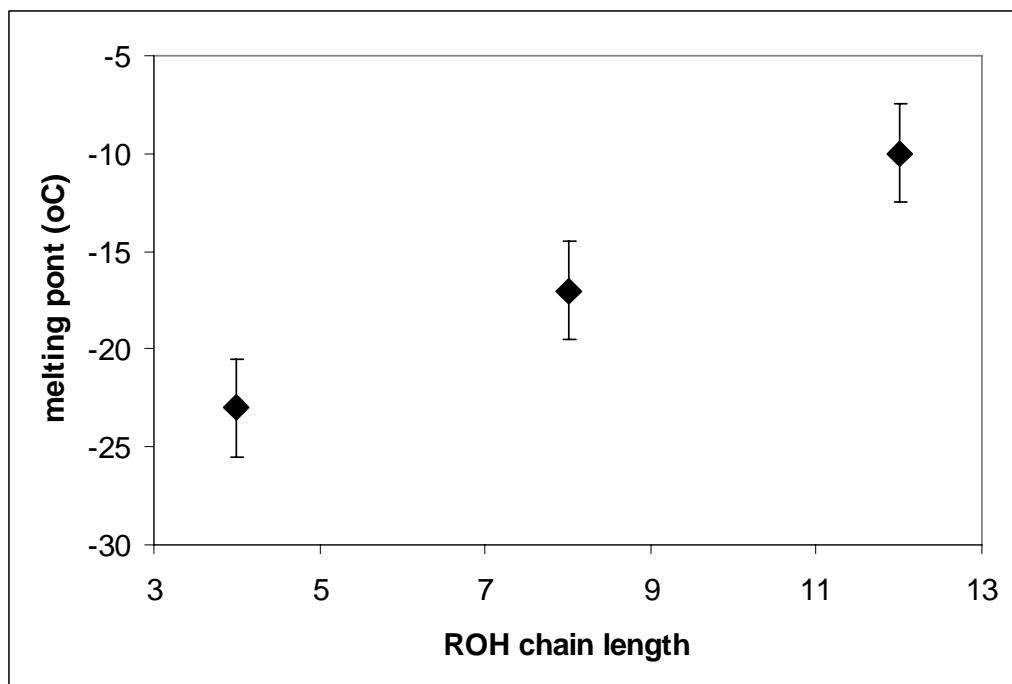
Fig 1.11: Melting points of the 2-butyl-1,1,3,3-tetramethylguanidinium alkylcarbonate RTILs

Nile Red was again used to measure polarity. The polarity of the ionic liquids depends greatly on the length of the alkyl chain, with the λ_{max} values falling well within the range found for non-switchable ionic liquids (**Table 1.2**).

Table 1.2: Comparison of common λ_{max} values with 2-butyl-1,1,3,3-tetramethylguanidinium alkylcarbonate RTILs and their neutral counterparts

Solvent	λ_{max} (Nile Red), nm
Ether	504.4
TMBG (neat)	524.8
Benzene	525.4
TMBG + DodecOH	528.0
TMBG + OctOH	530.1
TMBG + HexOH	531.1
TMBG + BuOH	532.0
CH_2Cl_2	535.2
TMBGH$^+$ + DodecOCO$_2$$^-$	536.5
$CHCl_3$	537.6
TMBG + MeOH	538.0
TMBGH$^+$ + OctOCO$_2$$^-$	541.1
DMF	541.2
Propanoic acid	542.4
1-Octanol	544.0
TMBGH$^+$ + BuOCO$_2$$^-$	544.4
TMBGH$^+$ + HexOCO$_2$$^-$	545.0
1-Propanol	545.6
[bmim]PF$_6$[1]	547.5
Methanol	549.6
TMBGH$^+$ + MeOCO$_2$$^-$	554.0
[eim]BF$_4$[2]	562.9

1. bmim = 1-butyl-3-methylimidazonium 2. eim = ethylimidazonium

1.3.4 Comparison of all synthesized 2-butyl-1,1,3,3-tetramethylguanidinium alkylcarbonates

Upon comparison of the methanol, 1-butanol, 1-hexanol, 1-octanol, and 1-dodecanol-based 2-butyl-1,1,3,3-tetramethylguanidinium RTILs, several conclusions can be made. The lowest boiling alcohol (methanol, bpt 64.7°C) produces the RTIL with the lowest melting point: 2-butyl-1,1,3,3-tetramethylguanidinium methylcarbonate (mpt –24 +/- 1°C). Accordingly, the highest boiling alcohol (dodecanol, bpt 260-262°C) generates an IL that has the highest melting point (-10.5 +/- 1°C). Furthermore, using shorter alcohols gives a greater difference between the polarities of the ionic and neutral forms of the solvent. This is made very clear by only comparing the polarities of TMBG-based ionic liquids to their neutral forms (**Fig 1.12**).
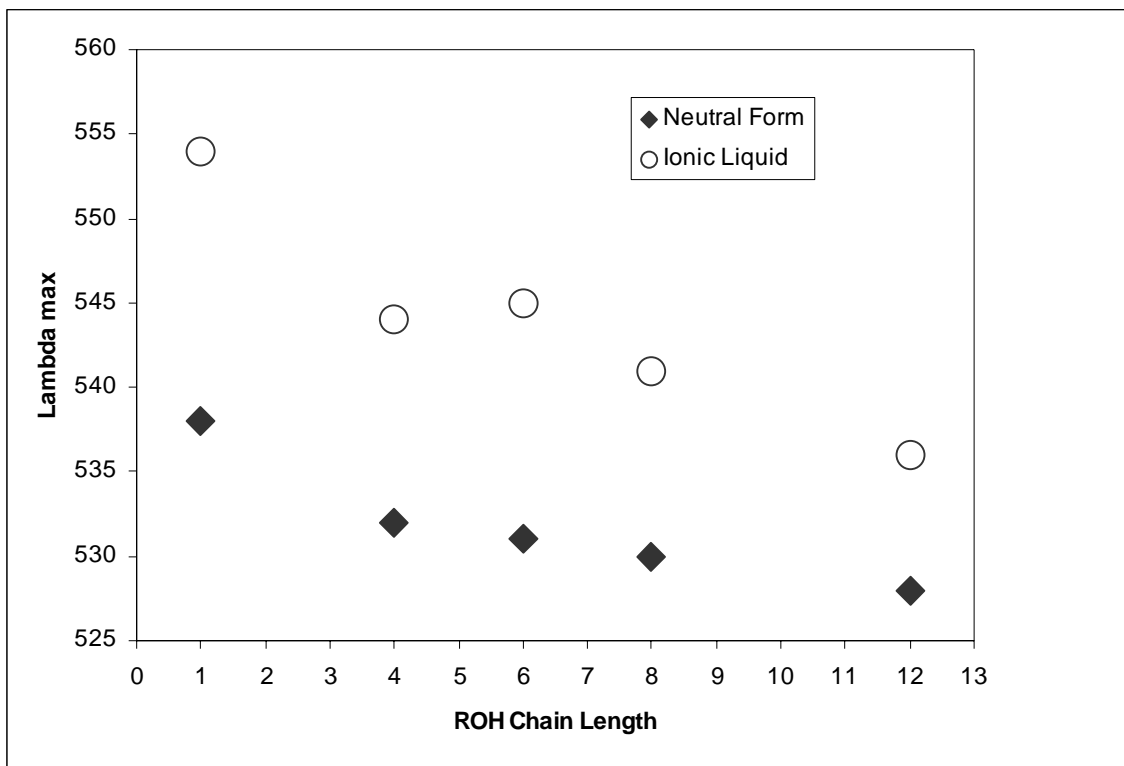
Fig 1.12: Polarities of TMBG-based ionic liquids and their neutral forms

Another characteristic we noticed was that as the alkyl chain of the alcohol increased, the viscosity of the 2-butyl-1,1,3,3-tetramethylguanidinium alkylcarbonates also increased. For example 2-butyl-1,1,3,3-tetramethylguanidinium dodecylcarbonate was so viscous, it seemed honey-like.

1.3.5 Reversibility and Reformation of 2-butyl-1,1,3,3-tetramethylguanidinium methylcarbonate

The reversibility and reformation of 2-butyl-1,1,3,3-tetramethylguanidinium methylcarbonate was demonstrated using two independent techniques: NMR (^{1}H and ^{13}C) and conductivity. In the NMR experiments, 2-butyl-1,1,3,3-tetramethylguanidine was combined in a 1:1 molar ratio with methanol. Figure **1.13A** is the NMR spectra of the initial equimolar solution of 2-butyl-1,1,3,3-tetramethylguanidine and methanol. CO_2 was bubbled through the mixture for 20min, or until the exothermic reaction ended (**Fig 1.13B**).
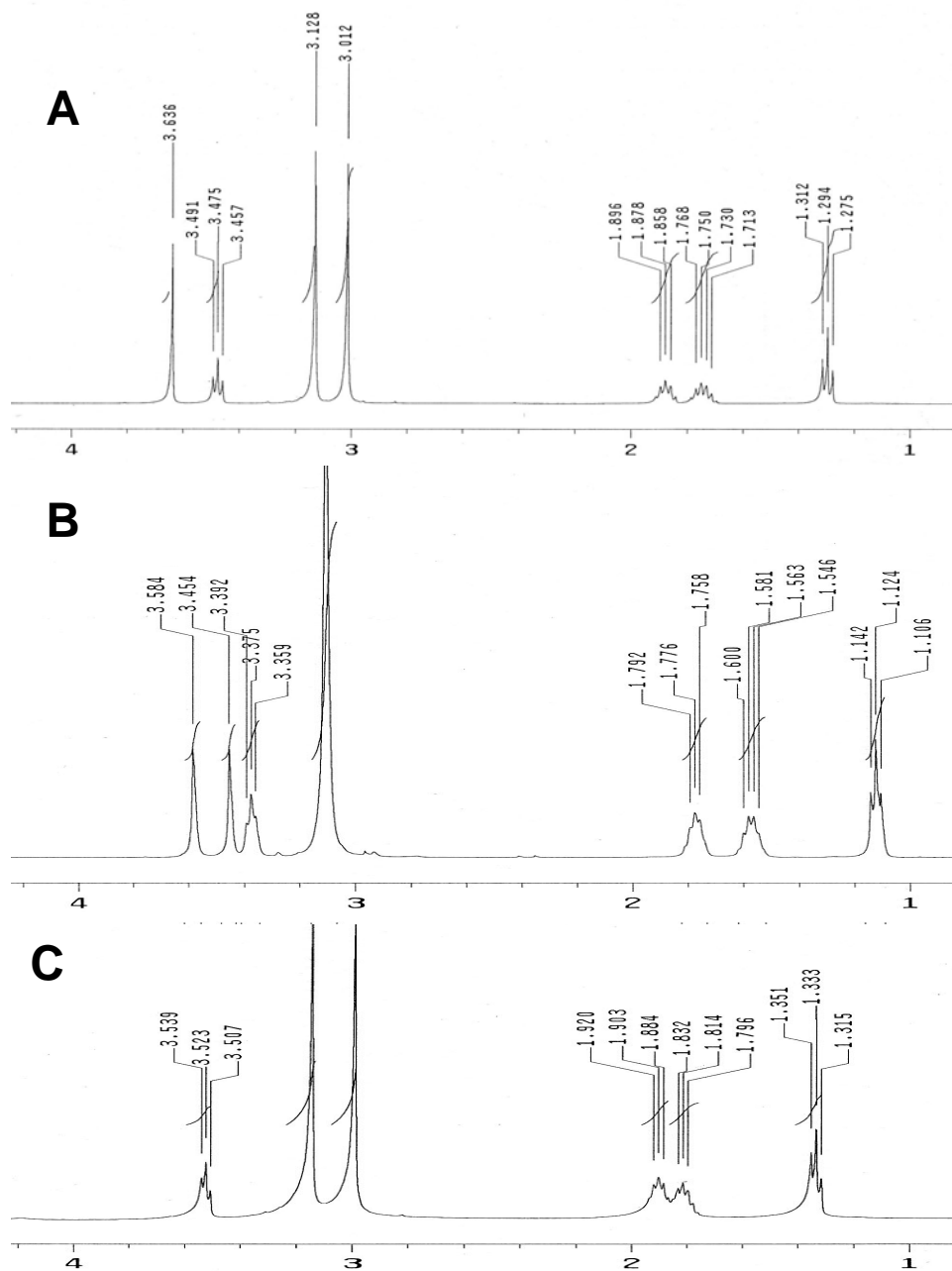
Fig 1.13: ^{1}H NMR of formation and reversal of 2-butyl-1,1,3,3-tetramethylguanidinium methylcarbonate switchable RTIL

Upon the addition of CO_2, protonation of the guanidine and formation of the methyl carbonate anion takes place. This is evidenced in ^{1}H NMR by an upfield shift in the aliphatic protons, and the collapse of the two N-Me peaks into one (**Fig 1.13B**). The ^{13}C NMR spectra exhibit the appearance of a characteristic carbonate peak at 161 ppm.

15

Furthermore, the chemical shifts of the methoxy peak, aliphatic carbons, and the change in N-Me peaks are clearly observed. Un-reacted CO_2 is not detected by ^{13}C NMR as no peaks are present at 120 ppm. Finally, Figure **1.13C** shows the ^{1}H NMR after nitrogen bubbling for 16 hours. The ionic liquid is indeed reversed to its original components. The exact same reversal was observed when 2-butyl-1,1,3,3-tetramethylguanidinium methylcarbonate was reversed by vacuum with stirring, except it took one hour.

The reversible formation of the ionic species has also been documented using conductivity (**Fig 1.14**). The conductivity experiment was carried out in the glove box to prevent water contamination. In this case, the experiment had to be done in solvent (chloroform) because the ionic liquid is too viscous for neat conductivity measurements.
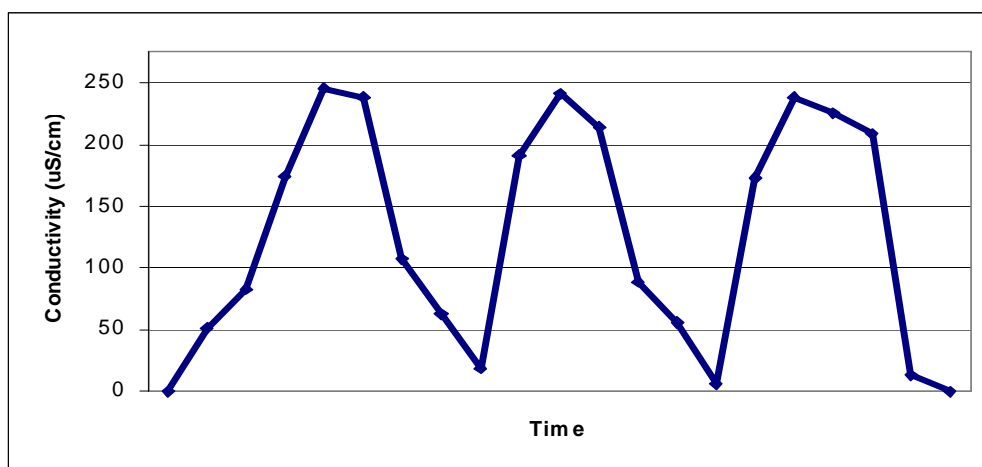
Fig 1.14: Conductivity of 2-butyl-1,1,3,3-tetramethylguanidinium methylcarbonate in chloroform

Thus, TMBG and methanol (5.56mmol each) were dissolved in 4mL of CDCl$_3$. Deuterated solvent was used to enable NMR co-observation. At the beginning of the experiment, the equimolar mixture of methanol and 2-butyl-1,1,3,3-tetramethylguanindine in chloroform does not conduct electricity (0 microSiemens(uS)/cm). However, as CO_2 is bubbled into the mixture, conductivity

increases up to 246uS/cm. This is consistent with the formation of the ionic species 2-butyl-1,1,3,3-tetramethylguanidinium and methyl carbonate. Upon heating, the conductivity decreases to 19uS/cm. This is in agreement with the 2-butyl-1,1,3,3-tetramethylguanidinium methylcarbonate reversing back to the starting materials, 2-butyl-1,1,3,3-tetramethylguanide and methanol, respectively. This cycle was repeated three times, showing similar observations as seen in Figure **1.14**.

Additionally, thermogravimetric studies document the reversal of RTIL upon solely heating (**Fig 1.15**).
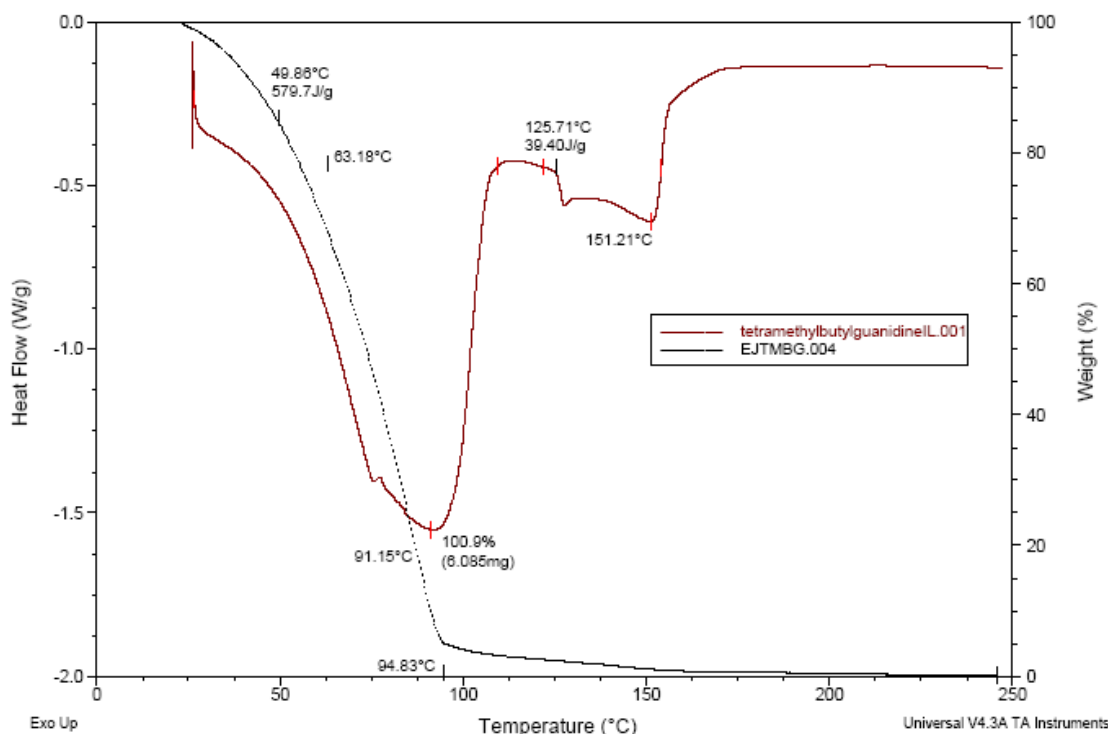
Fig 1.15: Thermogravimetric studies of 2-butyl-1,1,3,3-tetramethylguanidinium methylcarbonate

Above 50°C, the 2-butyl-1,1,3,3-tetramethylguanidinium methylcarbonate IL starts to reverse to guanidine, methanol and CO_2 as indicated by the weight loss and the temperature at which degradation begins (50°C, bpt of MeOH is 65°C).

All experiments indicate that 2-butyl-1,1,3,3-tetramethylguanidinium methyl carbonate IL can be formed **reversibly** from reacting an equimolar solution of 2-butyl-1,1,3,3-tetramethylguanide and methanol with CO_2. The reversal can be triggered by bubbling inert gases (Argon or Nitrogen), vacuum, or by simply heating above $50^{\circ}C$. When the switch is heat, both CO_2 and methanol are removed in the process as methanol is a low boiling point alcohol—however, both CO_2 and methanol can be easily recycled.

1.3.6 Reversibility and Reformation of 2-butyl-1,1,3,3-tetramethylguanidinium alkylcarbonates

The reversibility and reformation of the other 2-butyl-1,1,3,3-tetramethylguanidinium alkylcarbonates (butyl, hexyl, octyl, dodecyl) was demonstrated using NMR (^{1}H and ^{13}C). Analogous to 2-butyl-1,1,3,3-tetramethylguanidinium methylcarbonate, formation of the 2-butyl-1,1,3,3-tetramethylguanidinium alkylcarbonates were evidenced in ^{1}H NMRs by an upfield shift in the aliphatic protons, and the collapse of the two N-Me peaks into one, and the ^{13}C NMR spectrum exhibited a characteristic carbonate peak at 161 ppm. These RTILs were reversed by heating them at $80^{\circ}C$ since DSC-TGA data for 2-butyl-1,1,3,3-tetramethylguanidinium methylcarbonate indicated that the RTILs could be reversed by using heat.

1.3.7 Comparison of the Reversibility and Reformation of 2-butyl-1,1,3,3-tetramethylguanidinium alkylcarbonates

Each of the 2-butyl-1,1,3,3-tetramethylguanidinium alkylcarbonates (methyl, butyl, hexyl, octyl, and dodecyl) were easily formed by bubbling CO_2 into the

guanidine/alcohol mixtures. Furthermore, it is clear that heat is an efficient means to reverse the 2-butyl-1,1,3,3-tetramethylguanidinium alkylcarbonates to its original guanidine/alcohol components. The increase in the viscosity and melting point of the 2-butyl-1,1,3,3-tetramethylguanidinium alkylcarbonates as a function of chain length appear to have an effect on the amount of time the reversal from the 2-butyl-1,1,3,3-tetramethylguanidinium alkylcarbonate to the guanidine/alcohol mixture takes (**Fig 1.16**).
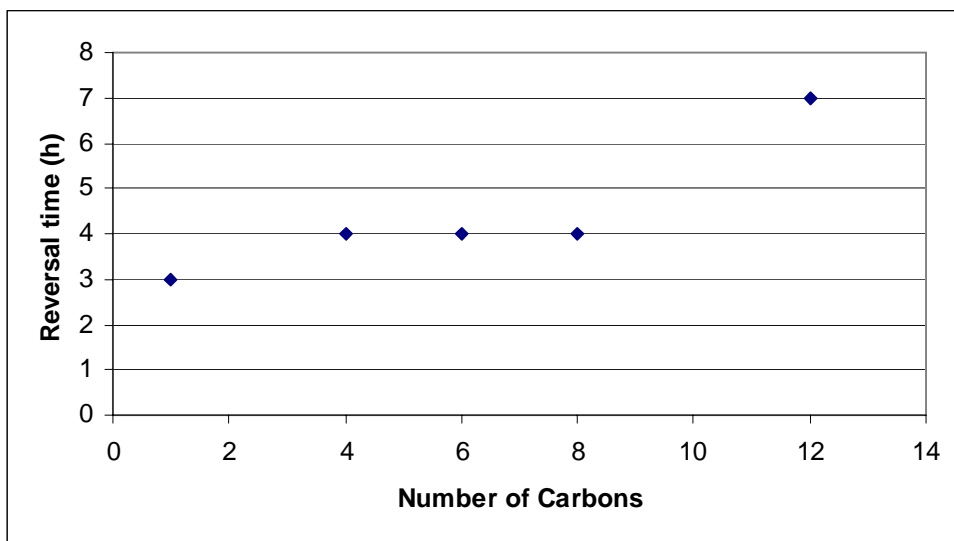
Fig 1.16: Reversal times of 2-butyl-1,1,3,3-tetramethylguanidinium alkylcarbonates
2-butyl-1,1,3,3-tetramethylguanidinium methylcarbonate reverses in merely three hours, whereas 2-butyl-1,1,3,3-tetramethylguanidinium dodecylcarbonate takes seven hours to reverse. The number of 2-butyl-1,1,3,3-tetramethylguanidinium alkylcarbonates that can be easily formed and reversed leads to opportunities where one not only has the choice of switching between a non-ionic liquid and a RTIL, one could also change the alcohol to reform a different ionic liquid between separation/reaction steps.

1.3.8 Miscibility studies

The miscibility of a range of solvents in 2-butyl-1,1,3,3-tetramethylguanidinium alkylcarbonate ILs has been investigated. The solvents tested in 2-butyl-1,1,3,3-tetramethylguanidinium methylcarbonate were pentane, hexane, heptane, octane, DMSO, chloroform, THF, toluene, and ethyl acetate. The solvents tested with the other 2-butyl-1,1,3,3-tetramethylguanidinium alkylcarbonates (butyl, hexyl, octyl, and dodecyl) were hexane, toluene, and ethyl acetate. Miscibility studies were conducted by adding the solvent (0.15mL) to an equimolar solution of 2-butyl-1,1,3,3-tetramethylguanidine and alcohol (0.88-1.23 mmol each). CO_2 was then bubbled into the system, and NMR was used to confirm the formation of the IL. Upon the formation of 2-butyl-1,1,3,3-tetramethylguanidinium methylcarbonate IL, the solvents octane, heptane, and pentane formed separate phases, while DMSO, chloroform, THF, and ethyl acetate remained soluble. Upon the formation of 2-butyl-1,1,3,3-tetramethylguanidinium alkylcarbonate IL, all solvents tested remained soluble. Furthermore, GC-MS and NMR indicated no cross-contamination between the ionic liquid phase and the octane, heptane, or pentane phase (95% purity). The solubilities of the 2-butyl-1,1,3,3-tetramethylguanidinium alkylcarbonate ILs are compared in **Table 1.3**.

Table 1.3: Solubilities of 2-butyl-1,1,3,3-tetramethylguanidinium alkylcarbonate ILs

R of guanidinium alkyl carbonate	Non-polar alkane	Toluene	EtOAc
Me	2 phases	1 phase	1 phase
Bu	1 phase	1 phase	1 phase
Hex	1 phase	1 phase	1 phase
Oct	1 phase	1 phase	1 phase
Dodec	1 phase	1 phase	1 phase

1.3.9 2-butyl-1,1,3,3-tetramethylguanidinium bicarbonate

As stated earlier, 2-butyl-1,1,3,3-tetramethylguanidinium methylcarbonate appeared to be sensitive to moisture. Thus, 2-butyl-1,1,3,3-tetramethylguanidinium bicarbonate was synthesized so that it could be studied (**Fig 1.17**).
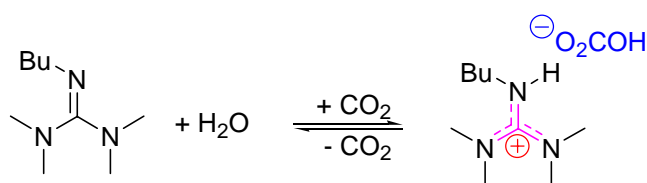
Fig 1.17: Reversible formation of 2-butyl-1,1,3,3-tetramethylguanidinium bicarbonate

CO_2 was bubbled into an equimolar mixture of TMBG and water. The exothermic formation of the bicarbonate salt was confirmed with NMR (^{1}H, ^{13}C). Unlike its alcohol analogues, the bicarbonate salt had to be heated at 80°C overnight to reverse. Furthermore, the bicarbonate reformed after reversal. More interestingly, in the presence of methanol, 2-butyl-1,1,3,3-tetramethylguanidinium bicarbonate appears to form a slurry

with very fine, sand like crystals. NMR analysis (^{1}H, ^{13}C), however, was inconclusive as to the exact components of the slurry.

1.3.10 Modification of alkyl groups in guanidine

A guanidine was synthesized where the alcohol moiety was directly attached to the molecule (**Fig 1.18**) as a means to avoid the addition and potential loss of the alcohol upon heat reversal, especially if the alcohol used were a low boiling one.
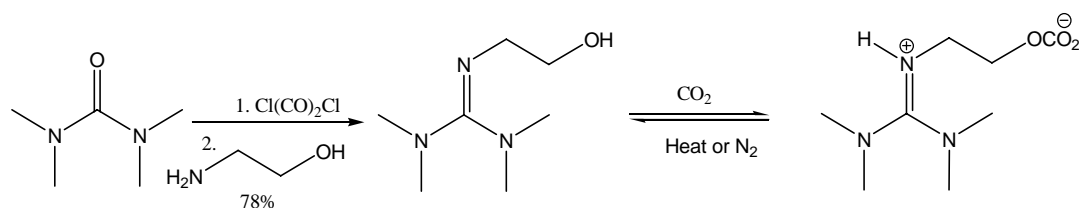
Fig 1.18: Amino-alcohol guanidine

2-[1-hydroxyethyl]-1,1,3,3-tetramethyl guanidine was synthesized using the same optimized protocol as 2-butyl-1,1,3,3-tetramethyl guanidine. Recrystallization in dichloromethane gave the desired solid product in 78% yield. Unfortunately, this hydroscopic compound (decomposition point 171°C) did not form a RTIL in the presence of CO_2. NMR data indicated that no reaction took place at all, and only the absorptions for 2-[1-hydroxyethyl]-1,1,3,3-tetramethyl guanidine were observed.

Another modification that was tested was the production of a 2-silylated guanidine (**Fig 1.19**). We chose to investigate silylated guanidines because RTILs are in general quite viscous and recent literature has indicated that silylated RTILs are less viscous.[23, 24] High viscosities may limit the usability of RTILs because they can complicate common laboratory tasks such as filtration, decantation, and dissolution. Furthermore, higher viscosities lead to slower rates in diffusion-controlled reactions. We

proposed to synthesize silyl-subsituted guanidines and determine if this simple silyl substitution will produce a less viscous liquid.

First, the aforementioned amino alcohol guanidine (2-[1-hydroxyethyl]-1,1,3,3-tetramethyl guanidine) was introduced to silylating conditions (**Fig 1.19**).
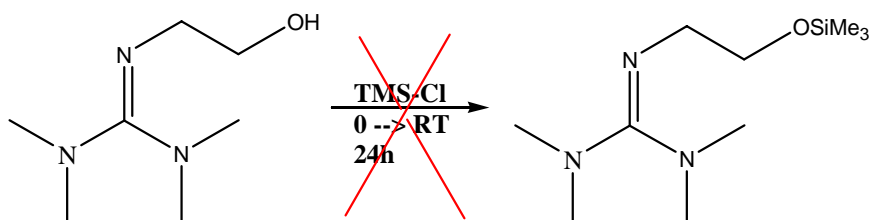
Fig 1.19: Silylation attempt of 2-[1-hydroxyethyl]-1,1,3,3-tetramethyl guanidine

NMR (^{1}H, ^{13}C) indicated that the desired compound was not generated by this scheme, and that the product isolated was unidentifiable. To synthesize the desired 2-[trimethylsiloxyethyl]-1,1,3,3-tetramethyl guanidine we then opted to synthesize trimethylsiloxyethylamine, and then use it in the protocol optimized for the synthesis of 2-butyl-1,1,3,3-tetramethyl guanidine (**Fig 1.20**).
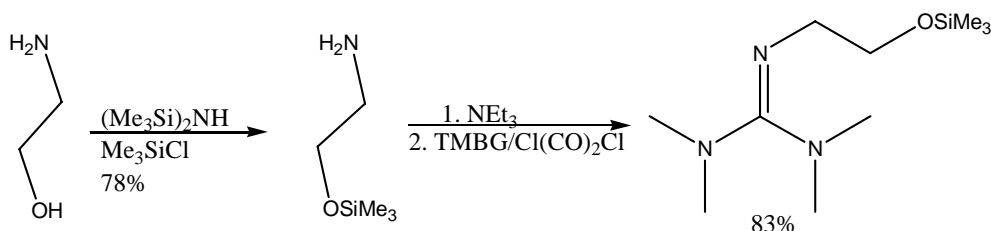
Fig 1.20: Synthesis of 2-[trimethylsiloxyethyl]-1,1,3,3-tetramethyl guanidine

This synthesis differed from the exact protocol for the synthesis of 2-butyl-1,1,3,3-tetramethyl guanidine in that triethylamine (1.5 equiv compared to the urea) was added along with 2-[1-hydroxyethyl]-1,1,3,3-tetramethyl guanidine to react with any hydrochloric acid and prevent deprotection of the silylated oxygen. Work-up gave the desired product in 83% yield as light yellow oil. When the 2-[1-trimethylsiloxyethyl]-

1,1,3,3-tetramethyl guanidine was mixed with methanol and introduced to CO_2, NMR did not indicate the formation of the desired 2-[1-trimethylsiloxyethyl]-1,1,3,3-tetramethyl guanidinium methylcarbonate RTIL (**Fig 1.21**).
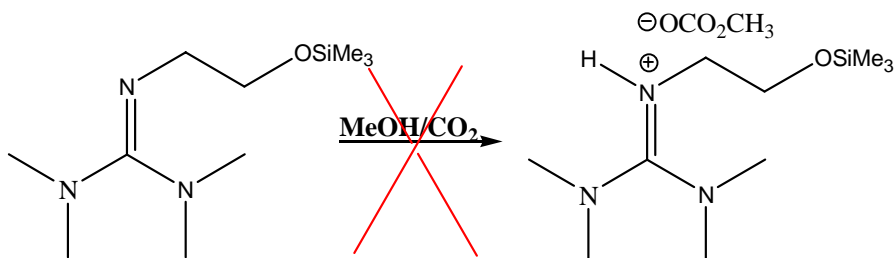
Fig 1.21: Attempt to form 2-[1-trimethylsiloxyethyl]-1,1,3,3-tetramethyl guanidinium methylcarbonate RTIL

2-[1trimethylsilylmethyl]-1,1,3,3-tetramethyl guanidine (**Fig 1.22**) was also synthesized. This compound was synthesized using the method optimized for the synthesis of TMBG.
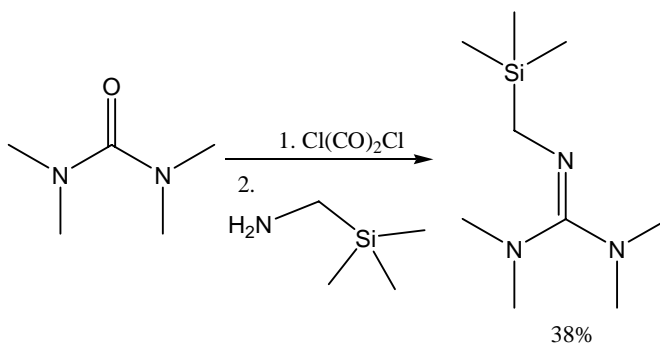
Fig 1.22: Silylated guanidine

Work-up and vacuum distillation produced the desired compound in 38% yield as a light yellow oil. When CO_2 was bubbled through an equimolar mixture of the 2-[trimethylsilanylmethyl]-1,1,3,3- tetramethylguanidine and methanol the 2-[trimethylsilanylmethyl]-1,1,3,3- tetramethylguanidinium methylcarbonate was formed. Unfortunately, it is a solid at room temperature (mp= 36°C) (**Fig 1.23**).
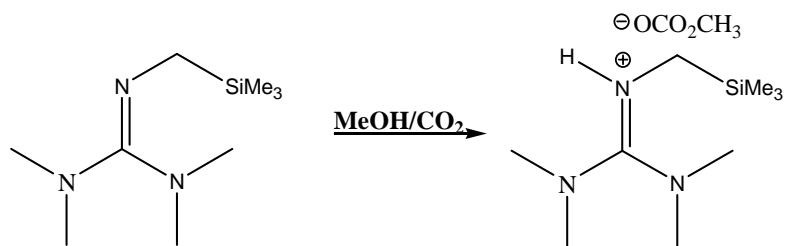
Fig 1.23: 2-[trimethylsilanylmethyl]-1,1,3,3- tetramethylguanidinium methylcarbonate

Since the melting point of 2-[trimethylsilanylmethyl]-1,1,3,3- tetramethylguanidinium methylcarbonate was not too high, we believed it had possibilities as an IL for reactions at higher temperatures. Unfortunately, heating barely past the melting point ($40^{o}C$) begins the reversal of this compound to the guanidine, possibly due to steric-driven elimination of CO_2.

1.3.11 Applications of TMBG/TMBG MC IL system

1.3.11.1 Reaction/recycle of TMBG-methanol IL systems

While we have demonstrated the reversible formation of the room temperature ionic liquids 2-butyl-1,1,3,3-tetramethyl guanidinium alkylcarbonate, their scope as reaction solvents still remains to be explored. We investigated organic transformations, product separations, and solvent recycle using the switchable ionic liquid 2-butyl-1,1,3,3-tetramethylguanidine/methanol system. The 1) Claisen-Schmidt condensation of 2-butanone and benzaldehyde, 2) cyanosilylation of cyclohexanone, 3) Michael addition between 2-cyclohexenone and dimethyl malonate, 4) Diels Alder reaction between anthrone and N-phenylmaleimide, 5) addition of aniline to chalcone, 6) Suzuki reaction between phenylboronic acid and bromobenzene, and 7) oxidation of benzyl alcohol with hypochlorite were studied. It was our goal to use these reactions as indications that

TMBG can be used in a complete chemical process that includes reaction, separation, reformation, and recycle (**Fig 1.24**).
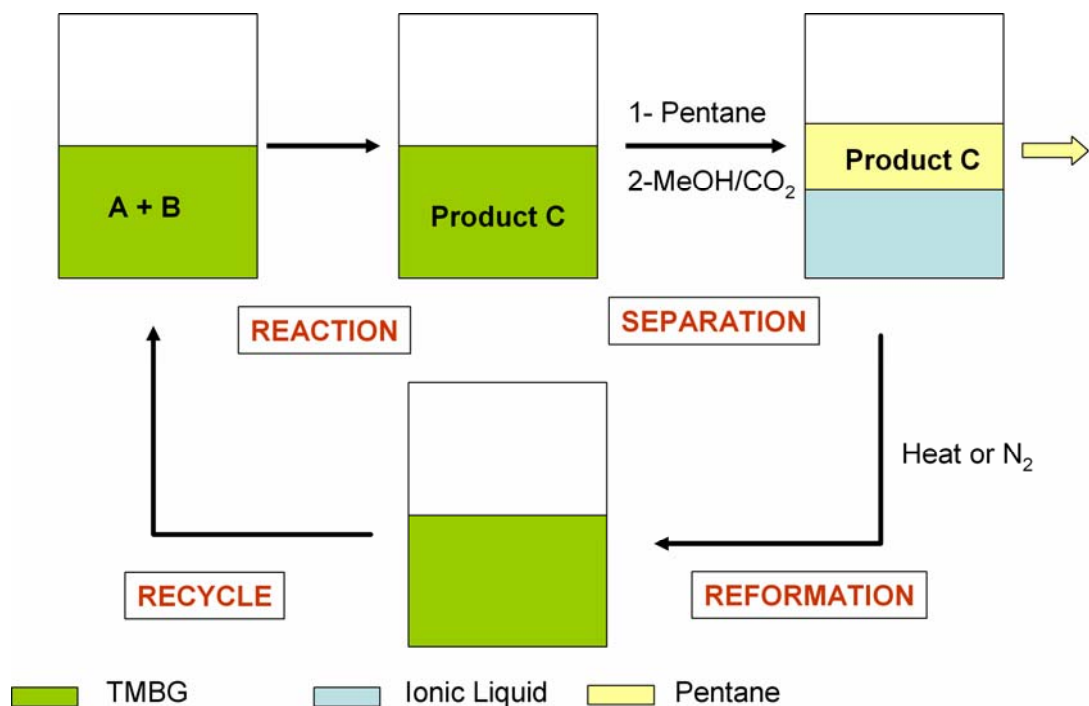
Fig 1.24: Complete Chemical Process

In this process, a reaction (A + B) could take place in the presence of TMBG to generate product C (**Fig 1.24**). After the reaction has reached completion, pentane (or heptane, octane, or dodecane) can be added along with methanol. Then, formation of the RTIL through bubbling CO_2 will cause a phase separation. The products would be anticipated to be soluble in the alkane phase, and the 2-butyl-1,1,3,3-tetramethylguanidinium methyl carbonate IL is a separate phase that can be removed, reversed, recycled, and reformed.

In the Claisen-Schmidt condensation of 2-butanone and benzaldehyde, the ratio between the internal and terminal enone products is dependent upon whether the reaction is done in basic or acidic conditions (**Fig 1.25**).[25-27]
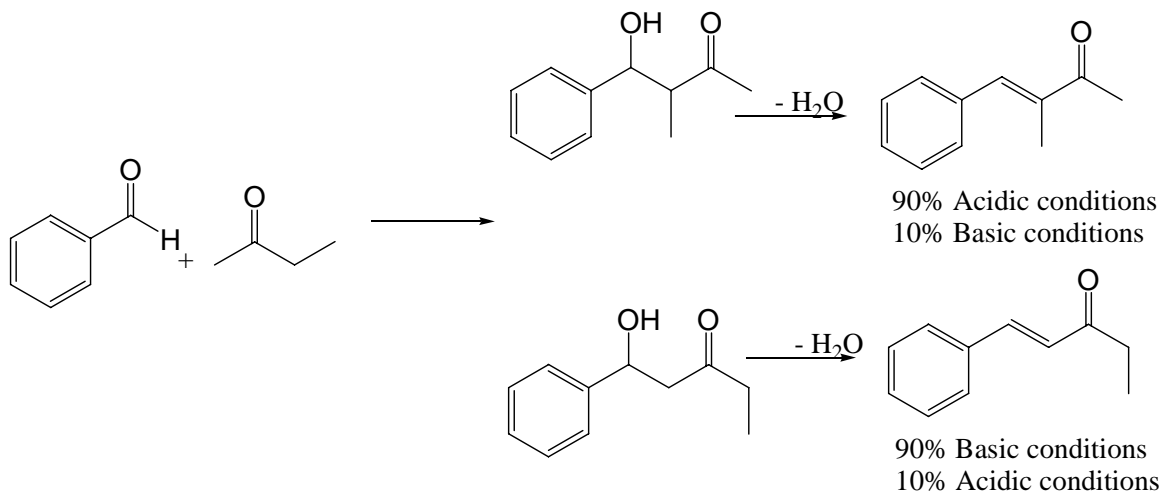
Fig 1.25: Claisen-Schmidt condensation of 2-butanone and benzaldehyde

In basic conditions, the terminal enone product is the predominant species formed, although both hydroxy ketols (internal and terminal) can be formed reversibly. Predominance is caused by faster rate of dehydration in the terminal enone as compared to the internal one.[27]   Thus the condensation of 2-butanone and benzaldehyde was investigated in the presence of TMBG. Since TMBG, like most guanidine moieties, is basic, the predominance of the terminal enone product was expected.[18, 28]   The reactions were run at room temperature in the glove box.   First, the optimal conditions for the reaction were investigated.   0.0024mol TMBG was mixed with .00024mol each of butanone and benzaldehyde. The samples were then stirred at either room temperature or at 80°C for between 1-24 hours (**Table 1.4**).

Table 1.4: Reaction conditions for the condensation of 2-butanone and benzaldehyde in the presence of TMBG

temp (C)	time (h)	Yield (%)
RT	24	48
80	1	13
80	2	24
80	3	44

Even though the yield at 80°C for three hours (44%) was similar to the yield at room temperature for 24 hours (48%), the heated sample became dark over time, indicating some type of degradation. The yield that is reported is a combination of the two expected products because it was difficult to estimate the ratio between the products at such low concentrations (0.0312-0.115mmol). Once it was clear the Claisen-Schmidt reaction was catalyzed by TMBG, the recycle was investigated (**Table 1.5**). The reactions were run at room temperature in the glove box, and GC-MS and NMR were used for characterization.

Table 1.5: Recycle of TMBG in Claisen-Schmidt condensation of 2-butanone and benzaldehyde

mol TMBG	mol benzalde hyde	mol buta none	time (h)	Pdt (%)
0.024	0.019	0.019	168	53
0.024	0.0012	0.002	96	83

In the first run, 1.3 equivalents of TMBG, compared to the reactants, was used as the catalyst and solvent (**Table 1.5**). After 168 hours, the reaction was stopped. Then, octane and methanol were added, and the mixture was bubbled with CO_2 to form 2-butyl-1,1,3,3-tetramethylguanidinium methyl carbonate. The enone product separated into the alkane phase and 2-butyl-1,1,3,3-tetramethylguanidinium methyl carbonate was removed with a pipette. Reduction of solvent led to an isolated yield of 53%. Next, 2-butyl-

1,1,3,3-tetramethylguanidinium methyl carbonate was then reversed by heating the RTIL at 50°C and reused. Since the reaction took so long the first time, the amount of reactants was decreased. In the second cycle, 10 equivalents of TMBG, compared to butanone, was used. This time, the isolated yield was 83% after reacting for 96 hours. Again, TMBG MC IL was heated so that it could reverse and be reused. At this point, however, the viscosity of the RTIL had greatly increased, which we attributed to bicarbonate formation from the water byproduct, TMBG, and CO_2. After the third cycle (same conditions as the second cycle), we were unable to quantify the final yield because the reaction mixture was so viscous. As stated earlier, this RTIL is not easily reversible, and therefore hindered the reaction process.

Because water accumulation (which leads to bicarbonate formation) hindered the recycling of the condensation reaction, an effort to counteract the problem of water accumulation was designed. The condensation reaction was allowed to run for a specified amount of time. After the reaction was stopped, appropriate amounts of methanol and heptane were added. Then, the solution was dried with magnesium sulfate and filtered. Finally, CO_2 was bubbled into the solution to allow for the formation of the TMBG MC IL which phase separated from the product containing heptane phase. In this experimental set-up, an equimolar solution of TMBG, benzaldehyde, and 2-butanone was refluxed (80°C) for four hours under an atmosphere of N_2, and GC-MS and NMR were used for characterization. Under these conditions, mostly terminal enone product was isolated (95%)

The reactions were stopped after four hours because it was found that the longer the reaction ran, the more side products were isolated (**Fig 1.26**).
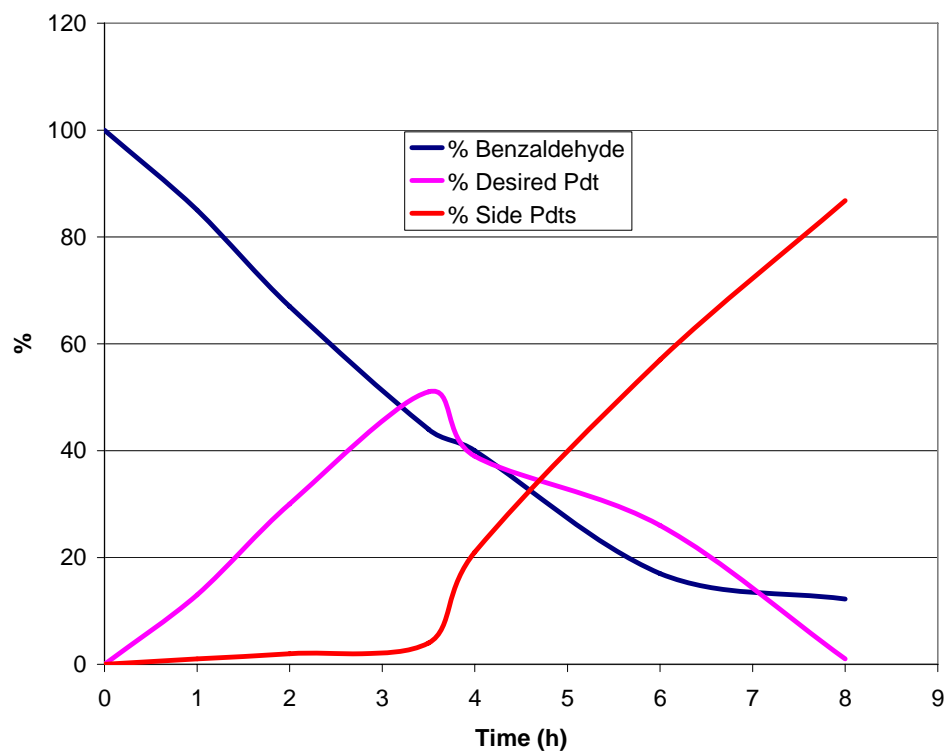
Fig 1.26: Change in product composition with time

As shown in **Fig 1.26**, as the conversion increases (decrease in benzaldehyde), the desired product peaks around four hours. After that time, the amount of desired product decreases and side products increase greatly. Side products include the higher addition adducts from additional condensation reactions, and oligomers.[29]

Using magnesium sulfate to dry the solution before CO_2-induced phase separation proved to be very successful (**Table 1.6**).

Table 1.6: Recycle of TMBG in Claisen-Schmidt condensation of 2-butanone and benzaldehyde, dried with MgSO₄

	mol TMBG	mol benzaldehyde	mol butanone	Pdt (%)
1-1	0.00585	0.00585	0.01	33
1-2	0.0076	0.0076	0.01	34
1-3	0.0076	0.0076	0.01	32
2-1	0.0117	0.0117	0.01	35
2-2	0.0117	0.0117	0.01	33
2-3	0.0117	0.0117	0.01	33

In run 1-1 (**Table 1.6**), 33% of the desired product was isolated from the reaction pot. Upon reversal and recycle, similar yields for found for two more cycles (34%, 32%, runs 1-2 and 1-3). Finally, reversing the TMBG MC IL and using acid-base work-up yielded pure TMBG in 85%. This sequence was repeated on a larger scale (runs 2-1 through 2-3) to give similar yields (33-35%), and 90% TMBG was recovered at the end of the recycle sequence.

1.3.11.1.2 Cyanosilylation of Cyclohexanone

Wang *et al.* demonstrated that a catalytic amount of 1,1,3,3-tetramethylguanidine (TMG, 2mol %) catalyzed the cyanosilylation of a number of ketones, benzaldehyde, and isobutyaldehyde in high yields (**Fig 1.27**).[30]
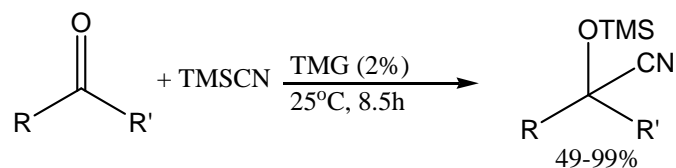
Fig 1.27: Cyanosilylation catalyzed by TMG

The cyanosilylation of cyclohexanone and benzaldehyde in TMBG was investigated. In these reactions, TMS-CN was slowly added to a mixture of TMBG and cyclohexanone

and allowed to react. When the reaction was stopped, heptane and methanol were added, and CO_2 was bubbled through the mixture to generate the 2-butyl-1,1,3,3-tetramethylguanidinium methylcarbonate IL (TMBG MC IL). TMBG MC IL phase separated from the product/heptane phase and could be easily removed via pipette (**Table 1.7**). GC-MS and NMR were used for characterization.

Table 1.7: Conditions for cyanosilylation catalyzed by TMBG

	mol TMBG	mol cyclohexanone	mol TMS-CN	time (h)	temp (C)	Pdt (%)
1	0.006	0.0005	0.0006	8	25	0
2	0.006	0.0005	0.0006	24	25	2
3	0.006	0.0005	0.0006	1	80	2
4	0.0001	0.005	0.006	1.5	25	100
5	0.0001	0.005	0.006	1.5	25	100
6	0.002	0.005	0.006	4	25	98
7	0.003	0.005	0.006	4	25	98
8	0.003	0.005	0.006	2.75	25	96
9	0.005	0.005	0.006	16	25	98

When TMBG were present as both catalyst and solvent in large excess (10 equivalents based on TMS-CN, **Table 1.7**, runs 1-3), only cyclohexanone was recovered, even when the reaction was heated. Since Wang *et al.* had used trace TMG as their catalyst, the exact conditions from the paper were used with TMBG as the catalyst (runs 4-5).[30] Although quantitative amounts of the desired product were found, the addition of heptane, methanol and CO_2 did not produce a separate phase, possibly because such low amounts of TMBG are soluble in the mixture. Next, the cyanosilylation of cyclohexanone was run where TMBG existed at 40 and 60 mol% (runs 6-7). After the addition of heptane, methanol, and CO_2, a phase separation occurred to give the desired

products in high yields (98%). Analysis of the TMBG MC IL phase indicated the formation of TMBG/TMS-CN salt , which has literature precedent (**Fig 1.28**).[30]
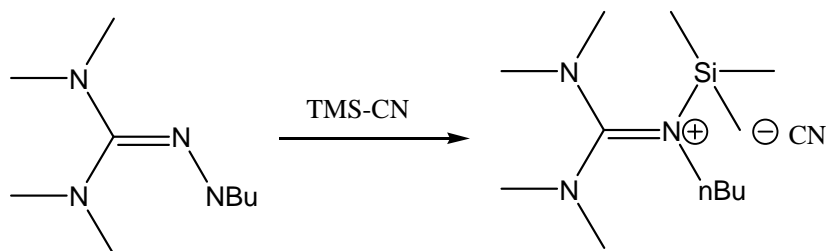
Fig 1.28: Formation of TMS-CN guanidinium salt

The formation of TMBG/TMS-CN salt seemed to be irreversible by heat or vacuum. Moreover, the combination of TMBG MC IL and the TMBG/TMS-CN salt was more viscous than TMBG MC IL alone. To minimize the formation of the TMBG/TMS-CN salt, the TMS-CN was diluted in heptane and then slowly added to a mixture of TMBG and cyclohexanone in an ice bath. Runs 8-9 show that the heptane had no detrimental effect on the yields (96-97%).

With high yields in hand and a minimal amount of the TMBG/TMS salt being formed, the recycle and reformation of the TMBG MC IL was attempted (**Table 1.8**).

Table 1.8: Recycle of TMBG in cyanosilylation of cyclohexenone

	mol TMBG	mol cyclohex anone	mol TMS-CN	time (h)	temp (C)	Pdt (%)
10-1	0.002	0.005	0.006	17	25	98
10-2	0.002	0.005	0.006	16	25	54
11-1	0.005	0.005	0.006	16	25	85
11-2	0.005	0.005	0.006	16	25	56

When the first cycle of the cyanosilylation of cyclohexanone was run, a high yield of product was found as usual (**Table 1.8**, run 10-1, 98%). After the TMBG MC IL was phase separated, its reversal was attempted using stirring and vacuum. Although it was

clear that a mixture of TMBG/TMS-CN salt and TMBG existed, it was still reused. The

second cycle showed a large decrease in yield (run 10-2, 54%), and the IL that phase

separated upon addition of methanol and CO_2 was even more viscous than before and

could not be reversed. In another run, the recycle and reformation were repeated using a

larger amount of TMBG (runs 11-1 and 11-2), but a large decrease was seen in the yield

after the second cycle again (85% to 56%).

1.3.11.1.3 Michael addition between 2-cyclohexenone and dimethyl malonate

Kumamoto *et al* showed that cyclopentenone and diphenyl malonate underwent

an asymmetric Michael reaction with good yields (75-77%) in the presence of a chiral

guanidine (0.1 equiv) (**Fig 1.29**).[31]
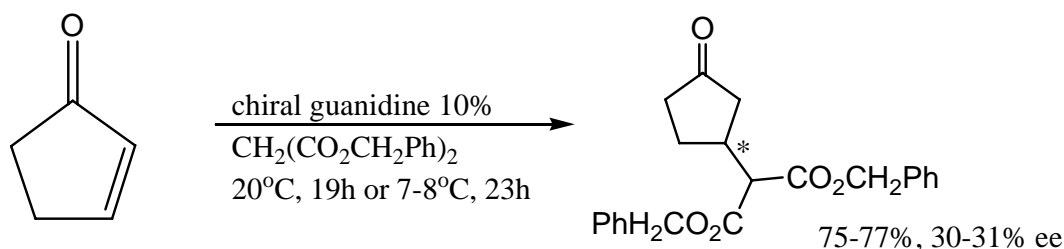
Fig 1.29: Michael addition between cyclopentenone and dimethyl malonate

In this work, the guanidine was recovered by acid-base extraction. A Michael addition

between 2-cyclohexenone and dimethyl malonate was investigated in TMBG (**Fig 1.30**).
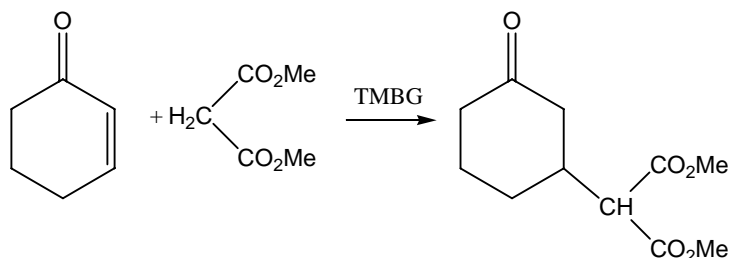
Fig 1.30: TMBG catalyzed Michael addition between 2-cyclohexenone and dimethyl malonate

Dimethyl malonate was added to a mixture of cyclohexenone and TMBG. After the reaction was stopped, hexane and methanol were added. The product would then be isolated from the hexane phase upon formation of TMBG MC IL by bubbling CO_2 (**Table 1.9**). GC-MS and NMR were used for characterization.

Table 1.9: Conditions for TMBG catalyzed Michael addition between 2-cyclohexenone and dimethyl malonate

	mol TMBG	mol MeMalonate	mol Cyclohexenone	solvent	time (h)	temp (C)	work up	Pdt (%)
1	0.006	0.006	0.006	neat	48	25	none	0
2	0.00175	0.00175	0.00175	neat	16	80	none	0
3	0.00175	0.00175	0.00175	neat	16	80	none	1
4	0.00175	0.00175	0.00175	MeOH	16	25	aq HCl	98
5	0.00175	0.00175	0.00175	MeOH	16	80	aq HCl	10
6	0.00175	0.00175	0.00175	neat	16	25	aq HCl	46
7	0.00175	0.00175	0.00175	neat	16	80	aq HCl	86

Attempts to isolate product from this procedure failed (**Table 1.9**, runs 1-3). Instead, treatment of the reaction mixture to 10% aqueous HCl and then extraction with diethyl ether provided the product in good yields (run 4: 98%, run 7: 86%). Necessary acidic work-up is attributed to the high acidity of the hydrogen atoms on the β-diester (**Fig 1.31**).
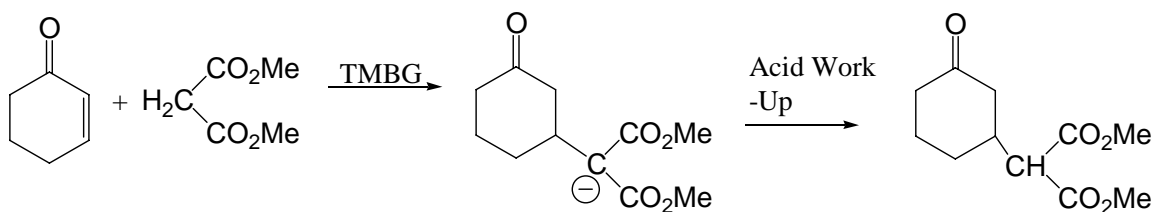
Fig 1.31: Quenching of β-diester

The α-carbon of the β-diester moiety is completely deprotonated, and only upon acid work-up is the product soluble in hexane. Although the TMBG could have been

recovered using acid-base extraction, this defeats the purpose of having an easily reversible IL. Thus our TMBG reformation/recovery process would not be applicable for this reaction even though the yields were high.

1.3.11.1.4 Diels Alder between Anthrone and N-phenylmaleimide

Shen *et al* designed a bicyclic guanidine (1,5,7-Triazabicyclo[4.4.0]dec-5-ene) which catalyzed Diels-Alder reactions between a variety of substituted anthrones and maleimides with yields ranging from 87-92% and ee's ranging from 85-99% (**Fig 1.32**).[32]
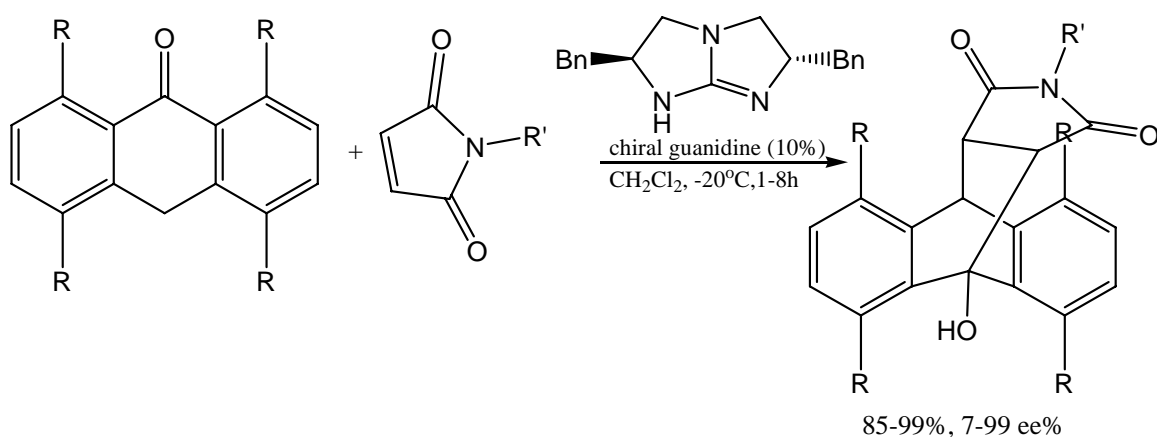
Fig 1.32: Diels-Alder catalyzed by chiral guanidine

The Diels-Alder reaction between anthrone and N-phenylmaleimide in TMBG was investigated (**Fig 1.33**).
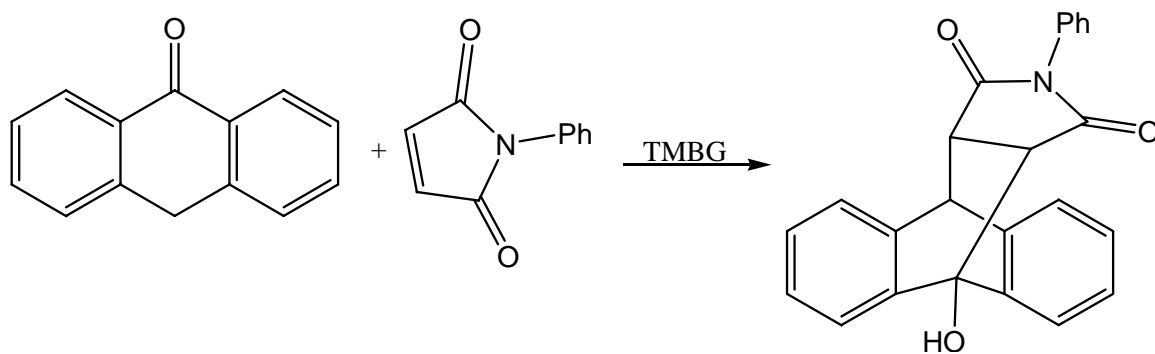
Fig 1.33: TMBG catalyzed Diels-Alder reaction between anthrone and N-phenylmaleimide

In this reaction, N-phenylmaleimide (0.006mol) was added to a mixture of TMBG (0.006mol) and anthrone (0.006mol). The heterogeneous mixture was then stirred at room temperature for 1, 16, and 48 hours. When the reaction was stopped, methanol and decane were added to the mixture. Then, CO_2 was bubbled through the solution to form the TMBG MC IL phase and phase separate the decane/product phase. GC-MS and NMR were used for analysis. Unfortunately, conversions were very low. After 48 hours, >5% of product was detected. However, Ye *et al* has shown that cyclic guanidines are far more basic than linear guanidines and often catalyze reactions where their linear counterparts fail.[33] Thus, TMBG may not have been basic enough to catalyze the reaction efficiently.

1.3.11.1.5 Addition of aniline to chalcone

Basic natural phosphate catalysts have been shown to catalyze the addition of amines to chalcone in methanol at room temperature with decent yields (50-95%).[34] The addition of aniline to chalcone was investigated using TMBG as a catalyst (**Fig 1.34**).
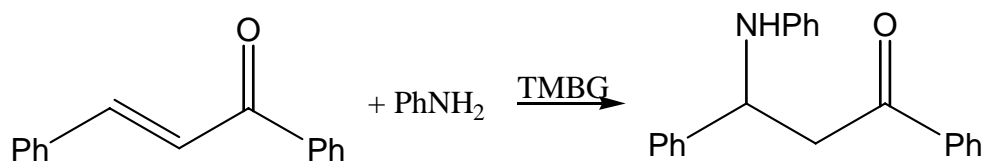
Fig 1.34 TMBG catalyzed addition of aniline to chalcone

In this reaction, aniline and chalcone were dissolved in solvent (methanol or methanol/heptane mixture). Then, TMBG was added and the mixture was allowed to react. After the reaction was completed, heptane was added if necessary, and CO_2 was bubbled throughout the mixture to form and phase separate the TMBG MC IL from the heptane/product phase (**Table 1.10**). GC-MS and NMR were used for characterization.

Table 1.10: Conditions for TMBG catalyzed addition of aniline to chalcone

	mol TMBG	mol chalcone	mol aniline	solvent	time (h)	temp (C)	Pdt (%)
1	0.0056	0.00263	0.00263	MeOH	15	RT	0
2	0.0056	0.00526	0.00526	MeOH	15	RT	0
3	0.011	0.00526	0.00526	MeOH/Heptane	16	RT	0
4-1	0.011	0.00526	0.00526	MeOH/Heptane	18	80	87
5-1	0.011	0.00526	0.00526	MeOH/Heptane	5.5	80	29
4-2	0.011	0.00526	0.00526	MeOH/Heptane	15.5	80	0
5-2	0.011	0.00526	0.00526	MeOH/Heptane	15.5	80	0

When this reaction was run at room temperature with just methanol as the solvent (**Table 1.10**, runs 1 and 2), the reactants only partially dissolved. Furthermore, after fifteen hours only starting material was recovered from the heptane phase upon the formation of the TMBG MC IL. When heptane (final ratio of 1:4 methanol/heptane) was added to homogenize the solution (run 3), still only starting material was recovered. Then, the mixture of heptane, methanol, chalcone and aniline was heated at 80°C overnight (runs 4-1 and 5-1). Once the reaction was stopped, extra methanol and heptane were added (0.5mL each), and CO_2 was bubbled through the solution to phase separate the TMBG MC IL from the product/heptane phase, and the desired product was isolated in decent

yields (87%, run 4-1). Upon recycle and re-use of the TMBG, however, no product was isolated; only starting material was recovered from the heptane phase. Analysis of the TMBG MC IL phase indicated that all unreacted starting materials were dissolved in the IL (run 4-1). Furthermore, after the second cycle was completed, not only were all of the accumulated starting materials dissolved in the TMBG MC IL, so was the desired product (45% conversion, run 4-2).

1.3.11.1.6 Metal-catalyzed reaction: Suzuki coupling reaction

A Suzuki reaction between phenyl boronic acid and bromobenzene was investigated with our TMBG system (**Fig 1.35**).
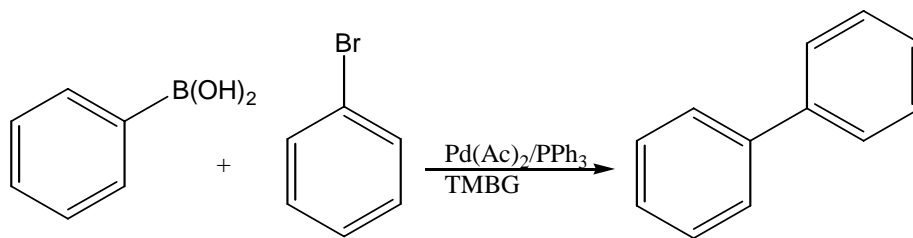
Fig 1.35: Suzuki reaction between phenyl boronic acid and bromobenzene, with TMBG as the base

This reaction was chosen for two reasons: 1) the diphenyl product is non-polar, making it very likely to be soluble in an alkane, and 2) if the metal ($Pd(Ac)_2$) and phosphine (PPh_3) could be immobilized in the TMBG MC IL, they could be recycled along with the IL and 3) at the end life of the catalytic system, the IL can be switched back to guanidine and methanol for purification and/or recovery of the metal and ligands.[35]

In this reaction, the solid boronic acid, palladium precatalyst, and phosphine were degassed together. Then, TMBG (stored under N_2) was added and the mixture was stirred. Finally, bromobenzene was added and the reaction was heated at $80^{\circ}C$. Once the

reaction was stopped, it was allowed to cool before heptane and methanol were added. Then, CO_2 was bubbled into the mixture to cause the formation and phase separation of the TMBG MC IL from the heptane/biphenyl phase (**Table 1.11**). GC-MS and NMR were used for characterization.

Table 1.11: Conditions for Suzuki reaction between phenyl boronic acid and bromobenzene, with TMBG as the base

	mol TMBG	mol boronic acid	mol bromobenzene	mol Pd(Ac)$_2$	mol PPh$_3$	time (h)	Pdt (%)	temp (C)
1	0.0035	0.00175	0.00117	5.9E-05	0.000118	16	9.38	80
2	0.0035	0.00175	0.00117	5.9E-05	0.000233	16	7.81	80
3	0.00525	0.00175	0.00117	5.9E-05	0.000118	16	6.99	80
4	0.00525	0.00175	0.00117	5.9E-05	0.000233	16	10.14	80
5	0.00526	0.000438	0.000293	1.5E-05	0.0000586	19	13.26	80
6	0.00526	0.000438	0.000293	1.5E-05	0.0000586	19	25.44	80
7	0.00526	0.000438	0.000293	1.5E-05	0.0000587	16	6.12	80
8	0.00175	0.00175	0.00117	5.9E-05	0.000118	16	2.75	80
9	0.00175	0.00175	0.00117	5.9E-05	0.000233	16	2.89	80

When 2-3 equivalents of TMBG was used in comparison to the boronic acid, the reaction mixture became very dark after 16 hours (**Table, 1.11**, runs 1-4). This change in color indicated that the palladium catalyst may be decomposing. Furthermore, yields were very low (6.99-10.14%). The ratio between TMBG and boronic acid was increased to 12:1 TMBG/boronic acid (runs 5-6). Although the reaction mixture no longer changed color, the yields still were not impressive (13.26%, 25.44%). Adding heptane as a solvent along with the TMBG also did not help the reaction (run 7); in fact, it seemed to detrimentally affect the yield (6.12%). The ionic liquid phase (TMBG MC IL) analysis along with the heptane/product phase is reported in **Table 1.12**).

Table 1.12: Analysis of heptane and IL phases in Suzuki reaction between phenyl boronic acid and bromobenzene, with TMBG as the base

	mol TMBG	mol boronic acid	mol bromobenzene	mol Pd(Ac)$_2$	mol PPh$_3$	time (h)	Pdt in heptane phase (%)	Pdt in IL phase (%)
10	0.00532	0.00175	0.00117	5.9E-05	0.000233	1	8.37	7.83
11	0.00532	0.00175	0.00117	5.9E-05	0.000233	2	8.59	8.1
12	0.00532	0.00175	0.00117	5.9E-05	0.000233	4	11.02	8.44
13	0.00532	0.00175	0.00117	5.9E-05	0.000233	4	10.69	8.03
14	0.00526	0.000438	0.000293	1.5E-05	0.0000585[1]	1	1.26	2.09
15	0.00526	0.000438	0.000293	1.5E-05	0.0000586[1]	19	7.71	1.18

[1]Phosphine used is actually 2-[di(tert-butyl)phosphino]-2',4',6'-triisopropyl-1,1'-biphenyl

Upon investigation, we found the biphenyl product equally soluble in both the TMBG MC IL and heptane phase (**Table 1.12**, runs 10-13). Furthermore, the TMBG MC IL/biphenyl mixture would not reverse. NMR (^{1}H) data indicated that in the TMBG MC IL phase was a mixture of biphenyl product, unreacted starting materials, and byproducts from the small of amount of reactants that had undergone Suzuki coupling. We theorized that if the yield could be greatly increased, then it would be easier to isolate the desired biphenyl product. Unfortunately, changing to a more reactive phosphine (2-[di(tert-butyl)phosphino]-2',4',6'-triisopropyl-1,1'-biphenyl) failed to increase the yield (**Fig 1.36**, **Table 1.12**, runs 14-15).
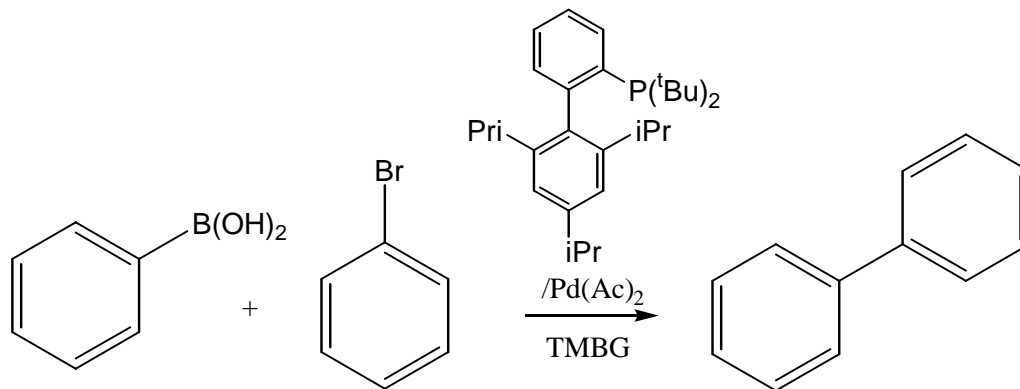
Fig 1.36: Suzuki reaction with 2-[di(tert-butyl)phosphino]-2',4',6'-triisopropyl-1,1'-biphenyl

Suzuki coupling proved to be very unsuccessful in our TMBG system. Two factors could have led to the low yields we encounter: 1) It was conjectured that the yields are so low because the boronic acid is not stable in the presence of large excesses of base (Boronic acid starting material is never seen in either phase upon work-up of the acid). 2) Other researchers have found Suzuki reactions where the base is DBU, DABCO, or 1,1,3,3-tetramethylguanidine fail when done without aqueous media present,[36] and our reactions also precluded an aqueous phase.

1.3.11.1.7 Oxidation of benzyl alcohol

Oxidation of benzaldehyde in the presence of a hexa-alkylguanidinium RTIL with sodium hypochlorite in water was reported (**Fig 1.37**).[37]
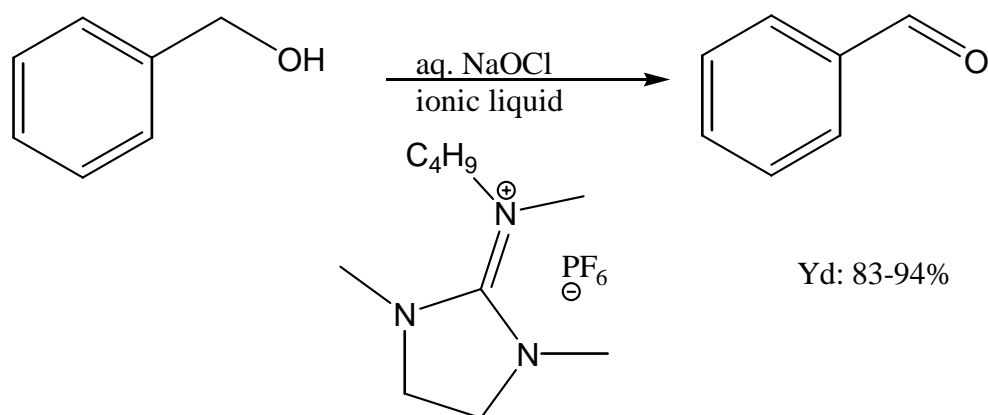
Fig 1.37: Oxidation of benzyl alcohol in hexa-alkylguanidinium RTIL

This biphasic system showed yields of 83-94% where the oxidized product was extracted in diethyl ether and the RTIL was recovered by dissolution in water and then drying under vacuum. For the oxidation of benzyl alcohol, a different strategy was investigated: the reaction would take place in the guanidine-based RTIL. Once the reaction reached completion, an alkane could be used to extract the product. In this reaction, we used calcium hypochlorite in our TMBG system because it was attainable in solid form (and therefore anhydrous) (**Fig 1.38**).
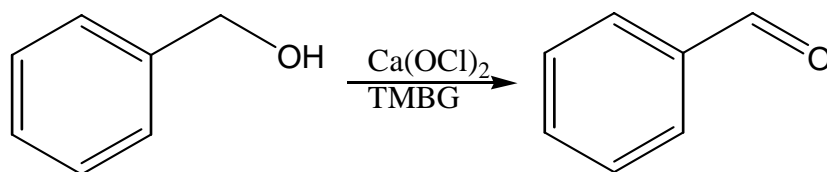
Fig 1.38: Oxidation of benzyl alcohol in TMBG

Calcium hypochlorite (0.789mmol) was added to a mixture of TMBG MC IL (5.26mmol) and benzyl alcohol (0.526mmol). After the reaction was run for 16 hours at room temperature, heptane was added to extract the benzaldehyde product. GC-MS and NMR analysis indicated that only benzyl alcohol was recovered. Calcium hypochlorite was

insoluble in TMBG MC IL. Perhaps if an oxidizing agent that is soluble in TMBG MC IL could be found, this reaction may work.

1.3.11.1.8 Summary of base-catalyzed reactions

We were able to successfully perform two reactions coupled with easy separation and recycle using our TMBG MC IL system: 1) Claisen-Schmidt condensation of 2-butanone and benzaldehyde and 2) cyanosilylation of cyclohexanone. The Claisen-Schmidt condensation of 2-butanone and benzaldehyde was successfully recycled in the TMBG MC IL system three times with fair yields (32.1-34.7%), and the TMBG was recovered in high yields (85-90%). The cyanosilylation of cyclohexanone was successfully recycled twice using our TMBG MC IL system two separate times with yields of 98% and 54%, and with yields of 85% and 56%. Decrease in yield is attributed to the formation of the TMBG/TMS-CN salt.

1.3.11.2 Separation of alkanes from tar sands/shale

Currently, it is very difficult to isolate octane from tar sand and shale.[38, 39] Tar sand and shale are mainly composed of bitumen which is a mixture of clay, Mg+, Ca+, and alkanes. We believed we could use the formation of the IL as a means to purify/isolate the octane from tar sands and shale (**Fig 1.39**).
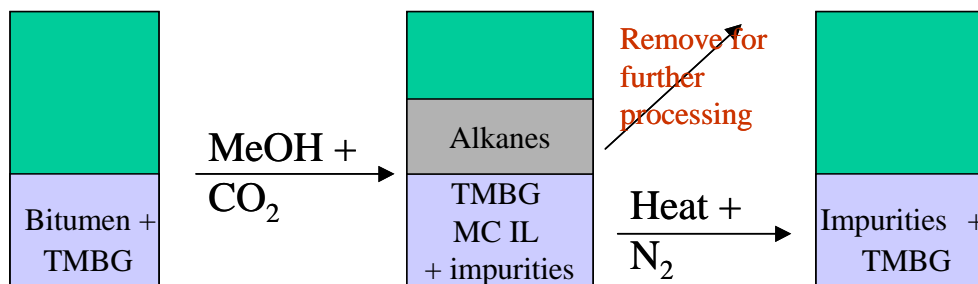
Fig 1.39: Separation of octane from tar sand or shale

Switching from the neutral TMBG/methanol solution to the TMBG MC IL could be an efficient means to isolate octane from impurities. Furthermore, the TMBG MC IL could be reversed and reused.

We first tested this hypothesis on crude oil, which is a mixture of alkanes. Crude oil was dissolved in TMBG. Then, methanol was added and CO_2 bubbled throughout the solution to form the TMBG MC IL and phase separate the alkane mixture (**Table 1.13**). % crude oil in mixture corresponds to the amount of oil in the total mixture (methanol, TMBG, and crude oil). Analysis was done by GC-MS.

Table 1.13: Separation of crude oil with TMBG MC IL

mol TMBG	g crude oil	% crude oil in mixture
0.00206	0.1	19.3
0.00199	0.1	19.7

Crude oil and TMBG are a homogeneous solution. However, upon the formation of TMBG MC IL, all of the crude oil phase separates (**Fig 1.40**).
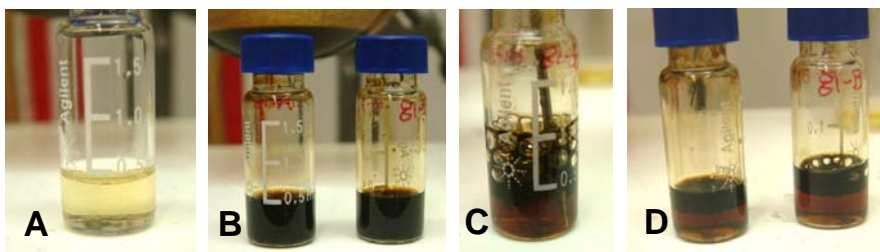
Fig 1.40: Separation of crude oil from TMBG via formation of TMBG MC IL, where A is TMBG; B is TMBG + crude oil mixture; C is CO_2 being bubbled into TMBG + crude oil mixture; and D is crude oil phase separated from TMBG MC IL

Analysis of the phases indicates trace TMBG is left in the crude oil (upper phase), but no crude oil is in the TMBG MC IL phase. The darkening of the TMBG MC IL could indicate the dissolution of inorganic impurities from the crude oil into the TMBG MC IL (**Fig 1.40D**).

This same procedure was repeated with a bitumen sample from ConocoPhillips. This bitumen sample is a mixture of clays, inorganic alkali metal salts, 1-3 wt% hydrogen sulfide, <2 wt% ethyl benzene, <1 wt% benzene, and crude oil.[40] Bitumen was dissolved in TMBG by stirring. Methanol is then added, and CO_2 is bubbled through the solution to form the separate TMBG MC IL and alkane phases (**Table 1.14**). Analysis was done with NMR (^{1}H, ^{13}C).

Table 1.14: Separation of bitumen with TMBG MC IL

	mol TMBG	g bitumen	% bitumen in mixture	Result after formation of TMBG MC IL
1	0.00409	0.142	14.6	1 phase
2	0.00409	0.103	10.2	1 phase
3	0.00409	0.009	1.07	2 phases
4	0.000567	0.003	2.54	2 phases
5	0.00067	0.006	4.25	1 phase
6	0.000544	0.007	5.96	1 phase
7	0.000421	0.008	8.56	1 phase
8-1	0.00725	0.016	1.07	2 phases
8-2	0.00772	0.017	1.07	2 phases
8-3	0.00316	0.007	1.07	2 phases

When high amounts of bitumen are mixed with TMBG, phase separation does not occur (**Table 1.14**, runs 1-2). However, when lower amounts of bitumen are used, phase separation occurs (run 3 through 5 and **Fig 1.41**). NMR (^{1}H, ^{13}C) was used to assess the quality and purity of the TMBG MC IL, but it is clear that the TMBG MC IL phase is much darker after separation from bitumen (**Fig 1.41D**). The NMR spectra display only the expected peaks for TMBG MC IL. Because of the polarities of the ionic species (which cannot be seen in NMR or GC-MS), it is believed that the inorganic species are retained in the ionic liquid phase. After separation with the TMBG MC IL, the bitumen phase is also noticeably less viscous. NMR analysis (^{1}H, ^{13}C) of untreated bitumen displays only alkane peaks, even though trace aromatics are in the mixture. NMR analysis of the treated bitumen shows the trace organic impurities (benzene, ethyl benzene) that were obscured when untreated bitumen was analyzed. Together, the data suggests that clay and other inorganics are dissolving in the TMBG MC IL and separating from the bitumen.
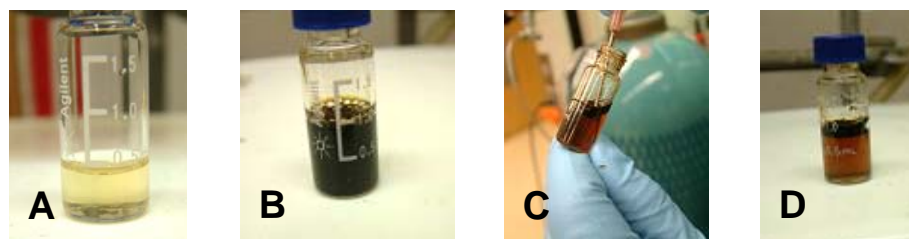
Fig 1.41: Separation of bitumen from TMBG via formation of TMBG MC IL, where A is TMBG; B is TMBG + bitumen mixture; C is CO_2 being bubbled into TMBG + bitumen mixture; and D is bitumen phase separated from TMBG MC IL

After the separated bitumen is removed, TMBG MC IL is reversed and fresh bitumen was introduced to the TMBG. The entire process (dissolution of bitumen in TMBG, TMBG MC IL formation/separation of bitumen, reversal of TMBG MC IL) can be repeated (**Table 1.14**, runs 8-1 through 8-3). After the second separation, the nearly black TMBG was run over a pad of silica gel with ethyl acetate to remove the accumulated inorganic impurities. The cleaner TMBG was then converted to the TMBG MC IL, phase separated, reversed, and bitumen was introduced once more. Formation of the TMBG MC IL through introduction of CO_2 once again phase separated the bitumen (run 8-3).

1.3.11.3 Separation of SO_2 and CO_2 from gas mixtures

We have found that TMBG reacts with SO_2 in the same manner as it does with CO_2: A 2-butyl-1,1,3,3-tetramethylguanidinium methylsulfite ionic liquid (TMBG MS IL) is formed (**Fig 1.42**).
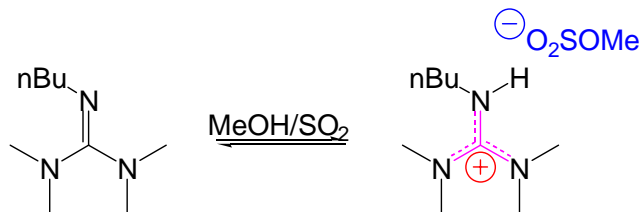
Fig 1.42: Formation of 2-butyl-1,1,3,3-tetramethylguanidinium methylsulfite (TMBG MS IL)

Examination of the IR spectra indicates formation of a sulfite (**Fig 1.43**). Absorbance of S=O stretching (1000 cm^{-1}) and S-O-C stretching (700 cm^{-1}) is observed. This is in agreement with the IR data for dimethyl sulfite, with a broad absorption peak at 1000cm^{-1} (S=O) and a peak at 700 cm^{-1} (S-O-C stretch).
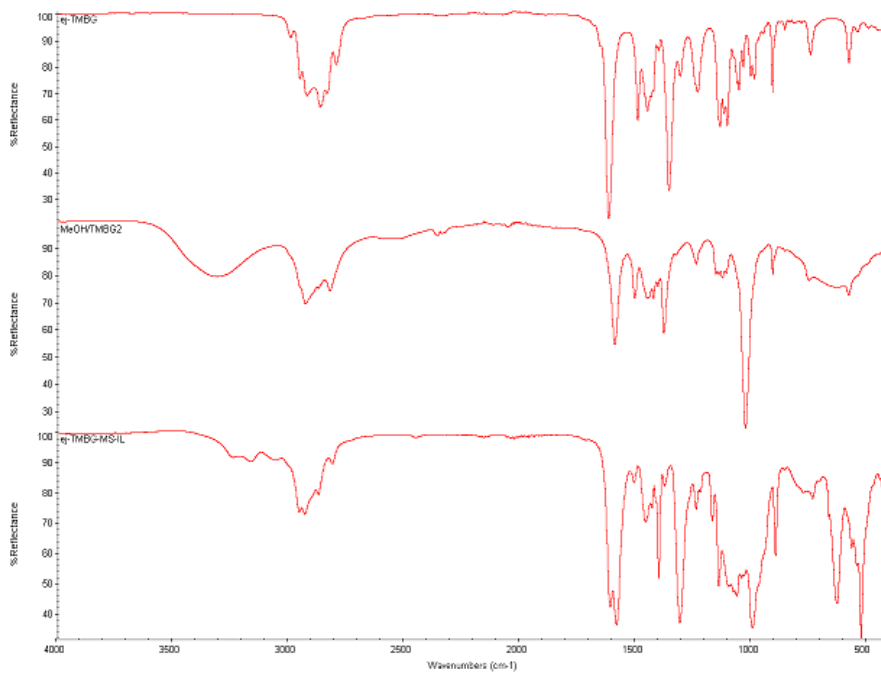
Fig 1.43: IR spectra of TMBG MS IL (bottom), compared with TMBG (top) and TMBG and MeOH (center)

49

Comparison of TMBG and methanol with TMBG MS IL show the maintenance of the C=N absorbance ($1500 cm^{-1}$). Just like TMBC MC IL, the DSC TGA thermogram indicates that TMBG MS IL is also reversible (**Fig 1.44**).
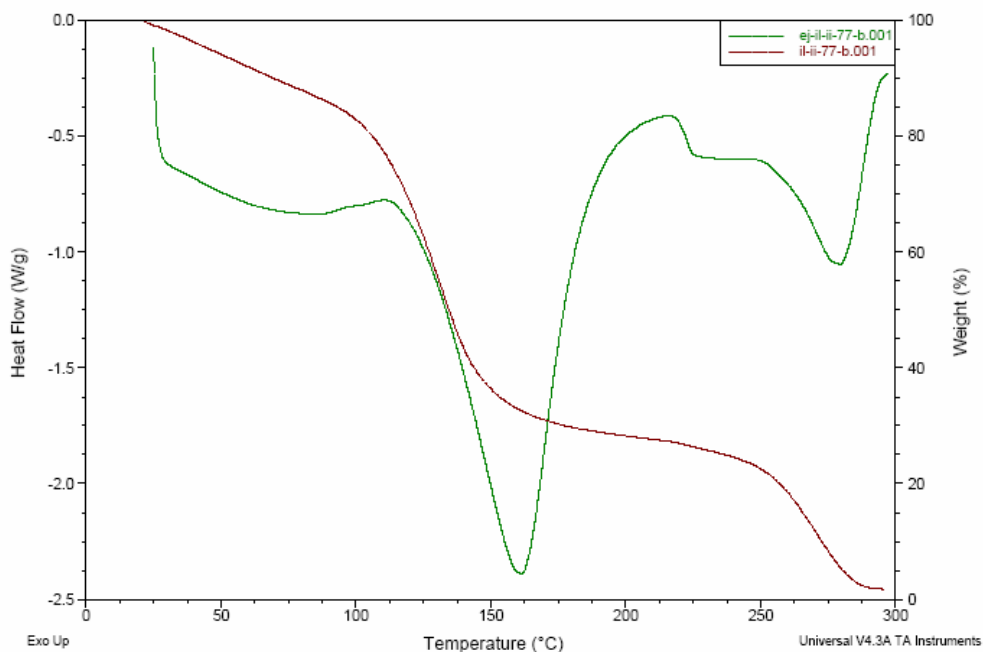
Fig 1.44: DSC-TGA of TMBG MS IL

From the DSC-TGA, TMBG MS IL begins to reverse at $100^{o}C$. In the lab, TMBG MS IL reverses after 2.5h at $160^{o}C$ or under vacuum in about one hour. More interestingly, when a 1:1 combination of TMBG MC IL and TMBG MS IL is made, they reverse at different temperatures (**Fig 1.45**).
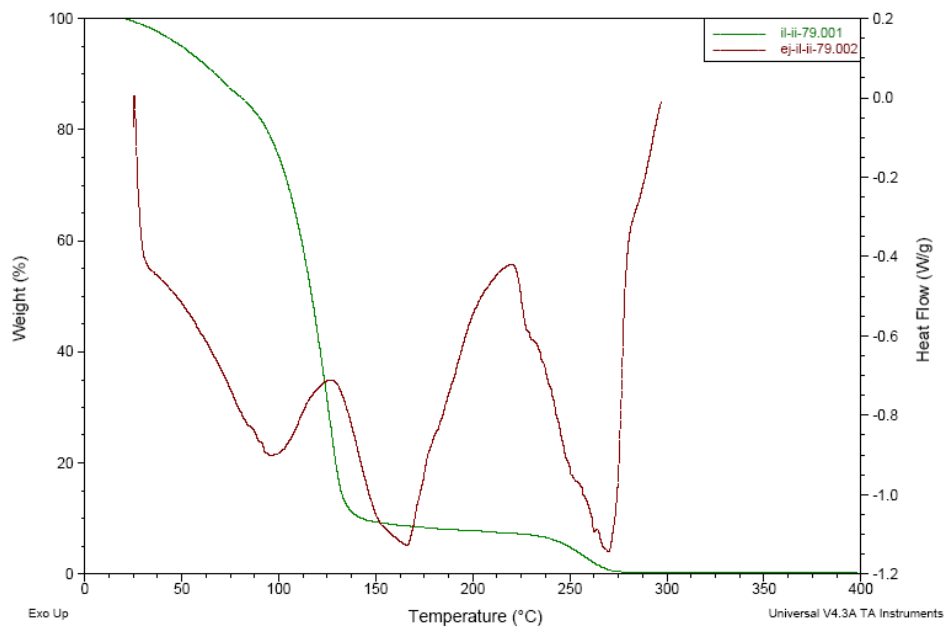
Fig 1.45: DSC-TGA of a mixture of TMBG MC IL and TMBG MS IL

As expected, the guanidinium methyl carbonate begins to reverse first at 50°C, and then the methyl sulfite begins to reverse at 120°C. At 270°C, the TMBG itself begins to degrade. This data indicates that TMBG could be a means to trap both CO_2 and SO_2. Then, by controlling the temperature, each gas could be recovered separately. This is important because there currently exists no easy/efficient means to trap and release SO_2 when necessary.[41] Furthermore, since guanidine reacts with both CO_2 and SO_2, industrial settings will not need to have two different systems to trap each gas, which is the current practice.

1.4 Conclusions

A new class of RTILs has been designed. These 2-butyl-1,1,3,3-tetramethylguanidinium alkylcarbonate RTILs are readily generated with the addition of

CO_2 and just as easily reversed to their original neutral states by the application of N_2 gas or mild heat.[42] Numerous reactions have been investigated in order to demonstrate a complete chemical process that includes reaction, separation, reformation, and recycle. Both the Claisen-Schmidt condensation of butanone and benzaldehyde and the cyanosilylation of cyclohexanone were successfully achieved, and the TMBG MC IL reversed and recycled three and two times, respectively. The reactivity of *2*-butyl-1,1,3,3-tetramethylguanidine tends to limit its applications as a solvent, but potentially new applications could be identified in the future.   For example, bitumen samples can be purified using TMBG MC IL. Upon optimization, this separation can be used to purify high-cost fuel samples. Additionally, sulfur dioxide based TMBG ILs can be generated, and separate at a different rate compared to TMBG MC IL, leading to CO_2 and SO_2 separation/sequestration opportunities.

1.5 Experimental

All chemicals were ordered from Aldrich and used a received, unless noted. NMR spectra were obtained from a Bruker DRX 500 and Varian-Mercury VX400 MHz spectrometer. NMRs of neat samples were calibrated to external $CDCl_3$ at 7.24ppm (^1H) and 77 ppm (^{13}C). GC-MS analysis was done on a HP GC 6890/ HP MS 5973. Thermal analyses studies were performed on TA instruments Differential Scanning Calorimeter (DSC) Model Q20 and Thermogravimetric Analyzer (TGA) Model Q50. Samples were heated at 5°C/ min for both DSC and TGA analyses. DSC experiments were performed in hermetically sealed pans with a pin-sized hole in the top.

Synthesis of TMBG

2-Butyl-1,1,3,3-tetramethylguanidine was synthesised by the literature procedure.[18] Tetramethylurea (0.08mol) was stirred in dry dichloroethane (80mL) for ~ 5min. Oxalyl chloride (0.18mol) was slowly added. The mixture was then heated at 60°C for 12h. Dichloroethane solvent was removed via vacuum after the mixture was cooled to RT. Dry acetonitrile (75mL) was used to dissolve the dichloride intermediate. The reaction vessel was then cooled to 0°C. Butylamine (0.16mol) was dissolved in 15mL of dry acetonitrile and the mixture was added dropwise to the dissolved dichloride intermediate. After the reaction warmed to RT, it was refluxed at 100°C for 16h. Solvent was then removed via the rotary evaporator, and the residue was treated with 30% aq NaOH (30mL). The product was then extracted with diethyl ether (3x20mL), dried with $MgSO_4$, and concentrated to give the desired product as a clear oil in 80 % yield.

2-Butyl-1,1,3,3-tetramethylguanidine: ^{1}H NMR (CDCl$_3$): 0.784 (t, 3H), 1.22 (m, 2H), 1.39 (m, 2H), 2.53 (s, 6H), 2.62 (s, 6H), 2.99 (t, 2H). ^{13}C NMR (CDCl$_3$):13.69, 20.32, 34.26, 38.39, 39.36, 48.69, 161.45. DEPT-135 (neat): up-13, 40, 42, 49; down-23, 36, 50. EA: calculated C, 59.37%; H, 11.96%; N, 20.77% N. Found: C, 59.21%; H, 12.3%; N, 21.5%

Formation of TMBG ILs

The 2-butyl-1,1,3,3-tetramethylguanidinium alkylcarbonate ionic liquids were formed by bubbling CO$_2$ into equimolar solutions of 2-butyl-1,1,3,3-tetramethylguanidine and the alcohol. The mixture was bubbled with CO$_2$ an additional 10-15 minutes after the exothermic reaction returned to room temperature, indicating full conversion of the neutral mixture to the ionic liquid.

2-butyl-1,1,3,3-tetramethylguanidinium methylcarbonate: ^{1}H NMR (neat): 1.12 (t, 3H), 1.51 (m, 2H), 1.78 (m, 2H), 3.1 (s, 12H), 3.38(t, 2H), 3.45 (s, 3H). ^{13}C NMR (neat): 14.35, 21.05, 33.48, 40, 46.59, 49.12, 51.79, 158.15, 161.16. DEPT-135 (neat): up-13, 39, 49, 51; down-20, 33, 46. EA: Theory 53.42 % C, 10.19% H, 16.99% N. Found 54.64% C, 11.1% H, 17.53% N.

2-butyl-1,1,3,3-tetramethylguanidinium butylcarbonate: ^{1}H NMR (neat): 1.11 (br s, 7H), 1.54 (m, 5H), 1.66 (m, 2H),1.8 (m, 2H), 3.1 (s, 12H), 3.39(t, 1H), 3.66 (m, 1H), 3.96 (s, 1H). ^{13}C NMR (neat): 13.6, 13.85, 19.16, 19.93, 32.39, 35.38, 39.27, 45.15, 60.65, 63.35, 157.22, 161.22

2-butyl-1,1,3,3-tetramethylguanidinium hexylcarbonate: ^{1}H NMR (neat): 1.03 (br s, 11H), 1.44 (br s, 14H), 1.62 (m, 4H), 1.77 (m, 2H), 3.15 (s, 12H), 3.33(t, 2H), 3.62 (m,

3H), 3.92 (s, 1H). ^{13}C NMR (neat): 13.83, 14.10, 20.16, 22.93, 26.07, 32.16, 33.36, 39.63, 61.38, 157.91, 161.81

2-butyl-1,1,3,3-tetramethylguanidinium octylcarbonate: ^{1}H NMR (neat): 1.1 (t, 6H), 1.46 (br s, 12H), 1.65 (m, 2H), 1.75 (m, 2H), 3.08 (s, 12H), 3.33(t, 2H), 3.62 (m, 1H), 3.92 (s, 1H). ^{13}C NMR (neat): 13.9, 14.09, 20.3, 22.84, 26.45, 29.65, 29.72, 30.54, 32.13, 32.97, 39.46, 46.04, 61.27, 63.95, 157, 160.9

2-butyl-1,1,3,3-tetramethylguanidinium dodecylcarbonate: ^{1}H NMR (neat): 1.1 (t, 7H), 1.49 (br s, 20H), 1.68 (m, 2H), 1.77 (m, 2H), 3.1 (s, 12H), 3.35(t, 2H), 3.65 (m, 1H), 3.95 (s, 1H). ^{13}C NMR (neat): 14.32, 14.49, 20.7, 23.25, 27.11, 30.03, 30.35, 32.55, 33.42, 39.85, 46.5, 61.69, 64.30, 157.74, 161.15

2-butyl-1,1,3,3-tetramethylguanidinium bicarbonate: ^{1}H NMR (neat): 0.84 (t, 3H), 1.26 (m, 2H), 1.4 (m, 2H), 2.67 (s, 12H), 3.02 (t, 2H), 3.38 (br s, 2H). ^{13}C NMR (neat): 13.67, 19.50, 31.46, 39.28, 44.26, 158, 160.62.

Nile Red Measurements

Polarity was measured using Nile Red dye on a Hewlet Packard 8453 UV-Vis system. Samples were measured at three different concentrations, three times each, for a total of nine measurements per sample.

Reversal of IL using vacuum

TMBG MC IL (1g) was dissolved in chloroform (10mL) and rotovapped for 1 hour. NMR indicated reversal to TMBG (methanol had evaporated).

Melting Points

Melting Points of TMBG salts were found as follows: A round bottomed flask was filled with ^{i}PrOH. In the flask was a thermometer and an NMR tube. In the NMR tube was freshly formed ionic liquid, which was sealed with an NMR septum and covered with parafilm. The flask was then cooled with a dry ice/acetone bath, and then allowed to warm up until the ionic liquid melted. The cool-heat cycle was performed three times for each sample.

Conductivity study

Conductivity was measured using a ThermoOrion Model 115 Meter. An equimolar solution of *2*-butyl-1,1,3,3-tetramethylguanidine and methanol (5.56 mmol) was dissolved in 4mL of deuterated chloroform. CO_2 was then slowly bubbled into the solution and measurements were taken until they no longer changed. After formation of the ionic species, the solution was heated and conductivity measurements were again taken until they no longer changed, indicating the reversal of the ionic species and reformation of the neutral species. Background measurements of solvents were substracted from acquired data. Procedure was repeated for three cycles. Cell constant = 1.

Water content

Water content was measured by injecting 1mL of solution into a Mettler Toledo DL31 Karl Fischer titrator.

<u>Miscibility studies</u>

Mixtures of solvent (3.5-5.84 mol) and TMBG (1.75-2.92 mol) were stirred together for ~15min. They were observed for miscibility. Then, methanol and CO_2 were added to the samples to form TMBG MC IL and left overnight. If the solvent phase separated, both phases were analyzed with GC-MS and NMR (^{1}H).

<u>Modifications to structure</u>

2-[1-hydroxyethyl]-1,1,3,3-tetramethyl guanidine: The same reaction conditions were used as for the synthesis of TMBG, with several exceptions: 1) 0.12mol of monoethanolamine was added dropwise to the dichloride in a mixture of Et_3N (23mL) and acetonitrile. 2)In the work-up, an acid-base work-up was utilized: 5% HCl (20mL) was added to the mixture, and extracted with CH_2Cl_2 (3x15mL). Residue from the organic extraction was then dissolved in water and basified using 30%NaOH (30mL). The organics were extracted with CH_2Cl_2 (3x15mL) to yield a yellow solid. Recrystallization gave the desired solid product in 78% yield; decomposition point 171°C; ^{1}H (CDCl$_3$): 1.09 (t, 2H), 2.27 (1H), 2.73-2.78 (m, 14H). ^{13}C (CDCl$_3$): 35.98, 44.51, 45.59, 59, 159.

2-[trimethylsiloxyethyl]-1,1,3,3-tetramethyl guanidine: The same reaction conditions were used as for the synthesis of TMBG, with an exception: 1) 0.12mol of 1-trimethylsiloxyethyl-2-amine was added dropwise to the dichloride in a mixture of Et_3N (23mL) and acetonitrile.83% yield as light yellow oil. ^{1}H NMR(d$_6$-DMSO): 0.03 (s, 9H),

2.75 (s, 4H), 2.78 (s, 8H), 3.58 (t, 2H), 4.18 (t, 2H) . ^{13}C NMR (d$_6$-DMSO): 1.5,38, 39, 52, 67, 161.

1-trimethylsiloxyethy1-2-amine:[43] To 0.5mol ethanolamine, 0.28mol of hexamethyldisilizane was slowly added via dropping funnel. One drop of Me$_3$SiCl was added and the mixture was heated to 130°C for 2h. Distillation under vacuum gave the liquid product in 78% yield. ^{1}H NMR(d$_6$-DMSO): 0.06 (s, 9H), 2,59 (t, 2H), 3.46 (t, 2H). ^{13}C NMR (d$_6$-DMSO): -0.66, 43.89, 64.63.

2-[1trimethylsilylmethyl]-1,1,3,3-tetramethyl guanidine: The same reaction conditions were used as for the synthesis of TMBG, except that 1-trimethylsilylmethyl amine was added to the dichloride intermediate. 38% yield as a light yellow oil. ^{1}H NMR(CDCl$_3$): -0.07 (s, 9H), 2.57 (s, 6H), 2.65 (s, 6H), 2.69 (s, 2H). ^{13}C NMR (CDCl$_3$): -2.48, 38.78, 39.63 40.81, 159.23.

2-[trimethylsilanylmethyl]-1,1,3,3- tetramethylguanidinium methylcarbonate: CO$_2$ was bubbled through an equimolar mixture of 2-[1trimethylsilylmethyl]-1,1,3,3-tetramethyl guanidine and methanol to yield solid at room temperature (mp= 36°C) ^{1}H NMR(d$_6$-DMSO): -0.02 (s, 9H), 2.69 (s, 12H), 3.15 (s, 2H).

Base-catalyzed reactions

Reagents were mixed as earlier described in TMBG. After the reaction ran to completion, hexane (or another non-polar alkane) and methanol were added. Next, CO$_2$ was bubbled into the mixture to cause the formation of two separate phases: hexane/product and TMBG MC IL. Each phase was analyzed by GC-MS to quantify the concentrations of reactants and products. Standard calibration curves of all starting

materials and most of the products were prepared. If the reaction was recycled, the desired products were isolated, characterized by NMR and compared to literature values. The TMBG MC IL was then reversed, more reagent was added, and the reaction started again.

1-phenyl-pent-1-en-3-one[44]: ^{1}H NMR: (CDCl$_3$): 1.16 (3H, t), 2.7 (2H, q), 6.7 (1H, d), 7.37-7.4 (3H, m), 7.5-7.6 (3H, m)

4-phenyl-3-methyl-3-buten-2-one[45, 46]: 66.5mL acetic acid was added to a round-bottomed flask over ice. 13.5mL 37wt% HCl was then added. Next, 7.88mL benzaldehyde was added. Finally, 13.95mL 2-butanone was added to the mixture and it was stirred until it returned to room temperature, and then for 36 more hours. The solution was neutralized with 125mL 10M NaOH after the addition of 50mL H$_2$O. The organics were separated with diethyl ether, washed again with 10 wt% NaHCO$_3$, and dried over MgSO$_4$ to give the desired product in 95% yield. [1]H(d$_6$-DMSO): 1.87 (d, 3H), 2.37 (s, 3H), 7.3-7.45 (m, 4H), 7.59 (s, 1H).

1-trimethylsilyloxy-1-cyclohexanecarbonitrile. [1]H (d$_6$-DMSO): 0.2 (s, 9H), 1.48-1.7 (m, 8H), 1.9 (m, 2H). [13]C (d$_6$-DMSO): 1.4, 22.4, 23.8, 38.6, 70.5, 121.

TMBG/TMS-CN salt: [1]H (d$_6$-DMSO): 0.1 (s, 9H), 0.82 (t, 3H), 0.98 (m, 2H), 1.25 (m, 2H), 2.8 (s, 12H). [13]C (d$_6$-DMSO): 1.1, 13.9, 18.8, 19.7, 31.7, 39.1, 123.4, 161.3.

3[bis(methoxycarbonyl)methyl]cyclohexanone. [1]H (CDCl$_3$): 1.4-1.55 (m, 1H), 1.65-1.8 (m, 2H), 1.9-2.0 (m, 1H), 2-2.15 (m, 1H), 2.3-2.55 (m, 5H), 3.3 (d, 1H), 3.75 (s, 6H).

3-(N-phenylamino)-1,3-diphenyl-1-acetone. ^{1}H (CDCl$_3$): 3.46 (d, 1H), 3.49 (d, 1H), 5.02 (m, 1H), 6.57 (d, 2H), 6.67 (m, 1H), 7.05 (m, 2H), 7.25 (d, 1H), 7.3-7.34 (m, 2H), 7.78-7.59 (m, 5H), 7.92 (d, 2H).

Separation of alkanes from tar sands/shale

Mixtures of TMBG and either crude oil or bitumen were stirred together. Addition of CO_2 into the mixture caused the formation of two separate phases: crude oil and TMBG MC IL. Each phase was analyzed by GC-MS or NMR for purity.

Bitumen before treatment with TMBG MC IL: ^{1}H NMR (CDCl$_3$): 0.87 (m), 1.26 (m). ^{13}C NMR (CDCl$_3$): 14.29, 22.83, 29.82

Bitumen after treatment with TMBG MC IL (TMBG peaks withheld for clarity): ^{1}H NMR (CDCl$_3$): 0.1 (s), 1.17 (s), 4.15 (p), 7.45 (m), 7.65 (m). 13C NMR (CDCl$_3$): 12.56, 23.47, 24.32, 29.51, 30.83, 30.97, 67.88, 129.43, 132.34, 132.83, 158.15, 165.43, 167.71, 206.

Separation of SO$_2$ and CO$_2$ from gas mixtures

Generation of TMBG MS IL

SO_2 was bubbled to equimolar solutions of TMBG and methanol to form TMBG MS IL. The mixture was bubbled with SO_2 an additional 10-15 minutes after the exothermic reaction returned to room temperature, indicating full conversion of the neutral mixture to the ionic liquid.

2-butyl-1,1,3,3-tetramethylguanidinium methylsulfite: ^{1}H NMR (neat): 1.19 (t, 3H), 1.63 (m, 2H), 1.9 (m, 2H), 3.30 (s, 12H), 3.49 (s, 6H). ^{13}C NMR (neat): 13.88, 20.04, 32.0, 39.84, 44.83, 46.53, 161.79

1.6 References Cited

1.   Launay, J.P. and C. Coudret, *Chemical Approaches of Molecular Switches* Annals of the New York Academy of Sciences, 1998(852): p. 116-132.

2.   Mendes, P.M., A.H. Flood, and J.F. Stoddart, *Nanoelectronic devices from self-organized molecular switches* Applied Physics A: Materials Science & Processing, 2005. **80**: p. 1197-1209.

3.   Jessop, P.G., et al., *A Reversible Ionic/Non-Ionic Switchable Solvent.* Nature, 2005. **436**: p. 1102.

4.   Gathergood, N., P.J. Scammells, and M.T. Garcia, *Biodegradeable ionic liquids Part III. The first readily biodegradeable ionic liquids.* Green chemistry, 2006. **8**: p. 156-160.

5.   M. T. Garcia, N. Gathergood, and, P.J. Scammells, *Biodegradeable ionic liquids Part II. Effect of the anion and toxicology.* Green chemistry, 2005. **7**: p. 9-14.

6.   K. M. Docherty, S. Z. Hebbeler, and C. F. Kulpa, Jr, *An assessment of ionic liquid mutagenicity using the Ames Test.* Green chemistry, 2006. **8**: p. 560-567.

7.   Nuno M. M. Mateus, et al., *Synthesis and properties of tetra-alkyl-dimethylguanidinium salts as a potential new generation of ionic liquids.* Green chemistry, 2003. **5**.

8.   Y. Gao, et al., *Guanidium-Based Ionic Liquids.* Inorg Chem., 2005. **44**: p. 1704-1712.

9.   P. Wang, et al., *Novel room temperature ionic liquids of hexaalkyl substituted guanidinium salts for dye-sensitized solar cells.* Applied Physics A: Materials Science & Processing, 2004. **79**: p. 73-77.

10.   H. Xie, S. Zhang, and H. Duan, *An ionic liquid based on a cyclic guanidinium cation is an efficient medium for the selective oxidation of benzyl alcohols.* Tet. Lett, 2004. **45**: p. 2013.

11.   T. Jiang, et al., *Ionic liquid catalyzed Henry reactions.* Tet. Lett, 2004. **45**: p. 2699-2701.

12.   A. Zhu, et al., *Direct aldol reactions catalyzed by 1,1,3,3-tetramethylguanidine lactate without solvent.* Green chemistry, 2005. **7**: p. 514-517.

13. A. Zhu, et al., *Study on guanidine-based task-specific ionic liquids as catalysts for direct aldol reactions without solvent.* New Journal of Chemistry, 2006. **30**: p. 736-740.

14. J. Huang, et al., *Pd Nanoparticles Immobilized on Molecular Sieves by Ionic Liquids: Heterogeneous Catalysts for Solvent-Free Hydrogenation.* Angewandte Chemie, Int Ed, 2004. **43**: p. 1397-1399.

15. Li, S., Lin, Y., Xie, H., Zhang, S., Xu, J. , *Guanidine Acid-Base Ionic Liquids: Novel Reaction Media for the Palladium-Catalyzed Heck Reaction* Org Lett, 2006: p. 391-394.

16. Akine, S.T., T; Dong, WK; Nabeshima, T, *Oxime-Based Salen-Type Tetradentate Ligands with High Stability against Imine Metathesis Reacation.* Inorg Chem., 2005: p. 1704.

17. Schuchardt , U., Vargas R.M.; Gelbard G., *Alkylguanidines as catalysts for the transesterification of rapeseed oil* Journal of Molecular Catalysis A: Chemical, 1995. **99**(2): p. 65-70.

18. Costa, M., et al., *Superbase catalysis of oxazolidin-2-one ring formation from carbon dioxide and prop-2-yn-1-amines under homogeneous or heterogenous conditions.* Journal of the Chemical Society-Perkin Transactions 1, 1998(9): p. 1541-1546.

19. L. Crowhurst, et al., *Sovent-solute interactions in ionic liquids.* Phys. Chem. Chem. Phys., 2003. **5**: p. 2790-2794.

20. Wataru Ogihara, T.A., Hiroyuki Ohno, *Polarity Measurement for Ionic Liquids Containing Dissociable Protons.* Chemistry Letters, 2004. **33**(11): p. 1414

21. Carmichael, A.J., & Seddon, Kenneth, R., *Polarity Study of Some 1-Alkyl-3-Methylimidazolium Ambient-Temperature Ionic Liquids with the Solvatochromic Dye, Nile Red.* J. Phys. Org. Chem., 2000. **13**: p. 591-595

22. Deye, J.F. and T.A. Berger, *Nile Red as a Solvatochromic Dye for Measuring Solvent Strength in Normal Liquids and Mixtures of Normal Liquids with Supercritical and Near Critical Fluids.* Anal. Chem., 1990. **62**: p. 615-622.

23. Shirota, H. and E.W. Castner, Jr., *Why Are Viscosities Lower for Ionic Liquids with -CH2Si(CH3)3 vs -CH2C(CH3)3 Substitutions on the Imidazolium Cations?* J. Phys. Chem. B., 2005. **109**(46): p. 21576.

24. Crosthwaite, J.M., et al., *Phase transition and decomposition temperatures, heat capacities and viscosities of pyridinium ionic liquids.* The Journal of Chemical Thermodynamics, 2005. **37**(6): p. 559-568.

25.	Carey, F.A. and R.J. Sunberg, *Advanced Organic Chemistry, Part B: Reactions and Synthesis*. 3rd ed ed. 1990, New York, NY: Plenum Press.

26.	S. Nolen, et al., *The catalytic opportunities of near-critical water: a benign medium for conventionally acid and base catalyzed condensations in organic synthesis.* Green chemistry, 2003. **5**: p. 663-669.

27.	M. Stiles, D. Wolf, and G. Hudson, *Catalyst Selectivity in the Reactions of unsymmetrical Ketones; Reaction of butanone with benzaldehyde and p-nitrobenzaldehyde*. JACS, 1959. **81**: p. 628-632.

28.	Toshio Isobe, K.F., and Tsutomu Ishikawa, *Modified Guanidines as Potential Chiral Superbases. 1. Preparation of 1,3-Disubstituted 2-Iminoimidazolidines and the Related Guanidines through Chloroamidine Derivatives,* Journal of Organic Chemistry, 2000. **65**(23): p. 7770 - 7773.

29.	Shane A. Nolen, et al., *The catalytic opportunities of near-critical water: a benign medium for conventionally acid and base catalyzed condensations for organic synthesis.* Green chemistry, 2003. **5**: p. 663-669.

30.	L. Wang, X.H., J. Jiang, X. Liu, X. Feng, *Catalytic cyanosilylation of ketones using organic catalyst 1,1,3,3-tetramethylguanidine.* Tetrahedron Letters, 2006. **47**: p. 1581-1584.

31.	T. Kumamoto, K.E., M. Endo, Y. Araki, Y. Fushimi, I. Miyamoto, T. Ishikawa, T. Isobe, K. Fukuda, *Guanidine-Catalyzed Asymmetric Addition Reactions: Michael Reactio nof Cyclopentenone with Dibenzyl Malonates and Epoxidation of Chalcone.* Heterocycles, 2005. **65**: p. 347-359.

32.	J. Shen, et al., *Chiral Bicyclic Guanidine-Catalyzed Enantioselective Reactions of Anthrones.* JACS, 2006. **128**: p. 13692-13693.

33.	W. Ye, et al., *1,5,7-triazabicyclo[4.4.0]dec-5-ene (TBD) catalyzed Michael reactions.* Tet. Lett, 2005. **46**: p. 6875-6878.

34.	Mohamed Zahouily, et al., *Natural Phosphate Modified with Sodium Nitrate: New Efficient Catalyst for the Construction of a Carbon-Sulfur and Carbon-Nitrogen Bonds* Letters in Organic Chemistry, 2005. **2**(4): p. 354-359.

35.	Nan Jiang, A.J.R., *Environmentally friendly synthesis of biaryls: Suzuki reaction of aryl bromides in water at low catalyst loadings.* Tet. Lett, 2006. **47**(2): p. 197-200.

36.   Chanthavong, F. and N. Leadbeater, *The application of organic bases in microwave-promoted Suzuki coupling reactions in water.* Tet. Lett, 2006. **47**: p. 1909-1912.

37.   Haibo Xie, S.Z., and Haifeng Duan, *An ionic liquid based on a cyclic guanidinium cation is an efficient medium for the selective oxidation of benzyl alcohols.* Tet. Lett, 2004. **45**(9): p. 2013-2015.

38.   L., P.F., *Supercritical tar sand extraction*, U.P. Office, Editor. 1980, Phillips Petroleum Company (Bartlesville, OK) USA.

39.   N., H.P., *Oil shale extraction process*, U.S. Patent, Editor. 1984, Union Oil Company of California (Los Angeles, CA) US.

40.   ConocoPhillips, *MSDS for bitumen sample (general).* 2007.

41.   Jun Huang, A.R., Peter Wasserscheid, Rasmus Fehrmann, *Reversible physical absorption of SO2 by ionic liquids.* Chemical Communications, 2006: p. 4027-4029.

42.   Lam Phan, D.C., David J. Heldebrant, Hillary Huttenhower, Ejae John, Xiaowang Li, Pamela Pollet, Ruiyao Wang, Charles A. Eckert, Charles L. Liotta, and Philip G. Jessop *Switchable Solvents Consisting of Amidine/Alcohol or Guanidine/Alcohol Mixtures.* I & EC Research, 2007: p. submitted.

43.   Mormann, W.L., Gabriele, *A simple and versatile synthesis of trimethylsiloxy-substituted isocyanates.* Synthesis, 1988 **12**: p. 990-2.

44.   Phillip Peac, D.J.C., Jennefer A. Kenny, Inderjit Mann, Ian Houson, Lynne Campbell, Tim Walsgrove, Martin Wills, *Asymmetric transfer hydrogenation of alpha,beta-unsaturated, alpha-tosyl and alpha-substituted ketones.* Tetrahedron, 2006. **62**: p. 1864-1876.

45.   Y. Kawai, K.S., K. HIda, D.H. Dao, A. Ohno *Sterochemical Control in Microbial Reduction XXVIII. Asymmetric Reduction of alpha-beta-Unsaturated Ketones with Bakers' Yeast.* Bull. Chem. Soc. Jpn, 1996. **69**: p. 2633-2638.

46.   Nolan, S.A., *Environmentally Benign Chemical Processing Using Supercritical Carbon Dioxide and Near-Critical Water*, in *School of Chemical Engineering.* 2001, Georgia Institute of Technology: Atlanta.

CHAPTER 2
PIPERYLENE SULFONE

2.1 Introduction

Solvents are vital to many industrial reaction processes. They affect reaction rates, chemical equilibria, the efficiency of heat and mass transfer, and facilitate intimate contact between mutually insoluble reactants. The literature is filled with reports of the development of novel solvents. These include ionic liquids,[1, 2] supercritical fluids,[3-6] gas-expanded liquids,[7-11] and perfluorinated solvents.[12-15] The choice of the right solvent is critical not only for a successful chemical transformation but also for the subsequent separation and purification processes.[16] The reactions of organic substrates with inorganic salts are particularly challenging because they traditionally need either a dipolar, aprotic solvent or a biphasic mixture of solvents combined with a phase transfer catalyst.[17] The latter is undesirable because the phase transfer catalysts are expensive and difficult to separate and recycle.[5, 11] The former option, dipolar, aprotic solvents, is expensive (in terms of money and energy) because such solvents are very difficult to remove by distillation. In addition, it is rarely practical to recycle and reuse such solvents. The pharmaceutical industry has emphasized the need for a dipolar, aprotic replacement for DMSO.[18]

We designed a separable and recyclable polar, aprotic solvent, piperylene sulfone (PS), which combines the excellent reaction medium properties of dipolar, aprotic solvents with the "volatility" of low boiling solvents necessary for facile isolation and purification of products. While piperylene sulfone is not volatile itself, it is readily converted (or "switched") into volatile species (**Fig 2.1**).

m.p. = −12 °C   b.p. = 42 °C   -10 °C
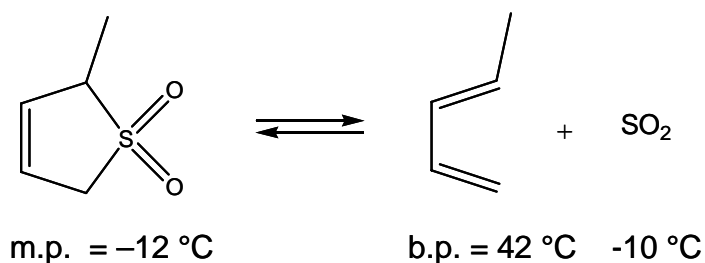
Fig 2.1: Degradation of piperylene sulfone

These volatile species can be collected elsewhere and recombined back into piperylene sulfone for re-use, making it an example of a switchable solvent.[7-11, 19] The utility of piperylene sulfone is demonstrated by showing that the rates of nucleophilic substitution reactions in piperylene sulfone are comparable to the rates of the same reactions in DMSO.

2.2 Background

2.2.1 The disadvantages of DMSO

DMSO is commonly used in reactions where the reactants include organic compounds and inorganic salts. After the reaction has run to completion, the reaction mixture is poured into water (or an aqueous phase), and the product precipitates or is extracted with an organic solvent. This procedure is both time and energy consuming, and produces large amounts of contaminated aqueous waste. Furthermore, the product is often contaminated with trace amounts of DMSO after work-up. Because of the high boiling point of DMSO (189°C), complete removal of the DMSO is difficult. It would be optimal to have a solvent that is comparable to DMSO in terms of solubility of substrates

(organic and inorganics), but has a straightforward means for the separation of products and recovery of solvent.

2.2.2 Retrocheletropic reactions

Literature review provided the melting points (**Fig 2.2**) and the rate of decomposition (**Fig 2.3**) of several interesting methyl-substituted sulfolenes. For example, sulfolene and 3-methylsulfolene melt around 64°C, while the disubstituted 3,4-methylsulfolene melts at 135°C. Piperylene sulfone stands out as it is liquid at room temperature; in fact its melting point is -12°C. Several substituted sulfolene are shown in **Figure 2.2**.[20]
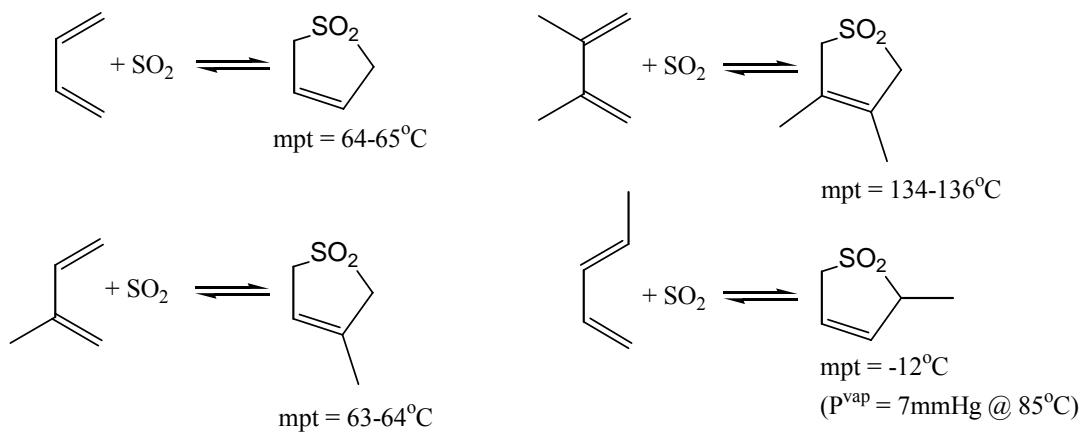
Fig 2.2: Melting Points of methyl-substituted Sulfolenes

The decomposition rates of butadiene sulfone, piperylene sulfone, and isoprene sulfone were also obtained from the literature (**Fig 2.3**).[21]
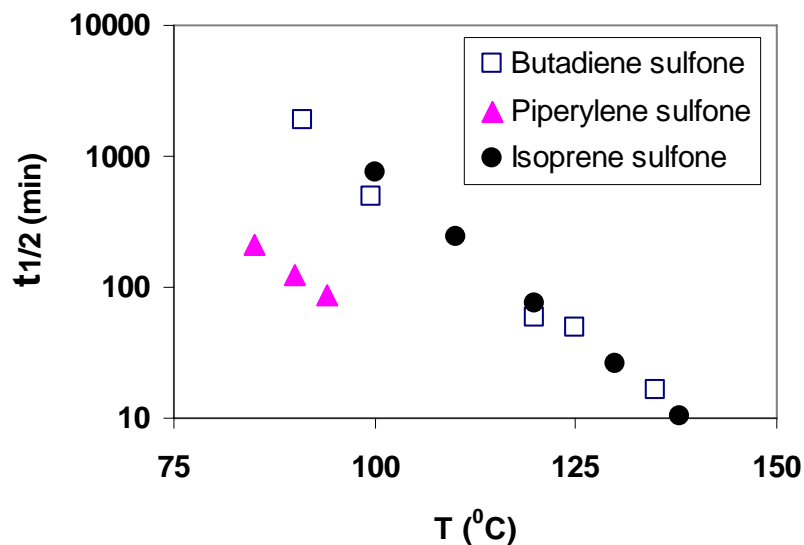
Fig 2.3: Decomposition Rates of Sulfolenes

The decomposition of PS occurs at lower temperature ($<100^{\circ}$C) compared to butadiene sulfone and isoprene sulfone ($\sim 140^{\circ}$C). Furthermore, when the decomposition rates are compared around the same temperature ($\sim 100^{\circ}$C), PS decomposes an order of magnitude faster than butadiene sulfone and isoprene sulfone. The melting point of PS and its decomposition rate led us to believe that PS could potentially be a labile DMSO replacement.

2.2.3 Piperylene sulfone

Piperylene sulfone (2,5-dihydro-2-methylthiophene-1-dioxide) is well known in the literature.[21-25] It is formed by the cheletropic reaction between piperylene and sulfur dioxide in the presence of phenyl-β-naphthylamine, which represses polymer formation (**Fig 2.4**).[24, 25]
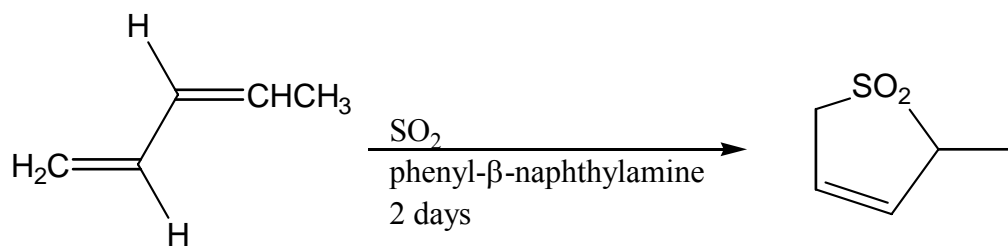
Fig 2.4: Synthesis of PS

In principal, both isomers of piperylene—cis and trans—can react with SO$_2$ to form PS, but the trans isomer primarily forms PS.[24]   When PS is decomposed via a retro-cheletropic reaction, only trans-piperylene and SO$_2$ are generated (**Fig 2.5**).[24]
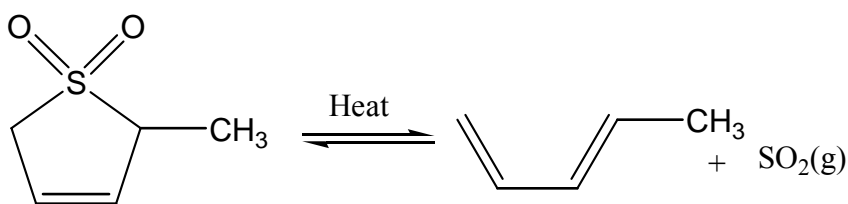
Fig 2.5: Decomposition of PS to generate SO$_2$ and trans-piperylene

2.3 Results and Discussion

2.3.1 Synthesis of PS

PS was synthesized by a modified method described by Grummitt *et al.* (**Fig 2.4**).[26]   The polymerization inhibitor N-phenyl-2-napthylamine was added to a steel bomb. The closed bomb was then briefly flushed with SO$_2$. Piperylene (mixture of cis and trans) was subsequently introduced to the bomb. Finally, the bomb was filled with SO$_2$ and stirred for two days at room temperature. After two days, the pressure was

slowly released and a thick orange oil was removed. This oil was then extracted with water three times. The aqueous phase was then back extracted with chloroform three times, and the organic phases were combined and dried and concentrated. PS was characterized via NMR (^{1}H and ^{13}C), and yield is based on amount of piperylene (mixture of cis and trans) used initially (**Table 2.1**). The piperylene was usually a mixture of 59-75% trans isomer and 21-41% cis isomer, but the ratio varies greatly from batch to batch.

Table 2.1: Synthesis of PS

	mol piperylene	mol inhibitor	vessel	yd(%)
1	0.25	0.0047	bomb	21.61
2	0.502	0.025	glass	20.77
3	0.25	0.0125	glass	28.14
4	0.25	0.0125	glass	39.34
5	0.25	0.0125	bomb	34.38
6	0.25	0.0125	glass	39.34

In our first attempt (**Table 2.1**, run 1), when the vessel was opened, the reaction mixture was very viscous and slimy, indicating a high amount of polymer formation. Thus, we increased the amount of inhibitor to 5 mol %. When the amount of initiator was initially doubled, we also moved to using the glass pressure vessel and doubled the amount of piperylene that was used (run 2). When the glass vessel was used for the synthesis of PS, it was shaken vigorously for two days at room temperature, but the work-up remained the same. At a ratio of 0.35 mol of piperylene and 0.0125 mol of inhibitor, the isolated yields were consistent at 35-40 % (runs 4-6).

2.3.2 Piperylene Sulfone as a DMSO replacement

The solvatochromic parameters (π^*,[27] α,[28] and β,[29] $E_T(30)$[30]) and the dielectric constant[31] of PS were measured since they are commonly used to compare solvent properties. The π^* parameter provides a comprehensive measure of the ability of a solvent to stabilize a solute molecule based on the local polarity of the solvent. It is a quantitative index of solvent dipolarity and polarizability.[32] The acidity α for a solvent is a measure of its strength as a hydrogen bond donor (HBD) - the ability to donate a proton in a solvent-to-solute hydrogen bond. The estimation of α is based on the experimental determination of π^* and $E_T(30)$. The $E_T(30)$ scale, developed by Reichardt *et al*., indicates solvent strength by combining polarity and HBD acidity, which itself serves as a useful solvent parameter for physicochemical correlations for a wide range of solvents.[30] The basicity parameter β denotes the solvent's hydrogen bond acidity (HBA) or an index of the solvent's ability to accept a proton in a solute-to-solvent hydrogen bond.

When compared to DMSO, the solvatochromic parameters and the dielectric constant indicate that piperylene sulfone is a dipolar aprotic solvent similar to DMSO. These values, along with other pertinent physical constants (boiling point, melting point, dipole moment) are summarized below (**Table 2.2**).

Table 2.2: Solvatochromic values and physical constants of PS and DMSO

Parameters	DMSO	Piperylene sulfone
Boiling point (^{o}C)	51 (7 Torr)	85 (7 Torr)
Melting point (^{o}C)	16-19	-12
Dipole moment (D)	4.27	5.32
α	0	0
β	0.76	0.46
$\pi*$	1.00	0.87
$E_T 30$ (KJ/mol)	189.0	189.0
ε	46.7	42.6

The only significant difference between the two solvents is the β-value, which indicates that DMSO is better than piperylene sulfone as a hydrogen bond acceptor.

2.3.3 Piperylene Sulfone as a Solvent for Chemical Processes

To demonstrate that piperylene sulfone can serve as a solvent for chemical processes, the new solvent has been tested as a medium for anionic nucleophilic substitution reactions. The rates of reaction of benzyl chloride with a variety of anionic nucleophiles were studied in both piperylene sulfone and DMSO at 40ºC (**Fig 2.6, Table 2.3**).
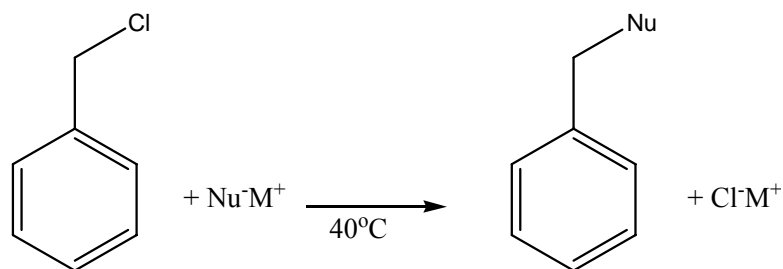
Fig 2.6: Anionic nucleophilic substitution reactions

In these reactions, 0.18 mmol of anionic nucleophile was added to 1.5mL of solvent (most of the reactions were run heterogeneously) and warmed to 40°C. 0.9 mmol of benzyl chloride was then added and stirred until the reaction was completed. In order to follow the rate of reaction, aliquots were taken every ten minutes over a period of one hour. After quenching with toluene, conversion was determined by GC-MS. NMR was used to characterize products. NMR experiments were used in the reactions with potassium thioacetate (KTA) and sodium pyrrolidinedithiocarbamate (NaPDTC) for kinetic measurements. In the NMR experiments, readings were taken every 30 seconds over a period of ten minutes.

Table 2.3: Rates of anionic nucleophilic substitution reactions
2nd Order Rate Constant k x10^1 (mL mol^{-1} sec^{-1})^a

Nucleophile	DMSO	DMSO (3% H$_2$O)	Piperylene Sulfone	Piperylene Sulfone (1% H$_2$O)
KTA[b]	> 1800	> 1800	> 1800	> 1800
NaPDTC[c]	> 1800	> 1800	> 1800	> 1800
KSCN	1.4 (± 0.1)	1.7 (± 0.1)	2.1 (± 0.1)	2.3 (± 0.2)
KOAc	3.4 (± 0.1)	11.0 (± 0.1)	0.013 (± 0.004)	0.19 (± 0.01)
KCN	5.8 (± 0.8)	17 (± 5)	--d	0.15 (± 0.01)
CsN$_3$	69 (± 1)	16.7 (± 0.9)	2.4 (± 0.9)	5.8 (± 0.9)
CsOAc	22.7 (± 0.6)	16.4 (± 0.2)	0.35 (± 0.04)	0.35 (± 0.06)

^{a} Only the rate constants for piperylene sulfone containing 1 wt% water are presented since the rates of reaction changed by only a factor of two for the entire water range studied. ^{b} KTA is potassium thioacetate. ^{c} NaPDTC is sodium pyrrolidinedithiocarbamate. ^{d} No reaction.

Even though the rates were comparable in both solvents, it was found that the presence of minimal amounts of water (as low as 0.1 wt%) dramatically affected the reaction rates (regardless of the solvent). It was discovered that traces of water added to the piperylene sulfone enhanced the rate of reaction. Indeed, no reaction was observed with potassium cyanide in dry piperylene sulfone (see **Table 2.3**). Only in the presence of a trace of water (0.1 wt%) did the reaction take place. In DMSO the reaction occurs much more slowly in the absence of water (58 vs. 170 x 10^{-1} mL mol^{-1} sec^{-1}). As a consequence, studies were conducted in dry DMSO, DMSO containing 3 wt% water, dry piperylene sulfone, and piperylene sulfone containing from 0.1 to 10 wt% water. It is

conjectured that, as in the case of solid-liquid phase transfer catalysis, small quantities of water enhance the rate of reactions in heterogeneous systems by facilitating a more rapid dissolution of the salts in the solvent phase.[17]

In general, the reactions are quantitative and the rates are a little slower in piperylene sulfone compared with DMSO. This latter observation could be attributed to the difference in hydrogen bond accepting ability, as indicated by the β-values of the two solvents. Perhaps DMSO solvates the cation more strongly than the PS facilitating greater ion-pair separation between the cation and the anion thus enhancing the nucleophilicity of the anion.[17]

2.3.4 Decomposition of PS

Piperylene sulfone undergoes a retro-cheletropic reaction with heat leading to two compounds: trans-1,3-pentadiene and sulfur dioxide (SO_2) (**Fig 2.7**).
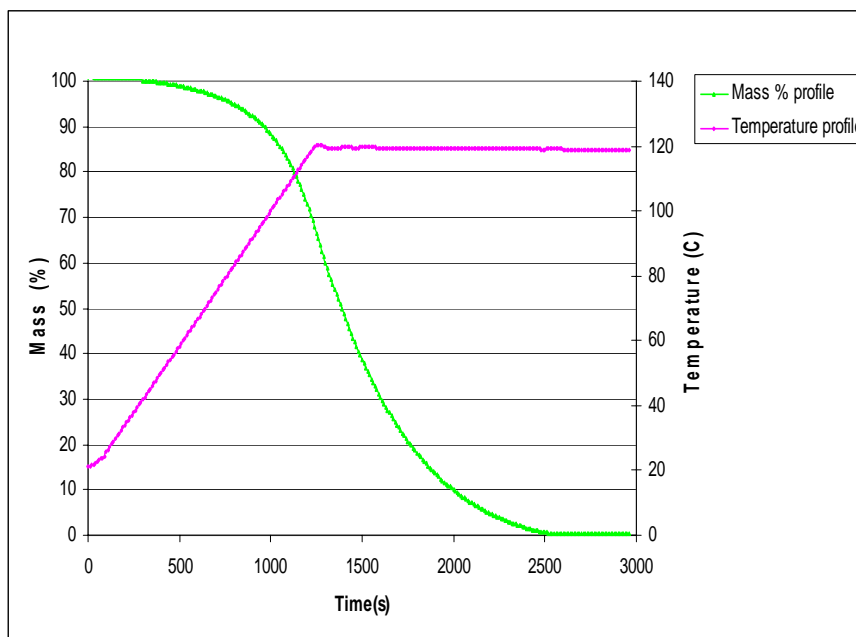
Fig 2.7: DSC-TGA of PS

It is clear from the TGA that when the temperature is held at 120°C, complete reversal of PS to gaseous trans-piperylene and SO_2 occurs, and no residue is left.

2.3.5 Complete chemical process

The retro-cheletropic reaction forming low boiling point products, trans-piperylene and gaseous sulfur dioxide, was exploited in the conduct of nucleophilic substitution coupled with a facile isolation of the products. First, the isolation of product from PS was tested. Benzylpyrrolidinedithiocarbamate (0.135 mmol) was dissolved in 1.5mL PS in a reaction vessel that had a cold finger (-30°C) attached to the top of the vessel. After heating the mixture at 110°C for 16 hours, pure trans-piperylene was found condensed on the cold finger and benzylpyrrolidinedithiocarbamate was left in the bottom of the reaction vessel. Both products were characterized by NMR (^{1}H).

PS was then used as a solvent for a nucleophilic substitution reaction and then decomposed to trans-piperylene and SO_2 for easy isolation of the product. Specifically, after the reaction of benzyl chloride (0.09mmol) with potassium thioacetate (0.18mmol) in piperylene sulfone (1.5mL) at 40°C (16h), the product reaction mixture was heated to 110°C overnight (16h). This initiated the decomposition of the solvent to gaseous *trans*-piperylene and sulfur dioxide. The residue was washed with water and then extracted with diethyl ether. Filtration over a short pad of silica gel and subsequent evaporation of the solvent, afforded pure benzyl thiocyanate in 97% yield. This process was repeated with sodium pyrrolidinedithiocarbamate to afford the product in 99% isolated yield. Products were characterized by GC-MS and ^{1}H NMR.

Finally, the complete process—preparing, using, decomposing and reforming the switchable solvent, piperylene sulfone—was carried out in our laboratory (**Fig 2.8**).
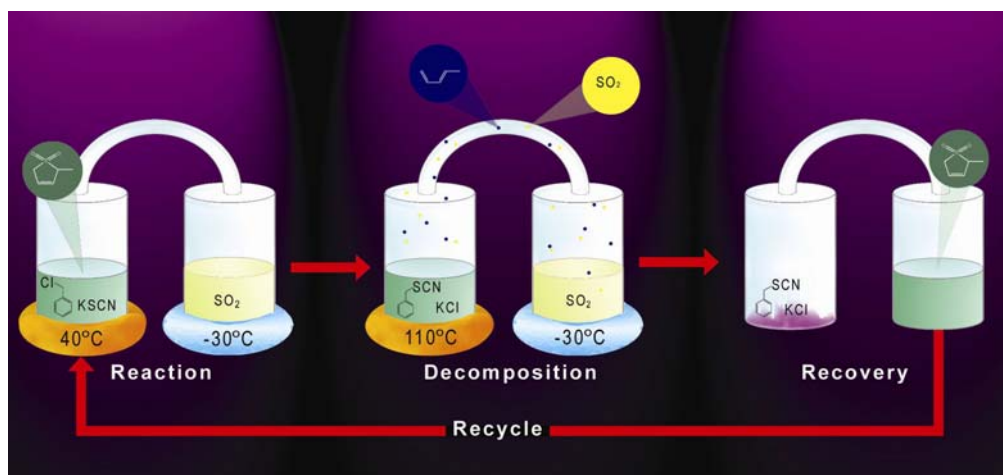
Fig 2.8: Illustration of complete process

Specifically, potassium thiocyanate (1.5 mmol) and PS (5mL) were placed in a vessel (40°C) connected to another vessel containing liquid SO_2 (-30°C). After 30 minutes of stirring benzyl chloride (0.75 mmol) was added to the first vessel. When all the benzyl chloride had reacted, the temperature of the first vessel was raised to 110°C to begin the decomposition process. This initiated the decomposition of the solvent to gaseous *trans*-piperylene and sulfur dioxide, leaving behind the solvent-free products of the nucleophilic substitution. The gases were collected in liquid sulfur dioxide at -30°C; this mixture was stirred for 48 hours. Subsequently the piperylene sulfone was reformed at ambient temperature and isolated in 87% yield using standard procedures. The residue of the first vessel was extracted with diethyl ether, washed with water, dried over $MgSO_4$, and filtered over a short pad of silica gel to afford pure benzyl thiocyanate in 96% yield.

Although the recovery of PS is relatively good (87%), it is lower than one would want for a real chemical process. This low recovery is due to losses because of the small

scale of the laboratory procedure – simple surface adhesion or adsorption accounts for most of these losses. Were the process scaled up, it is anticipated that the percent recovery would be near quantitative.

2.4 Conclusions

Piperylene sulfone is a unique solvent; it is a dipolar, aprotic solvent that can be switched to allow for an easy product recovery and solvent regeneration. Anionic nucleophilic substitution reactions have been performed in PS, the products were isolated in high yields, and then the PS was reformed for reuse. This novel system has been published and a patent application has been filed.[33-35] The high applicability and the operational simplicity of the piperylene sulfone highlights the potentials of reversible solvents.

2.5 Experimental

All chemicals were purchased from Sigma Aldrich and used without further purification, unless otherwise noted. ^{1}H and ^{13}C NMR spectra were recorded using a Varian Mercury Vx 400 spectrometer using residual CDCl$_3$ peak as an internal reference. Gas chromatography was performed on an HP GC 6890 . Mass spectrometry was performed on an HP MS 5973. TGA and DSC Thermal analyses studies were performed on TA instruments Differential Scanning Calorimeter (DSC) Model Q20 and Thermogravimetric Analyzer (TGA) Model Q50. All compounds synthesized are known in the literature; their ^{1}H NMRs were compared to literature values.

Synthesis of PS: PS was synthesized according to literature procedures.[26] 0.0125 mol (5 weight %) N-phenyl-2-napthylamine was added to a glass pressure vessel. The closed vessel was then briefly flushed with SO$_2$. 0.25 mol piperylene (mixture of cis and trans) was subsequently introduced to the vessel. Finally, the vessel was filled with SO$_2$ and shaken for two days at room temperature. After two days, the pressure was slowly released and a thick orange oil was removed. This oil was then extracted with water three times. The aqueous phase was then back extracted with chloroform three times, and the organic phases were combined and dried and concentrated. PS was characterized via NMR (^{1}H and ^{13}C), and yield is based on amount of piperylene (mixture of cis and trans) used initially. NMR data was compared to literature values.[36, 37]

^{1}H NMR (CDCl$_3$): 1.31 (d, 3H), 3.6-3.65 (m, 3H), 5.9 (s, 2H)

^{13}C NMR(CDCl$_3$): 131.3, 122.5, 59.3, 54.7, 12.9

TGA: In the thermo-gravimetric analysis (TGA) of piperylene sulfone the sample was heated at a rate of 5°C/min up to 120°C and held constant at 120°C for 30 minutes. No residual mass was left after 2500 sec.

Standard Procedure for the Kinetics of Reaction of Benzyl Chloride with Anionic Nucleophiles: A reaction vessel was charged with 0.3 mmol of the anionic nucleophile salt and 1 mL of solvent. The mixture was stirred at 40 °C for 30 minutes and then benzyl chloride (0.15 mmol) was added. Samples were taken at regular intervals of 10 minutes over 1 h period and quenched by dissolution in toluene. The concentrations of reactants and products were quantified by GC/FID analysis. The errors on the rate constant values were calculated as the standard deviation from the average value of multiple repetitions.

Procedure for Kinetics of thio-compounds: 0.06 moles of anionic thio-nucleophile was added to d_6-DMSO in an NMR tube. A ^{1}H NMR spectra was taken. Benzylchloride (0.06 moles) was added to the NMR tube and another ^{1}H NMR spectra was taken. The NMR tube was vigorously shaken (>5sec) and ^{1}H NMR spectra were taken every thirty seconds. Changes in the CH_{benzyl} peak were followed.

Isolation of Nucleophilic product from PS: Benzylpyrrolidinedithiocarbamate (0.135 mmol) was dissolved in 1.5mL PS in a reaction vessel that had a cold finger (-30°C) attached to the top of the vessel. After heating the mixture at 110°C for 16 hours, pure trans-piperylene was found condensed on the cold finger and benzylpyrrolidinedithiocarbamate was left in the bottom of the reaction vessel. The

products were quantified by GC/FID analysis and NMR. NMRs were compared to literature values, or commercial standards.

Trans-piperylene: ^{1}H NMR (d[6]DMSO): 1.7 (d, 3H), 4.9 (d, 1H), 5.0 (d, 1H), 5.67-5.76 (m, 1H), 6.0-6.1 (m, 1H), 6.2-6.3 (m, 1H)

Benzylpyrrolidinedithiocarbamate:[38] ^{1}H NMR (d[6]DMSO): 1.85-1.91 (p, 1H), 1.94-1.98 (p, 1H), 3.55-3.56 (t, 1H), 3.74-3.78 (t, 1H), 4.52 (s, 2H), 7.14-7.37 (m, 5H)

Complete chemical process: KSCN (1.5 mmol) and PS (5mL) were placed in a vessel (40 °C) connected to another vessel containing liquid SO_2 (-30 °C). After 30 minutes of stirring benzyl chloride (0.75 mmol) was added to the first vessel. When all BnCl had reacted, the temperature of the first vessel was raised to 110 °C to begin the decomposition process. PS decomposes into trans-piperylene and SO_2 which condense into the second vessel; this mixture was stirred for 48 hours. The residue of the first vessel was washed with water and then extracted with diethyl ether. Filtration over a short pad of silica gel and subsequent evaporation of the solvent, afforded pure benzyl thiocyanate in 96% yield (This preparative process was also repeated with the nucleophilic salts potassium thioacetate and sodium pyrrolidinedithiocarbamate to afford 97% and 99% isolated yields of products, respectively). The excess SO_2 was degassed from second vessel and aqueous/organic back extractions work-up afforded pure PS in 87% yield. NMRs were compared to literature values, or commercial standards.

Benzylthiocyanate - ^{1}H NMR (CDCl[3]): 4.03 (s, 2H), 7.27 (m, 5H)

Benzylthioacetate[39] - ^{1}H NMR (d[6]DMSO): 2.33 (s, 3H), 4.09 (s, 2H), 7.14-7.35 (m, 5H)

2.6 References Cited

1.   Rogers, R.D. and K.R. Seddon, eds. *Ionic Liquids as Green Solvents: Progress and Prospects. [In: ACS Symp. Ser., 2003; 856].* 2003, American Chemical Society: Washington, D. C. 599.

2.   Wasserscheid, P. and T. Welton, *Ionic Liquids in Synthesis.* 2003: WILEY-VCH Verlag GmbH & Co. KGaA, Weinheim.

3.   Brunner, G., ed. *Supercritical Fluids as Solvents and Reaction Media.* 2004, Elsevier B. V.: Amsterdam. 641.

4.   Jessop, P.G. and W. Leitner, eds. *Chemical Synthesis Using Supercritical Fluids.* 1999, WILEY-VCH Verlag GmbH & Co. KGaA: Weinheim. 480.

5.   Dillow, A.K., et al., *Kinetics of a phase-transfer catalysis reaction in supercritical fluid carbon dioxide.* Ind. Eng. Chem. Res., 1996. **35**: p. 1801.

6.   Brennecke, J.F., D.L. Tomasko, and C.A. Eckert, *Naphthalene/triethylamine Exciplex and Pyrene Excimer Formation in Supercritical Fluid Solutions.* J. Phys. Chem., 1990. **94**: p. 7692.

7.   Hallett, J.P., et al., *Probing the Cybotactic Region in Gas-Expanded Liquids (GXLs).* Acc. Chem. Res., 2006. **39**(8): p. 531-538.

8.   Eckert, C.A., et al., *Sustainable reactions in tunable solvents.* J. Phys. Chem. B, 2004. **108**: p. 18108.

9.   Broering, J.M., et al., *Biocatalytic Reaction And Recycling by Using CO2-Induced Organic Aqueous Tunable Solvents (OATS).* Angew. Chem. Int. Ed., 2006. **45**: p. 4670.

10.   Lu, J., et al., *Tunable Solvents for Homogeneous Catalyst Recycle.* Industrial & Engineering Chemistry Research, 2004. **43**(7): p. 1586-1590.

11.   Xie, X., Brown, James S., Joseph, Paul J,. Liotta, Charles L., Eckert, Charles A., *Phase-Transfer Catalyst Separation by CO2 Enhanced Aqueous Extraction.* Chemical Communications, 2002: p. 1156-1157.

12.   Ablan, C.D., et al., *Use and recovery of a homogeneous catalyst with carbon dioxide as a solubility switch.* Chem. Commun., 2003: p. 2972.

13.   Kho, Y.W., et al., *Solvent strength characterization of carbon dioxide expanded fluorinated solvents.* Ind. Eng. Chem. Res., 2003. **42**: p. 6511.

14.   Yu, M.S., D.P. Curran, and T. Nagashima, *Increasing fluorous partition coefficients by solvent tuning.* Org. Lett., 2005. **7**: p. 3677.

15.   West, K.N., et al., *CO2-Induced Miscibility of Fluorous and Organic Solvents for Recycling Homogeneous Catalysts.* Ind. Eng. Chem. Res., 2004. **43**(16): p. 4827.

16.   Reichardt, C., *Solvents and Solvent Effects in Organic Chemistry*. 3rd ed. 2003 Weinheim: WILEY-VCH Verlag GmbH & Co. KGaA. 653.

17.   Starks, C.M., C.L. Liotta, and M. Halpern, *Phase-Transfer Catalysis: Fundamentals, Applications, and Industrial Perspectives*. 1994, New York: Chapman & Hall. 688.

18.   Dunn, P.J., *Green Chemistry Institute Pharmaceutical Roundtable*, in *10th Annual Green Chemistry & Engineering Conference*. 2006: Washington, DC.

19.   Jessop, P.G., et al., *A Reversible Ionic/Non-Ionic Switchable Solvent.* Nature, 2005. **436**: p. 1102.

20.   Hamer, J., *1,4-Cycloaddition Reactions; The Diels-Alder Reaction in Heterocyclic Syntheses.* Organic Chemistry: A Series of Monographs, 1966. **8**: p. 530.

21.   Drake, L.R., S.C. Stowe, and A.M. Partanksy, *Kinetics of the Diene Sulfur Dioxide Reaction.* J. Am. Chem. Soc., 1946. **68**: p. 2521-2524.

22.   Krug, R.C. and J.A. Rigney, *Unsaturated Cyclic Sulfones. IV. Isomeric 2-Methyldihydrothiophene 1,1-Dioxide.* JOC, 1958. **23**: p. 1697-1699.

23.   Frank, R.L., R.D. Emmick, and R.S. Johnson, *cis- and trans-Piperylenes.* JACS, 1947. **69**: p. 2313-2317.

24.   Craig, D., *The Geometric Isomers of Piperylene.* J. Am. Chem. Soc., 1943. **65**: p. 1006-1013.

25.   Stadinger, H. and B. Ritzenthaler, *Uber die Anlagerung von Schwefeldioxd an Athylen-Derivate.* Berichte, 1935. **68**: p. 455-471.

26.   Grummit, O., A.E. Ardis, and J. Fick, *Thermal dissociation of methyldihydrothiophene 1-dioxides.* J. Am. Chem. Soc., 1950. **72**: p. 5167-5170.

27.   Kamlet, M.J., Abboud, J. L., Taft, R. W., *The solvatochromic comparison method 6. The pi* scale of solvent polarities.* J. Am. Chem. Soc., 1977. **99**: p. 6027.

28.   Taft, R.W., Kamlet, M. J., *The Solvatochromic Comparison Method. 2. The a-scale of solvent hydrogen-bond donor (HBD) acidities.* J. Am. Chem. Soc., 1976. **98**: p. 2886.

29. Taft, R.W. and M.J. Kamlet, *The solvatochromic comparison method. I. The beta-scale of solvent hydrogen-bond acceptor (HBA) basicities.* JACS, 1976. **98**: p. 377-383.

30. Reichardt, C., *Solvatochromic Dyes as solvent polarity indicators.* Chem. Rev., 1994. **94**: p. 2319.

31. Marcus, Y., *The properties of organic liquids that are relevant to their use as solvating solvents.* Chem. Soc. Rev, 1993. **22,**: p. 409.

32. L. Crowhurst, P.R.M., J.M.Perez-Arlandis, P.A. Salter, Tom Welton, *Sovent-solute interactions in ionic liquids.* Phys. Chem. Chem. Phys., 2003. **5**: p. 2790-2794.

33. D. Vinci, M.D., JP Hallet, EA John, P. Pollet, CA Thomas, JD Grilly, PG Jessop, CL Liotta, CA Eckert, *Piperylene sulfone: a labile and recyclable DMSO substitute.* Chem. Commun., 2007: p. 1427-1429.

34. Daniele Vinci, J.P.H., Ejae A. John, Pamela Pollet, Charles L. Liotta, Charles A. Eckert, *Piperylene Sulfone: A "Labile" and Recyclable DMSO Substitute.* Patent applied for Sept 2006.

35. Nan Jiang, D., Vinci, Ejae John, Pamela Pollet, Charles L. Liotta, Charles A. Eckert, and Arthur J. Ragauskas, *Piperylene Sulfone: A Recyclable DMSO Substitute for Copper Catalyzed Aerobic Alcohol Oxidation.* Ind. Eng. Chem. Res., submitted April 2007.

36. Ta-shue Chou, H.-H.T., Lee-Jean Chang, *Study of the alkylation reactions of sulphol-3-enes.* J. Chem. Soc. Perkin Trans, 1985: p. 515-520.

37. Sachiko Yamada, H.O., Takayoshi Suzuki, Hiroaki Takayama, *Stereoselective synthesis of (E)-, (E,Z)-, and (E, E)-conjugated dienes via alkylation of 3-sulfolenes as the key step.* J. Org. Chem., 1986. **51**: p. 4934-4940.

38. Azizi, N., F. Aryanasab, and M.R. Saidi, *Straightforward and Highly Efficient Catalyst-Free One-Pot Synthesis of Dithiocarbamates under Solvent-Free Conditions.* Org. Lett., 2006. **8**(23): p. 5275-5277.

39. Chakraborti, A.K. and Shivani, *Magnesium Bistrifluoromethanesulfonimide as a New and Efficient Acylation Catalyst.* J. Org. Chem., 2006. **71**(15): p. 5785-5788.

CHAPTER 3
RECYCLING HOMOGENEOUS CATALYSTS

3.1 Introduction

Homogeneously catalyzed reactions are highly efficient in terms of selectivity (i.e. enantiomeric excesses) and reaction rates.[1] Unfortunately, catalyst recovery can be very difficult, and product contamination by residual catalyst or metal species can be a problem. In contrast, heterogeneously catalyzed reactions allow easy and efficient separation of high value products from the catalyst and metal derivatives. However, selectivity and rates are often limited by the multiphasic nature of this system and/or variations in active site distribution.[1] We have developed a fluorous immobilized system that uses CO_2-expanded liquids for performing homogeneous reactions while maintaining the facile separation of heterogeneous systems.

3.2 Background

3.2.1 Gas-Expanded Liquids (GXLs)

GXLs are formed by dissolution of a gas, frequently CO_2, in an organic liquid. They are intermediate in properties between normal liquids and gases, both in solvating power and in transport properties (**Fig 3.1**).
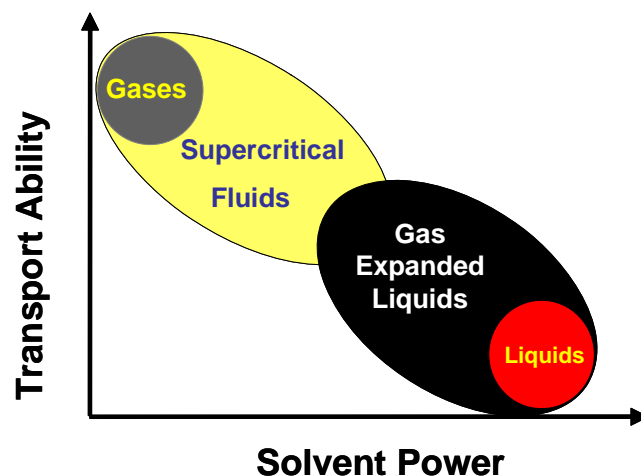
Fig 3.1: Solution properties of tunable solvents

As seen in figure **3.1**, gases have high transport ability but low solvent power whereas liquids have high solvent power but low transport ability. GXLs, however, are much better solvents than gases, with better transport ability properties compared to liquids. Furthermore, GXLs are highly tunable by simple variations of pressure of the gas.
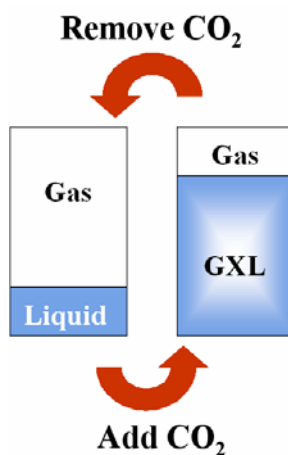
Fig 3.2: Cartoon of GXL concept

Figure 3.2 shows the reversible formation of a GXL. Adding CO_2 to a closed system containing an organic solvent causes the CO_2 to dissolve in the organic solvent. Furthermore, by releasing CO_2 pressure the expansion phenomenon is reversed. CO_2 has considerable solubility in many organic solvents (alcohols, ketones, ethers, esters, etc.)

providing the opportunity to alter the physicochemical properties of the solvent such as density, viscosity, solubility, dielectric constant and polarity. CO_2 is a poor solvent, while typical organic solvents such as methanol and acetone are good solvents. By combining CO_2 with organic solvents we can access a wide range of properties that are easily tuned by changing the pressure. Furthermore, CO_2 is an ideal anti-solvent since it is cheap, environmentally benign, easily removed, and recyclable.

3.2.2 Fluorous Biphasic Catalysis (FBC)

In chiral reactions, FBC is a powerful technique that combines the high enantioselectivity and activity of homogeneous catalysis with the post reaction catalyst recovery and re-use of heterogeneous catalysis (**Fig 3.3**).
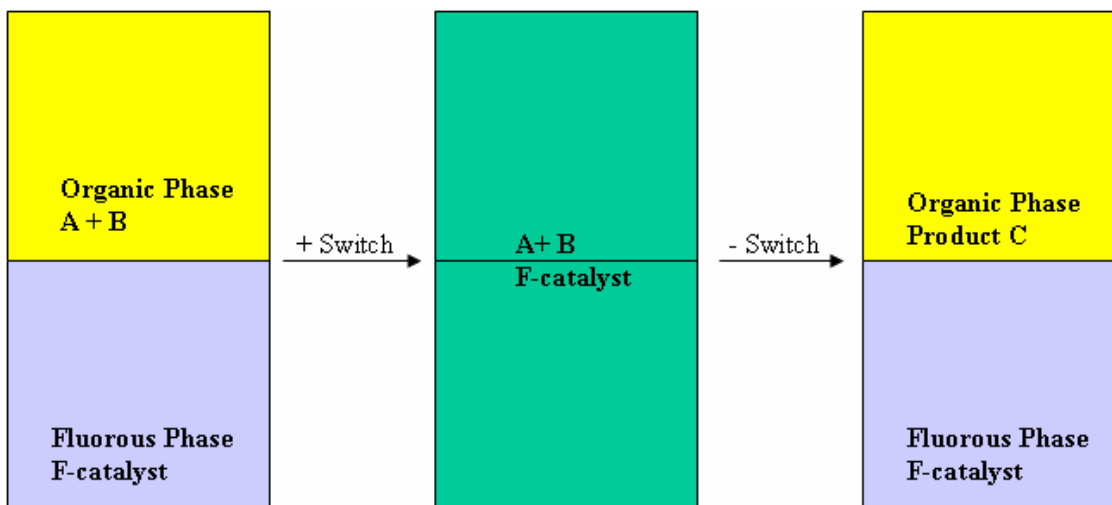
Fig 3.3: Illustration of FBC

This is achieved by having a system where a fluorous catalyst is in the fluorous phase (perfluoroalkane, perfluoroether or perfluoroamine)[2] while the immiscible organic phase (methanol, toluene, or other hydrocarbons) contains the reactants. The reaction can occur across the phase boundary, [3] or homogeneously when a switch (heat, [4, 5] CO_2[6,

[7]) is used to make the two liquid phases miscible. Then, reversal of the switch regenerates the separate fluorous phase (containing the fluorous catalyst) while the organic phase now holds the newly formed product. The product-bearing organic phase can then be removed, and the fluorous catalyst-containing phase can be re-used.

When Horvath and Rabai published the first FBC systems, they investigated the hydroformylation of 1-decene in the biphasic system of perfluoro(methylcyclohexane) and toluene (**Fig. 3.4**). The authors used vigorous stirring to overcome the transport limitations of the biphasic system and reaction occurred at the interface.[3] Their fluorinated catalyst was formed *in-situ* from $Rh(CO)_2(acac)$ (acac = acetylacetonate) and $P[CH_2CH_2(CF_2)_5CF_3]_3$ (P/Rh = 40).

$L = P[CH_2CH_2(CF_2)_5CF_3]_3;\ R = C_8H_{17}$
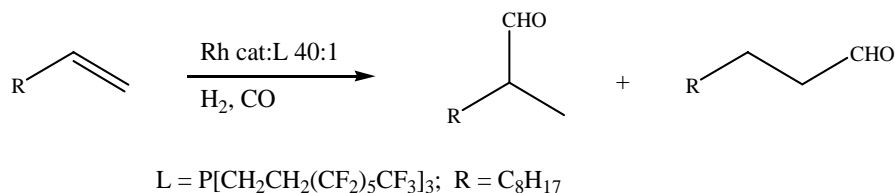
Fig 3.4: Hydroformylation of 1-decene using FBC

Decene underwent 85% conversion with a linear/branched ratio of 2.9 (n-nonanal vs. i-nonanal). Successful recycle was reported (2 cycles), however the authors failed to quantify the leaching of their fluorinated catalyst into the organic phase.

To overcome the transport limitations of FBC, alternatives have been developed including heat,[4, 5] and CO_2.[6, 7] The Eckert-Liotta group has shown that CO_2 can be used to induce miscibility of fluorocarbon-hydrocarbon mixtures and organic solvents such as methanol.[6]

0.1 MPa CO₂	**3.2 MPa CO₂**	**3.3 MPa CO₂**
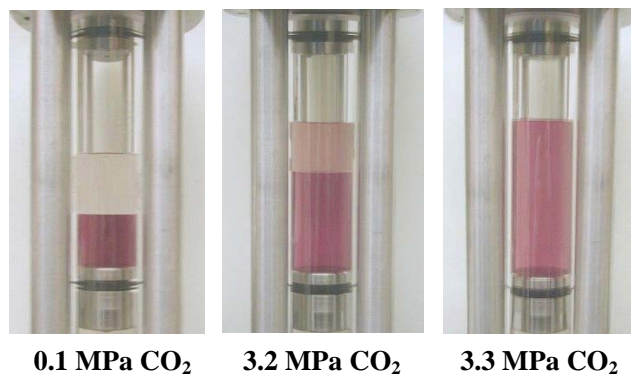
Fig 3.5: CO_2 used to homogenize an organic (toluene, clear liquid) and a fluorous (FC-75, colored liquid) phase

Figure 3.5 illustrates how CO_2 can be used to induce miscibility of fluorocarbon-hydrocarbon mixtures: Under normal conditions, the organic phase (toluene) is immiscible with the fluorous phase (perfluoro-2-n-butyl THF, FC-75). In the fluorous phase a fluorous cobalt catalyst-mimic $Co-[CO_2-(OCF_2)_{3-4}-(OCF(CF_3)-CF_2)_2-OCF_3]_2$ (aka $Co(CO_2PFPE)_2$, **Fig 3.6**) is dissolved, coloring the fluorous phase dark pink (left panel, **Fig 3.5**).
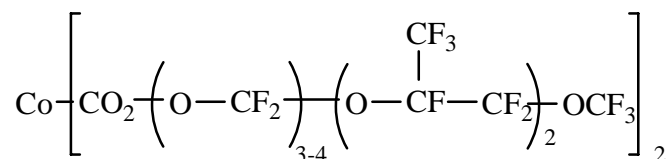
Fig 3.6: $Co(CO_2PFPE)_2$

Adding CO_2 to the organic and fluorous phases homogenizes them. With a slight pressure of CO_2 (0.1MPa), a minor coloration of the organic phase is noticeable (middle panel, **Fig 3.5**), indicating initial GXL formation. Once the enough CO_2 is in the GXL, both phases are completely miscible (right panel, **Fig 3.5**).

This CO_2 "miscibility switch" was demonstrated on two model reactions: the hydrogenation of allyl alcohol and the epoxidation of cyclohexene (**Fig 3.7**).[6] In each of these experiments, a fluorous-soluble catalyst was dissolved in the fluorous solvent FC-

40 (a mixture of perfluoro 12 carbon aromatics) or FC-75 and added to a system containing a neat organic reactant phase. In both cases, addition of enough CO_2 to homogenize the phases increased the average turnover frequency (TOF, mole product produced per mole catalyst per time) relative to the biphasic system by 50-70%.[6, 8]
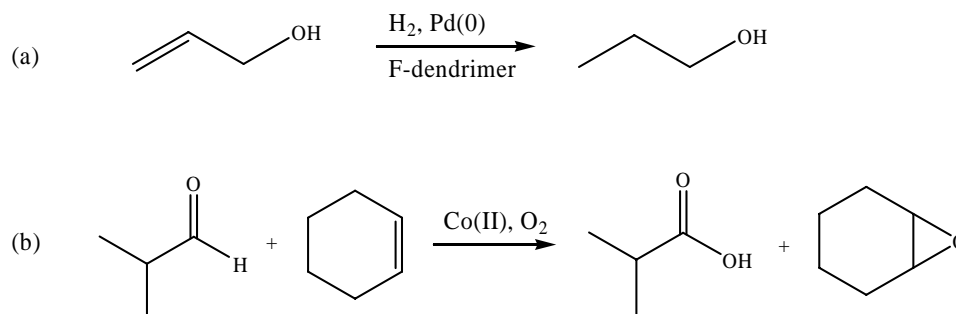
Fig 3.7: Hydrogenation and oxidation using CO_2 as the switch in FBC

For example, in the hydrogenation of allyl alcohol in **Figure 3.7A** the TOF was enhanced by 70%, going from a TOF of 1093 ± 62 h^{-1} under biphasic conditions (THF/FC-75) to a TOF of 1858 ± 57 h^{-1} under monophasic conditions (FC-40, 56 bars of CO_2). Additionally, the epoxidation of cyclohexene was also enhanced (**Fig 3.7B**), going from a TOF of 2.25 ± 0.02 h^{-1} under biphasic conditions to a TOF of 3.37 ± 0.06 h^{-1} under monophasic conditions.

Although these examples illustrate the effectiveness of the CO_2 switch for addressing mass transfer limitations of fluorous biphasic reactions, fluorinated solvents are undesirable because of high expense and environmental persistence.[9, 10] Furthermore, very little has been accomplished in reducing the leaching of fluorous compounds (catalyst and/or solvent) into the organic phase commonly associated with FBC. Through the use of CO_2-gas expanded liquid (GXL) technology and an immobilized micro-fluorous phase, solvent loss by leaching and the amount of

fluorinated solvents can be minimized while maintaining the recycling strategy and efficiency of FBC.

3.2.3 Immobilized fluorous phase

An immobilized fluorous phase, fluorinated silica, was proposed, synthesized, and used in our lab as a replacement for the fluorous liquid solvent.[11] Fluorinated silica provides a fluorinated layer around the silica core that can be visualized as a "micro" fluorinated phase. The silica (SiO_2) was surface-modified using a standard two-step process. First, the tetrachlorosilane was reacted with the alcohol terminated perfluoropolyether (PFPE) of average molecular weight 650.[12] The stoichiometry of the reactants was adjusted to mainly form the di-substituted product: the di(perfluoropolyether)-dichlorosilane. Then, this intermediate was reacted with silica (SiO_2) to form the perfluorinated modified silica, which was carefully washed to eliminate by-products such as HCl and the residual un-reacted dichlorosilanes. **Figure 3.8** depicts a representation of the surface modified silica (F-silica).
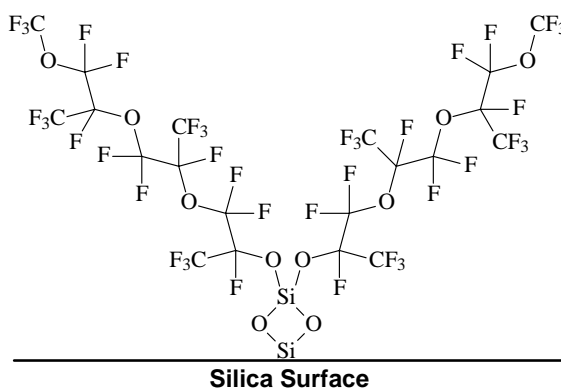
Fig 3.8: Schematic of Fluorous Silica

It is believed that the fluorinated tails on the surface of the silica are reversibly adsorbing the perfluorinated catalyst species according to **Figure 3.9**. In the absence of CO_2, the

fluorophilic species congregate. Upon formation of the GXL, the fluorophilic nature of CO_2-expanded liquids causes the fluorinated tails on the silica to extend and release the fluorinated catalyst into the now fluorophilic solution.
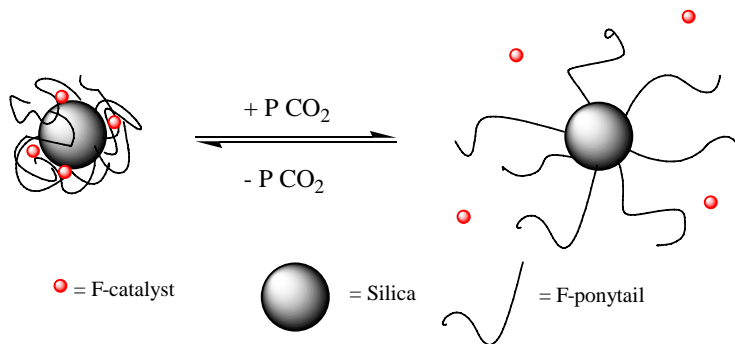
Fig 3.9: Behavior of immobilized fluorous phase with CO_2

A fluorinated catalyst mimic ($Co(CO_2PFPE)_2$) was investigated to demonstrate this concept (**Fig 3.10**).[11] This mimic was chosen because it has two PFPE chains and is colored, making spectroscopical monitoring easy. $Co(CO_2PFPE)_2$ was added to F-silica and cyclohexane at atmospheric pressure. At this time, 1% of the fluorinated mimic is detected in cyclohexane. Once a moderate pressure of CO_2 (68.3 bar) is added to cyclohexane and a CO_2 GXL is formed, and solubility increases to 99%.
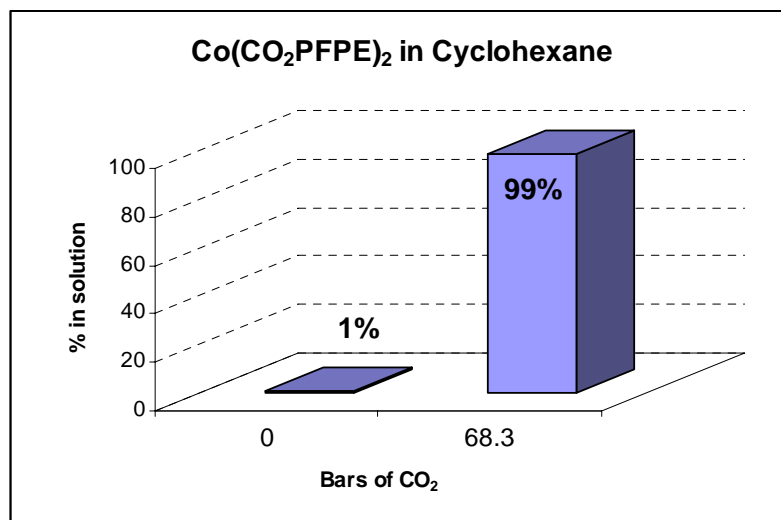
Fig 3.10: Partitioning Data of Co(PFPE)$_2$ in Cyclohexane

This data further supports our theory on the behavior of the F-catalyst and F-silica: in GXLs the fluorous catalyst is soluble in the fluorophilic environment whereas in gas/liquid conditions it is not. Particularly noteworthy is the fact that this system was switched between GXL and gas/liquid conditions several times with identical results.

3.2.4 Use of Fluorous Immobilized Phase

As proof of principle, a fluorinated Wilkinson's catalyst in cyclohexane in the presence of fluorinated silica was used for the hydrogenation of styrene (**Fig 3.11**).[7]
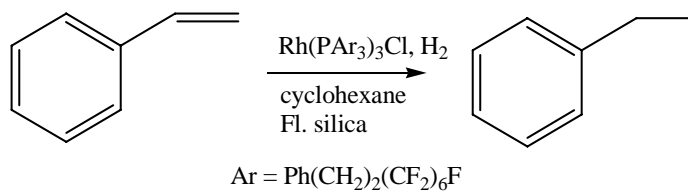
Fig 3.11: Hydrogenation of styrene using F-immobilised phase and GXL

The hydrogenation was performed under mixed CO_2 (60 bar) and H_2 (30 bar) pressure, the former to afford catalyst solubility and the latter as the hydrogen source for reaction. After reaction, depressurization, recovery and analysis of products, fresh reactants and

94

solvents were introduced and the reaction was run again. Using this method the catalyst was recycled four times with little change in activity as is seen in the conversions shown in **Table 3.1**.

Table 3.1: Hydrogenation of styrene using fluorous silica recycling method

Catalyst	Conversion (%)
Fresh	100
1st reuse	100
2nd	100
3rd	> 99
4th	100

Using the fluorous-immobilised concept, the turnover number (TON, moles of product per moles catalyst) was increased from 280 to 1400. Furthermore, Rh leaching was less than 20 ppm (ICP/AA detection limit) making the fluorous silica an attractive method to recycle homogenous catalysts.

Although this work demonstrated the viability of immobilized fluorous phases for reversibly sequestering a homogeneous catalyst, the reaction used to demonstrate the principle is of little importance to industrial synthetic processes. Realistically, for this concept to be attractive to the industrial community, it must be advantageous both economically and environmentally. Therefore, we chose to focus on asymmetric catalyzed reactions that provide enantiomerically pure intermediates. These intermediates are particularly important in pharmaceutical, agrochemical, or other fine chemical fields.

Asymmetric catalysts are usually prepared from expensive chiral ligands, and expensive and/or toxic metals. Considering the quality requirements of the final product, the economics, and the environmental policies, it is critical to efficiently separate these catalysts from the product and eventually to recycle them. Furthermore, in asymmetric catalysis of high value-added chemicals (HVAC), especially for pharmaceutical applications, contamination by metals must be avoided. An immobilized fluorous phase would provide a novel way to achieve these goals in a sustainable fashion.

3.3 Results and Discussion

The asymmetric hydrogenation of α-acetamidocinnamic acid methyl ester was carried out and the separation of the chiral catalyst and its recycling investigated (**Fig 3.12**).

Ligand = F-Monophos (**8**) or Monophos
$PCO_2 = 60$ bar, $PH_2 = 110$ bar
Solvents = EtOAc, Hexane, Dioxane
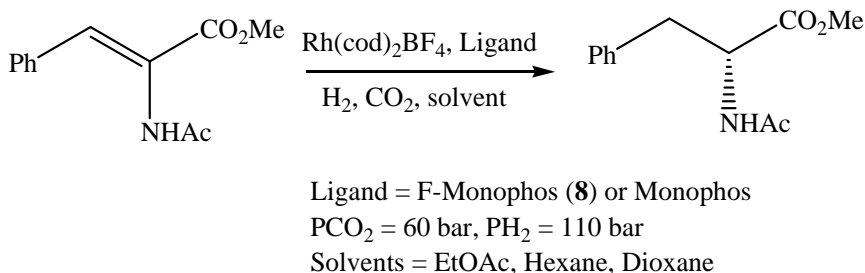
Fig 3.12: Hydrogenation of α-acetamidocinnamic acid methyl ester using F-immobilized phase and GXL

The asymmetric ligands used and compared were the well-known MonoPhos and a fluorinated version of MonoPhos. The asymmetric ligand (9,14-bis[tris(3,3,4,4,5,5,6,6,7,7,8,8,8-trideca-fluorodecyl)silyl]-(R)-(3,5-dioxa-4-phospha-cyclohepta[2,1-a;3,4-a']dinapthalen-4-yl)-dimethyl amine, or F-MonoPhos (**8**), was synthesized, characterized, and its partitioning properties between organic and fluorous

phases were studied. MonoPhos was chosen because it is a well known system that is used in industry already.[13, 14]

3.3.1 Synthesis of F-Monophos

The preparation of (R)- and (S)- fluorinated MonoPhos (**8**) is described in **Figure 3.13**.
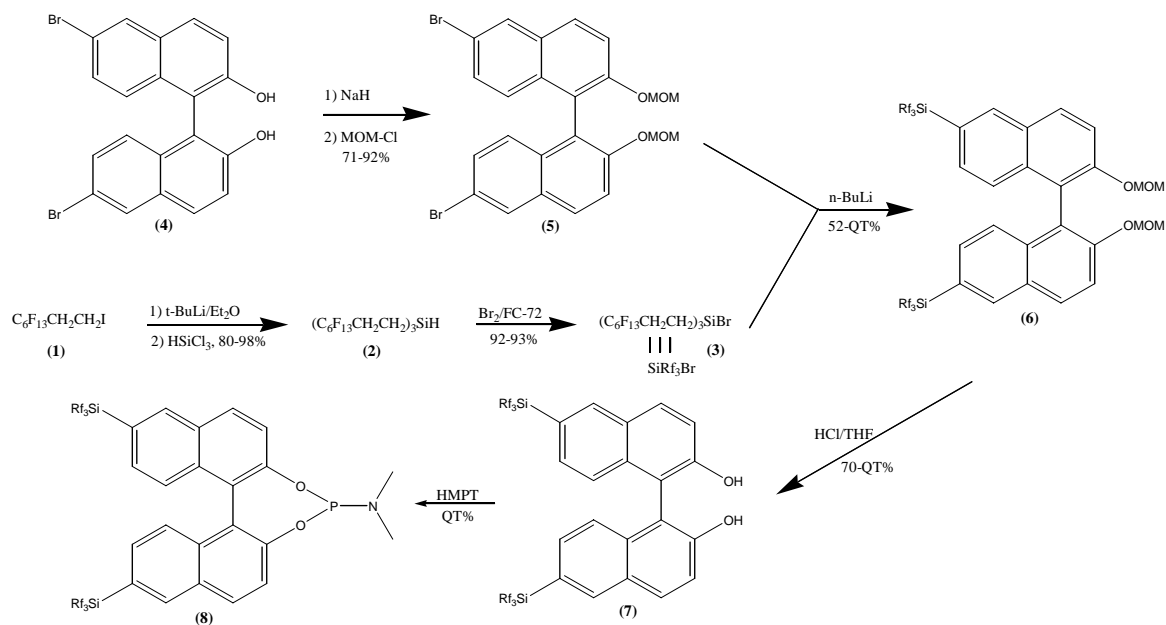
Fig 3.13: Synthetic procedure for the preparation of both (*R*) and (S)-F-MonoPhos

Although, compounds **3**,[15] **4**, **5**, (R)-**6**,[16] and (R)-**7**[16] are known in the literature, the fluorinated MonoPhos ligand **8** has never been reported. The lack of satisfactory separation methods for fluorinated materials required the optimization of all reaction conditions. Thus, only reactions yielding high purity products were acceptable, as discussed below.

3.3.1.1 Tris-(1H, 1H, 2H, 2H-perfluorooctyl)silane (2)

The initial route that was investigated to make the tris(1H,1H,2H2H-perfluorooctyl)silane from the 1H,1H,2H,2H-perfluorooctyl iodide and trichlorosilane used a Grignard reagent generated *in-situ* based upon the method of Boutevin *et al*. (**Fig 3.14**).[17]

$$Rf_3CH_2CH_2I + Mg \xrightarrow[\text{35 °C}]{\text{diethyl ether}} Rf_3CH_2CH_2MgI \xrightarrow{HSiCl_3} (Rf_3CH_2CH_2)_3SiH$$
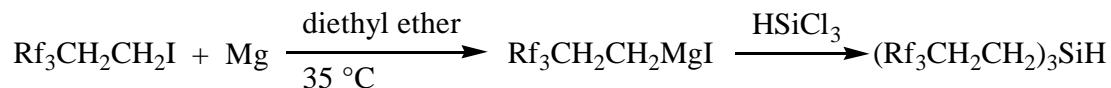
Fig 3.14: Synthesis of f-silane via Grignard reagent formation

After two attempts with no indication of coupling to the silane, we opted for halogen-metal exchange followed by reaction with the trichlorosilane using a lithium reagent—*tert*-butyl lithium (**Fig 3.15**).

$$Rf_3CH_2CH_2I \xrightarrow[\substack{\text{ether} \\ \text{-78 °C}}]{^tBuLi} Rf_3CH_2CH_2Li \xrightarrow{HSiCl_3} (Rf_3CH_2CH_2)_3SiH$$
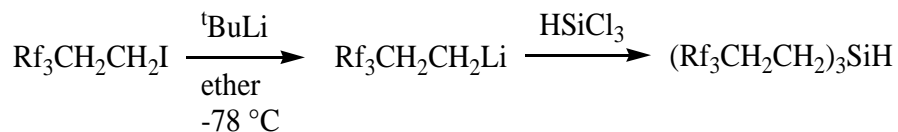
Fig 3.15:Synthesis of f-silane via lithiation

This reaction was conducted at -78°C, adding the F-iodide 1H,1H,2H,2H-perfluorooctyl iodide **1** slowly to the lithium solution. Our studies showed that the addition of the iodide must be precisely controlled (drop-by-drop) over 30 minutes to maintain the reaction temperature at -78^oC +/- 5^oC. In reactions where the addition was made more rapidly, lower conversions were obtained. With controlled addition this method led to approximately 87% conversion based on trichlorosilane. Attempts to separate unreacted

fluorous iodide from the tris(fluorinated silane) by column chromatography were unsuccessful—even using fluorinated silica as the stationary phase as described by Curran *et al*.[4] The reaction was also determined to be sensitive to dilution. While initial runs were performed at ~0.6 M F-iodide, diluting by a factor of about 20 (~0.03 M F-iodide) showed higher conversions. Optimizing for both dilution and temperature, yields of about 98% were finally obtained. This step is crucial for the overall success of the synthesis, as any fluorinated impurities produced in this step will be carried throughout the entire synthesis.

Several other factors complicate this synthesis: variation in starting material, precise stoichiometry, and time of reaction were all problems encountered with this preparation. Fluorous Technologies, Inc. (FTI), a supplier of fluorinated chemicals, encountered the same difficulties with the production of this fluorinated silane, and subsequently discontinued production of these types of fluorinated species.

3.3.1.2 Tris(1H,1H,2H,2H-perfluorooctyl)silyl bromide (**3**)

Bromination of silane **2** was achieved via reaction with bromine in FC-72 at room temperature. This step proceeded smoothly when the starting silane was pure. Without the means of purification of any fluorinated impurity from the starting material or product, the bromination reaction was optimized to run to complete conversion. This required extending the reaction time from the literature value of 8 hours to 16 hours to give a quantitative yield.[15] Furthermore, the product **3** was sensitive to moisture, so it was stored under Argon atmosphere at reduced temperature (0-4°C). The coupling

reaction with 6,6'-bis[tris(1H,1H,2H,2H-perfluorooctyl)silyl]-1,1'-bi-2-napthol **6** was done as soon as possible to avoid complications arising from the hydrolysis of **3**.

3.3.1.3 6,6'-Dibromo-2,2'-bis(methoxymethoxy)-1,1'-binapthalene (**5**)

Formation of the MOM-protected binaphthol was achieved with sodium hydride and MOM-Cl at 0°C. The protection went smoothly, according to literature;[16] however, careful purification was critical to the success of the next step. The desired product (**5**) was obtained in highly purified form by column chromatography and/or re-crystallization from dichloromethane, with a yield of 97%.

3.3.1.4   6,6'-Bis-[tris(1H,1H,2H,2H-perfluoroctyl)silanyl]-2,2'-bis(methoxymethoxy)-[1,1']binaphthalene (**6**)

The coupling of the bromosilane **3** and the methoxymethyl protected BINOL **5** occurs through a halogen-metal exchange. In this step, **5** is added to freshly distilled THF and cooled to -78 °C, followed by slow addition of the butyllithium. Again, adding the lithiated base slowly maintains optimal conditions in which the Li complex is most stable; however, adding the reagent too slowly can allow decomposition of the Li complex. From experience with this reaction, it was determined that addition needs to be complete in less then 30 minutes, with the addition done in aliquots of approximately 0.3 mL. Extraction with FC-72 was used to separate any un-reacted **5** from the product **6.** Quantitative yields were obtained for this reaction.

3.3.1.5   6,6'-Bis-[tris(1H,1H,2H,2H-perfluoroctyl)silanyl]-[1,1']binaphthalenyl-2,2'-diol (**7**)

The deprotection of the MOM-protected fluorinated BINOL was achieved by dissolving **6** in THF and slowly adding concentrated HCl to the solution.[16] The mixture was then heated, and optimal conversion was accomplished in sixteen hours, as opposed to four in the literature. Extraction with FC-72 yielded the desired compound **7** in near quantitative yield (>99%).

3.3.1.6   (9,14-Bis-(tris1H,1H,2H,2H-perfluoroctylsilanyl)-3,5-dioxa-4-phospha-cyclohepta[2,1-a;3,4-a']dinaphthalen-4-yl)-dimethyl amine (**8**)

Hulst *et al*. reported the conversion of BINOL into MonoPhos using the air-stable reactant hexamethylphosphor-triamide (HMPT).[18] Applying this methodology to our F-BINOL however was not as straightforward as we had anticipated. While the HMPT reaction with 6,6'-dibromo-1,1'-dinapthyl-2,2'-diol was complete in 4 hours at 40 °C, our substrate **8** required 48 hours to achieve completion (93% yd).   Furthermore, sometimes this reaction produced highly impure products, even when all efforts to remove experimental variances had been taken. Best results were obtained when rigorously excluding water; still, some reactions did not produce satisfactory results under anhydrous conditions.

3.3.2 Reversible immobilization: Partitioning coefficient

The reversible immobilization of the F-MonoPhos precursor (*R*)-6,6'-bis[tris(1H,1H,2H,2H-perfluorooctyl)silyl]-1,1'-bi-2-napthol (**7**) (F-BINOL) on the fluorous immobilized phase was studied (**Fig 3.16**).
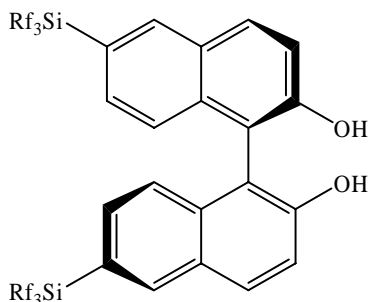
Fig 3.16: F-BINOL (7)

Using the fluorous silica and **7** in cyclohexane, measurements were taken in the presence and absence of CO_2 pressure. The addition of CO_2 greatly increased the solubility of **7** in the GXL. Without CO_2, 0.29% of **7** was detected in cyclohexane, but after applying only 39.7 bars of CO_2 GXL formation induces complete miscibility of the fluorous materials, and 99.56% of **7** was seen in cyclohexane-CO_2 phase.   These results indicated that the amount of fluorination of the ligand (60% fluorine by weight) is appropriate for efficient reversible immobilization.[19]

3.3.3 Asymmetric hydrogenation with catalyst recycling

3.3.3.1 In the presence of solid support

The asymmetric hydrogenation of the pro-chiral olefin α-acetamidocinnamic acid methyl ester was studied. Conversion, enantiomeric excess, recycling, and leaching of fluorinated species into the bulk phase were investigated using both regular MonoPhos and our fluorinated MonoPhos **8**. Both versions of MonoPhos were used in the hydrogenation of α-acetamidocinnamic acid methyl ester (**Fig 3.17**).[14]

Ligand = F-Monophos (**8**) or Monophos
PCO_2 = 60 bar, PH_2 = 110 bar
Solvents = EtOAc, Hexane, Dioxane
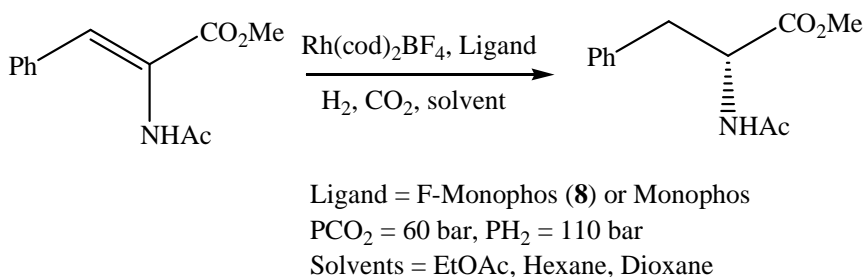
Fig 3.17: Hydrogenation of α-acetamidocinnamic acid methyl ester

We first checked to be sure the fluorinated support would not racemize the product (N-acetylphenylalanine methyl ester. Enantiomerically enriched N-acetylphenylalanine methyl ester was placed in reaction conditions with F-silica. Upon analysis no change in the enantiopurity of the product was observed. Thus, it was concluded that no racemization of the product occurs due to interaction with the fluorinated silica.

Next, we investigated the hydrogenation of α-acetamidocinnamic acid methyl ester using our F-immobilized system. The Rh complex with F-MonoPhos (**8**) showed excellent ability to induce enantioselectivity in ethylacetate and hexane (**Table 3.2, run 2**). Significantly, the non-fluorinated MonoPhos showed nearly identical ee's under the same conditions (**run 1**). This indicates the electron withdrawing effect of the

fluorination has been successfully isolated from the catalytic metal center.[20] The result

of hydrogenation with F-MonoPhos (**8)** in the presence of fluorous silica surprised us:

when the two were used together, no detectable enantiomeric excess was observed (**run**

3).

Table 3.2: Results of hydrogenation of α-acetamidocinnamic acid methyl ester

	Ligand	Solid Support	Solvent	Conversion	ee%
1	MonoPhos	none	EtOAc	100	94
2	F-MonoPhos	none	EtOAc	100	89
3	F-MonoPhos	F-silica	EtOAc	100	0
4	MonoPhos	F-silica	EtOAc	100	93.3

However, when Monophos is used in the presence of F-silica, enantiomeric excess is

maintained (**Table 3.2, run 4**). How the support affects the fluorinated catalyst and/or its

activity is not yet fully understood. It should be noted that van den Berg *et al*. reported

that P-N bonds are susceptible to cleavage, especially in the presence of acid.[14]

3.3.3.2 With traditional biphasic catalysis

Attempts were made to recycle the F-MonoPhos (**8**)-Rh catalyst using a liquid

fluorous/organic biphasic system. Using ethyl acetate as the organic solvent, the

hydrogenation of α-acetamidocinnamic acid methyl ester was performed using conditions

identical to the previous reactions. After depressurization of the system,

perfluoro(methylcyclohexane) was added and the mixture stirred. The initially yellow

organic phase became colorless, while the initially colorless fluorous phase became yellow. ^{31}P NMR showed a singlet corresponding to ligand **8**, plus several other unidentified peaks. After separation, the catalyst-containing fluorous phase was put in contact with a fresh substrate bearing organic phase and the reaction was re-run. The results are shown in **Table 3.3**.

Table 3.3: Homogeneous catalyst recycles by type of fluorous phase

Entry	Fluorous phase	Conversion (1st & 2nd run)	ee% 1st run	Ee% 2nd run
1	Perfluorohexanes (FC-72)	> 99, > 99	83	61
2	FC-72/EtOAc	> 99, > 99	68	30
3	Fluorous silica	> 99, >99	15	0

While the catalyst retained activity toward hydrogenation, the enantiomeric excess suffered upon reuse. Moreover, the ee is worst when F-silica is used (**Table 3.3, run 3**). This may further support the contention that the phosphoramidite ligand is unstable under reaction conditions.

After we had obtained these results, Reetz *et al.* published a study comparing BINOL-based monophosphites, phosphonites, and phosphoramidites (**Fig 3.18**).[13]
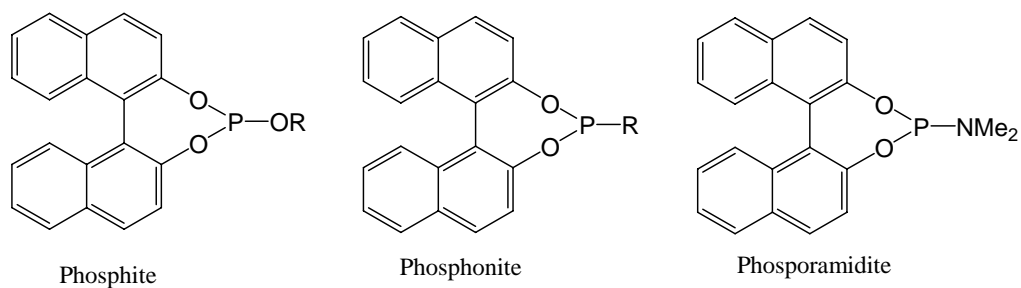
Fig 3.18: BINOL-based phosphite, phosphonite, and phosphoramidite

Rh-based catalysts made with the three groups were compared through the catalysis of the hydrogenation of itaconic acid dimethyl ester (**Fig 3.19**).
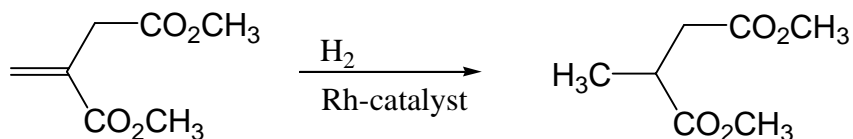
Fig 3.19: Hydrogenation of itaconic acid dimethyl ester

It was demonstrated that the phosphonite system was most active (based on speed of reaction) while the phosphoramidite system was the least reactive catalyst system. They explained this by suggesting that catalyst activation competes with hydrogenation for a significant portion of the reaction when the phosphoramidite catalyst is used.

3.4 Conclusions

We designed an immobilized microphase system that uses F-MonoPhos (**8**) to induce high enantioselectivities. Although recycling was achieved, we saw reduced enantioselectivity for subsequent cycles. Later experiments and literature indicate several weaknesses in the combination of F-Monophos (**8**) and our F-immobilized phase.

Alternatives that address these drawbacks will be discussed in the Recommendations

chapter.

3.5 Experimental

All reagents were purchased from Aldrich and used without purification except for the following: 1H,1H,2H,2H-perfluorooctyl iodide was purchased from Fluorous Technologies Inc. and dried with $MgSO_4$ before use. FC-72, FC-75, and FC-40 solvents were purchased from 3M.   (R)-(+)-6,6'-Dibromo-2,2'-bis(methoxymethoxy)-1,1'-binapthalene was purchased from Strem Chemicals Inc. and recrystallized from dry MeOH before use. Diethyl ether and THF were distilled from sodium and benzophenone before use. Hexamethylphosphorous triamide (HMPT) was distilled under an inert atmosphere (N_2 or Ar) and stored over activated 4 Å molecular sieves. Benzyltrifluoride (BTF) was dried with oven-activated molecular sieves.

^{1}H, ^{13}C, ^{19}F and ^{31}P NMR spectra were recorded using a Varian Mercury Vx 400 spectrometer. NMR spectra were referenced according to the following: ^{1}H and ^{13}C NMR used residual $CDCl_3$ peak as an internal reference, ^{19}F used α,α,α-trifluorotoluene ($\delta = -67.7$ ppm) as an external reference, and ^{31}P used 85% H_3PO_4 as an external reference. UV-visible spectra were recorded on a Hewlett-Packard 8453 spectrometer. Mass spectrum analysis was done on an Agilent 1100 Series LC coupled to an Agilent 1100 Series electrospray mass selective detector run in positive ion mode, or MALDI-TOF MS collected by the Bioanalytical Mass Spectrometry Facility. Elemental analyses were submitted to Atlantic Microlabs, Inc. The optical rotations were obtained with a Perkin-Elmer 341 polarimeter.

Synthesis

Tris(1H,1H,2H,2H-perfluorooctyl)silane (**2**)

100mL of freshly distilled ether is added to an oven-dried round bottom flask that has been flushed with argon and then cooled to -78°C. 13.25mL of 1.7M t-butyl lithium in pentane (1.2 eq) is added. 5g of 1H,1H,2H,2H-perfluorooctyl iodide (**1**) (1eq) in 5mL ether is very slowly added and allowed to react at -78°C for 30min, and then -40°C for 30min. Finally, the solution is cooled to -78°C again and 0.32mL HSiCl$_3$ (0.3 eq) is added. The mixture is allowed to react and warm to room temperature overnight. 15mL of saturated NH$_4$Cl solution is added, stirred, and the contents are concentrated *in vacuo* until 2/3 of the organic layer has evaporated. The mixture is then transferred to separatory funnel and extracted 3 times (10mL) with FC-72. The combined fluorous layers are dried with MgSO$_4$, and the solvent is removed *in vacuo* to yield 3.4g (90%). ^{1}H NMR (CDCl$_3$): δ(ppm)= 3.95 (s, 1H); 2.1 (m, 6H); 0.9 (m, 6H). ^{19}F NMR (CDCl$_3$): δ(ppm) = -102.4, -108.5, -109.4, -109.7, -109.8, -112.7.

Tris(1H,1H,2H,2H-perfluorooctyl)silyl bromide (**3**)

3 was prepared by the method of Studer and Curran.[21] To a 250 mL round bottom flask containing 7.18 g. (6.4 mmol) of tris(1H,1H,2H,2H-perfluorooctyl)silane (**2**) was added 30 mL of FC-72 and stirred vigorously under N$_2$ flush. 0.5 mL of Br$_2$ (9.7 mmol) was added dropwise over 30 minutes and the mixture was stirred for 16 hours. After transfer to a separatory funnel, the mixture was washed with 10 mL of methylene chloride. The fluorinated phase was then separated and the solvent was removed *in-vacuo*. NMR data were compared to literature values.[21] ^{1}H NMR (CDCl$_3$): δ(ppm) = 2.19 (br m, 6H), 1.27 (quintet, 6H). ^{19}F NMR (CDCl$_3$): δ(ppm) = -81.4, -116.4, -122.6, -123.5, -123.9, -126.8.

(R)-6,6'-dibromo-2,2'-bis(methoxymethoxy)-1,1'-binapthyl (**5**)

5 was prepared by the method of Chin *et al.*[22] To a 25 mL flask flushed with dry nitrogen was added 0.1 g (7 mmol) of NaH and 5 mL of THF. To this a solution of 0.5 g (1.1 mmol) of (R)-6,6'-dibromo-1,1'-bi-2-napthol in 3 mL of THF was added dropwise at room temperature. After 1 hour the reaction mixture was quenched with water, and the aqueous layer was extracted with ethyl acetate (3 x 5 mL). The combined organic layers were dried over $MgSO_4$, filtered, and the solvents removed *in-vacuo*. The white solid was recrystallized from dichloromethane to afford 0.58 g (97%). NMR data were compared to literature values.[22] ^{1}H NMR ($CDCl_3$): δ(ppm) = 8.03 (d, 2H), 7.86 (d, 2H), 7.59 (d, 2H), 7.27 (d, 2H), 6.97 (d, 2H), 5.04 (dd, 4H), 3.18 (s, 6H). ^{13}C NMR ($CDCl_3$): δ(ppm) = 152.7, 132.3, 130.7, 129.7, 129.6, 128.6, 127.0, 120.6, 117.9, 94.9, 56.0.

(S)-6,6'-dibromo-2,2'-bis(methoxymethoxy)-1,1'-binapthyl (**5**)

Yd: 92%. NMR data were compared to literature values.[22] ^{1}H NMR ($CDCl_3$): δ(ppm) = 8.03 (d, 2H), 7.87 (d, 2H), 7.61 (d, 2H), 7.27 (d, 2H), 6.99 (d, 2H), 5.08 (dd, 4H), 3.16 (s, 6H). ^{13}C NMR ($CDCl_3$): δ(ppm) = 152.7, 132.3, 130.7, 129.7, 129.6, 128.6, 127.0, 120.6, 117.9, 94.9, 56.0.

(*R*)-6,6'-Bis[tris(1H,1H,2H,2H-perfluorooctyl)silyl]-2,2'-bis(methoxymethoxy)-1,1'-binapthalene (**6**)

150 mL of freshly distilled THF is placed in a dry, N_2 flushed 500 mL 2-neck flask, and then cooled to -78 °C. 4.2 mL of 1.6 M *n*-butyl lithium in hexanes (6.7 mmol.) is added followed by addition of 1.67g (3.1 mmol) of (R)-(+)-6,6'-dibromo-2,2'-

bis(methoxymethoxy)-1,1'-binapthalene in 10 mL of THF. After reacting for 1 hour, 7.95 g (6.6 mmol) of tris(1H,1H,2H,2H-perfluorooctyl)silyl bromide (**3**) is added slowly in 10 mL of THF and allowed to react for 16 hours while the temperature is allowed to rise to r.t. 30 mL of saturated NH_4Cl solution is added, allowed to stir for 5 minutes, and the contents are transferred to a separatory funnel. The organic layer is removed, and the aqueous layer is extracted 3 x 20 mL with FC-72. The combined fluorinated layers are dried with $MgSO_4$ and the solvent is removed *in vacuo* to yield 7.87 g (99.7%). NMR data were compared to literature values.[16] ^{1}H NMR ($CDCl_3$): δ(ppm) = 7.98 (m, 4H); 7.68 (d, 2H); 7.23 (m, 4H); 5.09 (dd, 4H); 3.15 (s, 6H); 2.02 (br m, 12H); 1.19 (m, 6H); 0.95 (m, 6H). ^{19}F NMR ($CDCl_3$): δ(ppm) = -102.4, -108.5, -109.4, -109.7, -109.8, -112.7.

(*S*)-6,6'-Bis[tris(1H,1H,2H,2H-perfluorooctyl)silyl]-2,2'-bis(methoxymethoxy)-1,1'-binapthalene (**6**)

Yd: Qt. ^{1}H NMR ($CDCl_3$): δ(ppm) = 8.00 (m, 4H); 7.69 (d, 2H); 7.26 (m, 4H); 5.07 (dd, 4H); 3.16 (s, 6H); 2.02 (br m, 12H); 1.19 (m, 6H); 0.95 (m, 6H). ^{19}F NMR ($CDCl_3$): δ(ppm) = -102.4, -108.5, -109.4, -109.7, -109.8, -112.7.

(*R*)-6,6'-Bis[tris(1H,1H,2H,2H-perfluorooctyl)silyl]-1,1'-bi-2-napthol (**7**)

7.8 g of (*R*)-6,6'-bis[tris(1H,1H,2H,2H-perfluorooctyl)silyl]-2,2'-bis(methoxy methoxy)-1,1'-binapthalene (6.6 mmol) is dissolved in 100 mL of THF to which is slowly added 50 mL of conc. HCl after which the mixture is heated to 60 °C for 16 hrs. After cooling, extract with FC-72 3 x 20 mL; dry over $MgSO_4$, and removal of the

solvent *in-vacuo* yields 7.6 g (>99%). NMR data were compared to literature values.[16]

^{1}H NMR (CDCl$_3$): δ(ppm) = 8.04 (d, 2H); 8.0 (s, 2H); 7.47 (d, 2H); 7.31 (d, 2H); 7.22 (d, 2H); 5.17 (s, 2H); 2.04 (br m, 12H); 1.19 (m, 6H). ^{13}C NMR (CDCl$_3$): δ(ppm) = 154.3, 135.8, 134.7, 132.2, 131.0, 129.4, 126.7, 124.8, 119.0, 110.7, 108.5, 25.9, 25.7, 25.4, 25.2, 24.9, 4.5, 1.7, 1.3. ^{19}F NMR (CDCl$_3$): δ(ppm) = -102.4, -108.5, -109.4, -109.7, -109.8, -112.7. MALDI-TOF MS: 2422, 1410, 1354.

(*S*)-6,6'-Bis[tris(1H,1H,2H,2H-perfluorooctyl)silyl]-1,1'-bi-2-napthol (**7**)

Yd: 90%. Mass (HP1100) 2421 [M-1]. ^{1}H NMR (CDCl$_3$): δ(ppm)= 8.04 (d, 2H); 8.0 (s, 2H); 7.47 (d, 2H); 7.3 (d, 2H); 5.16 (s, 2H); 2.05 (m, 12H); 1.19 (m, 6H); 0.94 (m, 6H). ^{13}C NMR (CDCl$_3$): δ(ppm)= 154.29; 135.81; 134.70; 132.27; 130.97; 129.41; 126.7; 124.79; 118.92; 115.93 111.20; 110.65; 26.16; 25.91; 25.67; 25.43; 24.93; 4.91; 1.76. ^{19}F NMR (CDCl$_3$): δ(ppm)= -102.4, -108.5, -109.4, -109.7, -109.8, -112.7. [a]^{25} +42.6 (c= 100, in 1:1 MeOH, BTF).

(*R*)-6,6'-Bis[tris(1H,1H,2H,2H-perfluorooctyl)silyl-2,2'-O,O'-1(1,1'-Binapthyl)-O,O'-dioxo-N,N'-dimethylphospholidine (F-MonoPhos) (**8**)

In a 100mL round bottom flask, 0.5 g of (*R*)-6,6'-bis[tris(1H,1H,2H,2H-perfluorooctyl)silyl]-1,1'-bi-2-napthol (0.2 mmol) is dissolved in 25mL of α,α,α−trifluorotoluene under Argon. 39.6 μL (0.21 mmol) of hexamethylphosphortriamide (HMPT) is added and the mixture is heated to 45 °C for 48 h. Removal of all liquids *in-vacuo* yields 0.51 g. (93%). ^{1}H NMR (CDCl$_3$): δ(ppm) = 8.04 – 7.94 (m, 4H); 7.76 – 7.35 (m, 4H); 7.22 (m, 2H); 2.57 (d, 6H); 2.06 (br m, 12H);

1.19 (m, 6H). ^{1}H (d-THF): δ(ppm)= 8.37 (d, 2H); 8.2 (d, 2H); 7.7-7.5 (m, 4H); 7.4 (d, 2H); 2.58 (d, 6H); 2.26 (br m, 12H); 1.3 (m, 6H); 1.1 (m, 6H). ^{13}C NMR (d^8-THF): δ(ppm) = 150.9, 137.5, 134.3, 133.2, 131.2, 130.1, 128.0, 126.3, 122.3, 119.7, 117.1, 112.4, 110.0, 37.8, 34.8, 31.0, 27.7, 5.1, 1.95. ^{19}F NMR (CDCl$_3$): δ(ppm) = -102.4, -108.4, -109.4, -109.7, -109.8, -112.7. ^{31}P NMR (CDCl3): δ(ppm) = 14.6. ESI-MS: 2497 (M+1).

(*S*)-6,6'-Bis[tris(1H,1H,2H,2H-perfluorooctyl)silyl-2,2'-O,O'-1(1,1'-Binapthyl)-O,O'-dioxo-N,N'-dimethylphospholidine (F-MonoPhos) (**8**)

Yd: 97%. ^{1}H NMR (CDCl$_3$): δ(ppm)= 8.04-7.94 (m, 4H); 7.63-7.41 (m, 4H); 7.22 (m, 2H); 2.6 (d, 6H); 2.06 (br m, 12H); 1.19 (m, 6H); 0.9 (m, 6H). ^{19}F NMR (CDCl$_3$): δ(ppm)=,-102.5 -108.5, -109.4, -109.6, -109.7, -112.7. ^{31}P NMR (CDCl3): δ(ppm) = 14.4. ESI-MS: 2497 (M+1).

Hydrogenation Reactions

Reactions were carried out in a stainless steel autoclave (Parr Inst. Co.) under inert atmosphere conditions. Substrate, ligand **8,** and a solution of Rh(COD)$_2$BF$_4$ (in hexane, EtOAc, or dioxane) were added to the vessel and sealed; 60 bar of CO$_2$ pressure was applied and the system was stirred for 30 minutes after which H$_2$ was added to a total pressure of 110 bars. Conversion and ee% were measured by GC-FID using a Daicel Chiralpak AD-H column.

3.6 References Cited

1.   Crabtree, R.H., *The Organometallic Chemistry of the Transition Metals*. 3rd ed. 2001, New Haven: Wiley - Interscience Publications.

2.   Luis P. Bartel-Rosa, J.A.Gladysz, *Chemistry. in fluorous media: a user's guide to practical considerations in the application of fluorous catalysts and reagents.* Coordination Chemistry Reviews, 1999. **190-192**: p. 587-605.

3.   Horvath, I.T. and J.Rabai, *Facile Catalyst Separation Without Water: Fluorous Biphase Hydroformylation of Olefins.* Science, 1994. **266**: p. 72-75.

4.   Curran, D.P., *Strategy-level separations in organic synthesis: from planning to practice.* Angewandte Chemie, International Edition, 1998. **37**(9): p. 1175-1196.

5.   Fish, R., H., *Fluorous biphasic catalysis: A new paradigm for the separation of homogeneous catalysts from their reaction substrates and products.* Chemistry, A European Journal, 1999. **5**(6): p. 1677-1680.

6.   West, K.N., et al., *CO2-Induced Miscibility of Fluorous and Organic Solvents for Recycling Homogeneous Catalysts.* Industrial & Engineering Chemistry Research, 2004. **43**(16): p. 4827-4832.

7.   Ablan, C.D., et al., *Use and recovery of a homogeneous catalyst with carbon dioxide as a solubility switch.* Chemical Communications, 2003. **24**: p. 2972-2973.

8.   Chechik, V. and R.M. Crooks, *Dendrimer-Encapsulated Pd Nanoparticles as Fluorous Phase-Soluble Catalysts.* JACS, 2000. **122**: p. 1243-1244.

9.   Cavalli, F., et al., *Atmospheric lifetimes, infrared spectra and degradation products of a series of hydrofluoroethers.* Atmospheric Environment, 1998. **32**(21): p. 3767-3773.

10.   Ravishankara, A.R., et al., *Atmospheric lifetimes of long-lived halogenated species.* Science, 1993. **259**(5092): p. 194-9.

11.   Thomas, C.A., *Reactions and Separations in Tunable Solvents*, in *Chemistry and Biochemistry*. 2006, Georgia Institute of Technology: Atlanta.

12.   Ablan, C.D., et al., *Use and recovery of a homogeneous catalyst with carbon dioxide as a solubility switch.* Chemical Communications (Cambridge, United Kingdom), 2003(24): p. 2972-2973.

13.   Manfred T. Reetz, A.M., Gerlinde Mehler, Klaus Angermund, Martin Graf, Walter Thiel, Richard Mynott, Donna G. Blackmond, *Why are BINOL-Based*

monophosphites such efficient ligands in Rh-catalyzed asymmetric olefin hydrogenation? JACS, 2005. **127**: p. 10305-10313.

14. van den Berg, M., et al., *Monodentate phosphoramidites: A breakthrough in rhodium-catalyzed asymmetric hydrogenation of olefins.* Advanced Synthesis & Catalysis, 2003. **345**(1+2): p. 308-323.

15. Studer, A. and D.P. Curran, *A strategic alternative to solid phase synthesis: preparation of a small isoxazoline library by "fluorous synthesis".* Tetrahedron, 1997. **53**(19): p. 6681-6696.

16. Chin, J., et al., *Chiral Shift Reagent for Amino Acids Based on Resonance-Assisted Hydrogen Bonding.* Organic Letters, 2004. **6**(15): p. 2591-2593.

17. Boutevin, B., et al., *Study of the alkylation of chlorosilanes. Part I. Synthesis of tetra(1H,1H,2H,2H-polyfluoroalkyl)silanes.* Journal of Fluorine Chemistry, 1993. **60**(2-3): p. 211-223.

18. Hulst, R., N. Koen de Vries, and B.L. Feringa, *a-Phenylethylamine based chiral phospholidines; new agents for the determination of the enantiomeric excess of chiral alcohols, amines and thiols by means of 31P NMR.* Tetrahedron: Asymmetry, 1994. **5**(4): p. 699-708.

19. P. Bhattacharyya, et al., J. Chem. Soc., Perkin Trans. 1, 1997: p. 3609.

20. L. J. Alvey, R.M., T. Soos, P. Bernatis, and J. A. Gladysz, Eur. J. Inorg. Chem, 2000: p. 1975.

21. Studer, A. and D.P. Curran, *A strategic alternative to solid phase synthesis: preparation of a small isoxazoline library by \"fluorous synthesis\".* Tetrahedron, 1997. **53**(19): p. 6681-6696.

22. Chin, J., et al., *Chiral Shift Reagent for Amino Acids Based on Resonance-Assisted Hydrogen Bonding.* Organic Letters, 2004. **6**(15): p. 2591-2593.

CHAPTER 4
POLYETHYLENIMINE-CO$_2$ GELS

4.1 Introduction & Background

4.1.1 Gels: A Brief Introduction

A Gel is defined as a substance that 1) has a continuous structure with macroscopic dimensions that is "permanent" on the time scale of an analytical experiment and 2) is solid-like in its rheological behavior.[1] In simpler terms, a gel is simply a matrix with a substance trapped inside of it that does not flow. However, the more common definition is "If it looks like Jell-O, it must be a gel."[2] This chapter focuses on organogels, where an organogel is defined as a gel that is composed of a gel-forming agent (gelator) and an organic liquid,[3] specifically organogels formed by low-molecular mass organic gelators.

4.1.2 Low-Molecular Mass Organic Gelator Gels

Low-molecular mass organic gelator (LMOG) gels' distinctive characteristic is that they are usually thermally reversible.[4] One example of thermally reversible LMOG gels makes use of well-known carbamate chemistry: It is known that primary and secondary amines reversibly react with CO$_2$ to form ammonium carbamates (**Fig 4.1**).[5]
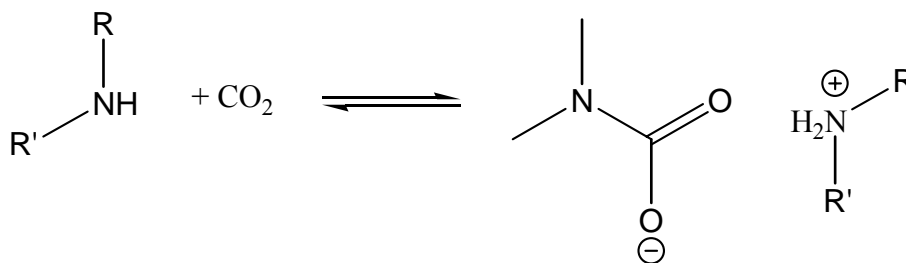
Fig 4.1: Formation of ammonium carbamates

These ammonium carbamates can be formed and reversed many times without detectable degradation to the system. Using this well-known chemistry, George and Weiss published a series of papers dealing with thermally reversible organogels where they combined amines, other liquids (silicone oil, hexane, n-octane, ethanol, 1-butanol, 1-pentanol, 1-octanol, benzyl alcohol, toluene, DMSO, and CCl_4) and CO_2 to form gels (**Fig 4.2**). [6]

R	**R'**
$C_{18}H_{37}$	H
$C_{16}H_{33}$	H
$C_{10}H_{21}$	H
C_8H_{17}	C_8H_{17}
$C_{18}H_{37}$	CH_3
$H_2NC_{12}H_{24}$	H
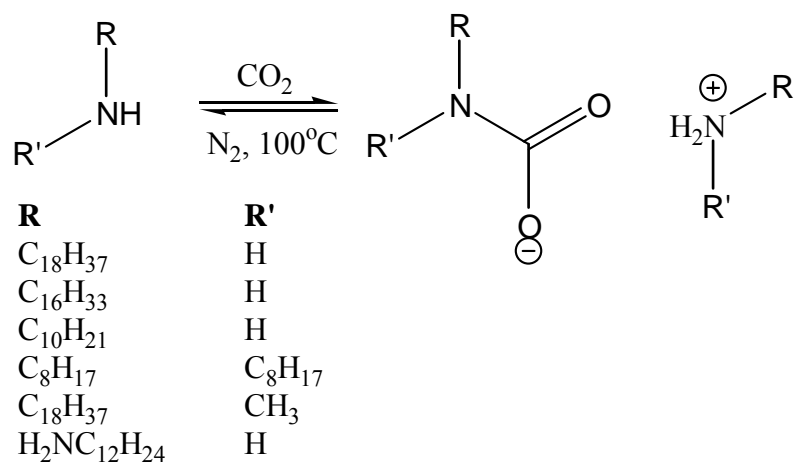
Fig 4.2: Formation of ammonium carbamate gels

The liquids formed gels in the presence of amine (5%) and CO_2. The gels were reversed by bubbling N_2 through them at $\geq 100^{\circ}C$. Amines do not form gels in the presence of the aforementioned liquids by themselves. Instead, the amines must chemically react with CO_2 which then causes the liquids to be gelled in between the carbamates.[7] Thus, the amines were latent gelators with CO_2: when ammonium carbamates combined with a solvent, they formed networks that immobilized the liquid component.

4.1.3 Polyamine Gels

Another example where an amine and CO_2 exist as a latent gelator is with polyallylamine (PAA) (**Fig 4.3**).[8]
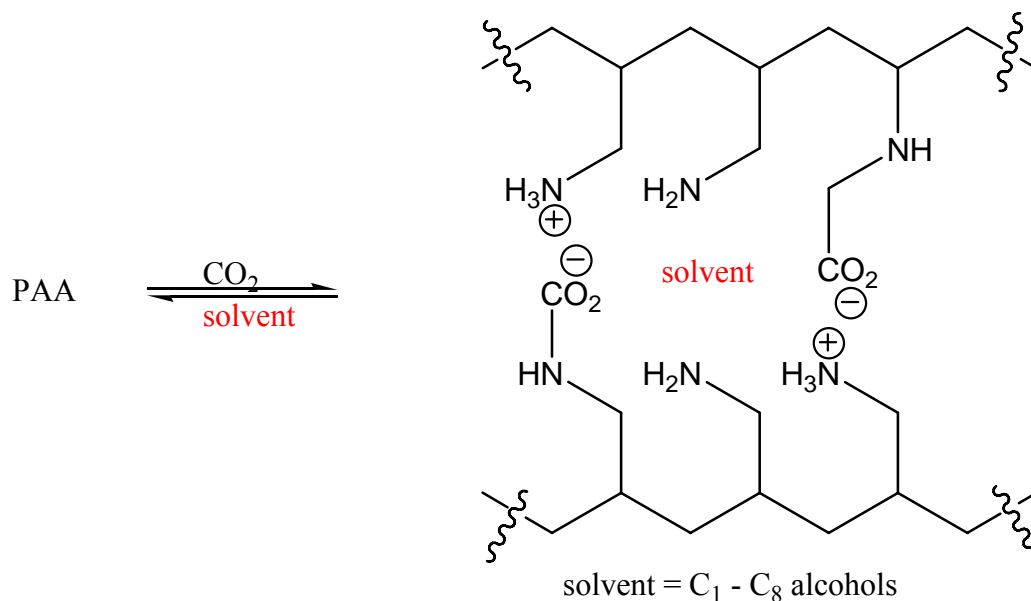
Fig 4.3: Formation of polyallylamine ammonium carbamate gels

When the interactions between polymer chains and a cross-linking agent are electrostatic, gels with well-ordered structures are possible.[9] Caretti *et al.* found that bubbling CO_2 through PAA causes the formation of ionic species (carbamate and ammonium centers). Thus, he theorized a well-ordered gel structure could form with polyallylamine, CO_2 and a suitable gelator. Caretti *et. al.* tested polyamines dissolved in methanol, ethanol, 1-propanol, 1-butanol, 1-pentanol, 1-hexanol, 1-heptanol, 1-octanol, 1-methyl-2-pyrrolidone, DMSO, and dichloromethane. Upon the addition of CO_2, the PAA chains are cross-linked through interchain ion-paired centers with the solvent trapped inside. DCS-TGA analysis indicates that 66% of the amines in PAA react with CO_2 in these gels, and they reverse at $80^{\circ}C$.

4.1.4 CO_2-diamine and hydrazine gels

It has recently been reported that CO_2 readily reacts with neat hydrazine, monomethylhydrazine, and ethylenediamine to form gels (**Fig 4.4**).[10]
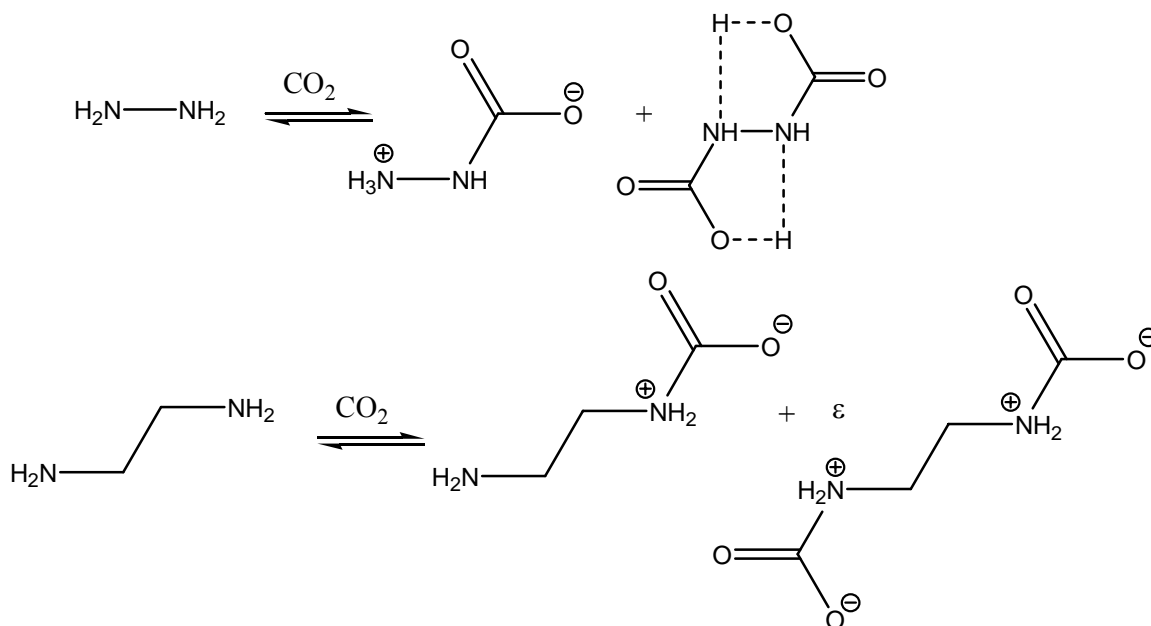
Fig 4.4: Reaction of ethylenediamine and hydrazine with CO_2, resulting in gels

The resultant materials are called gels because they consist of a matrix and trapped solvent molecules, and when these materials are placed in a vial which is then turned upside down they do not flow. Characterization of these hydrazine, monomethylhydrazine, and ethylenediamine gels has shown that the matrix is formed from the ammonium carbamate salts, and the trapped molecules are the un-reacted hydrazines or diethylamine. These gels are different from the previous examples because the amine source behaves as both the matrix (upon reaction with CO_2) and the substance trapped inside.

4.1.5 Polyethyleneimine (PEI)

Polyethyleneimine (PEI) is a polymer that contains approximately 25% primary amine, 50% secondary amine, and 25% tertiary amine groups (**Fig 4.5**).

119
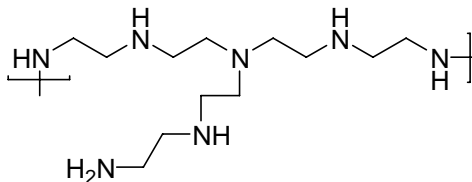
Fig 4.5: Polyethyleneimine structure

It is food-safe, non-toxic, inexpensive and available in a variety of molecular weights. PEI is known as an effective gene delivery polymer because it encapsulates DNA through strong electrostatic interactions.[11, 12]

4.2 Results and Discussion

It was recently found that after thorough mixing of PEI with octanol, introduction of CO_2 leads to the formation of a stable gel. The proposed gel structure is shown in **Fig 4.6**.
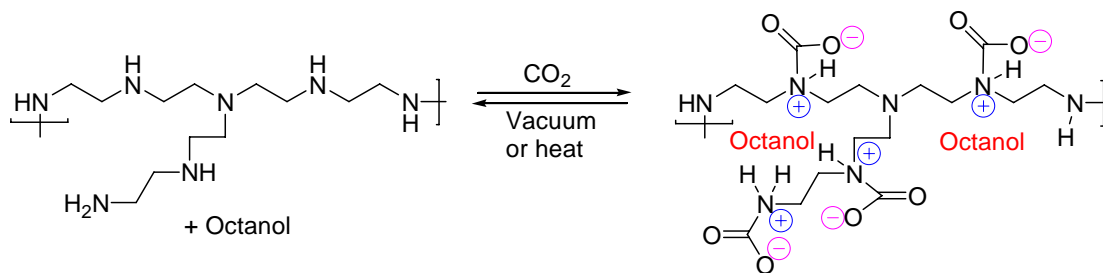
Fig 4.6: Proposed structure of formation of PEI-based gels

It is believed that upon reaction with CO_2, PEI ammonium carbamate salts form the matrix while octanol is the guest.

4.2.1 Synthesis of PEI-CO$_2$ gels

Mixtures of PEI (MW 600, 1200, 1800) and a variety of organic solvents (1-octanol, ethyl acetate, methyl ethyl ketone (MEK), isopropanol, ethanol, dimethyl

sulfoxide, and tertbutanol) were reacted with CO_2. It was found that the gelation depends on 1) the nature of the organic solvent, 2) the PEI MW and 3) the ratio PEI/organic solvent.

The solvents were mixed in varying amounts of PEI. Then, gaseous CO_2 was bubbled into the mixtures for several minutes to induce carbamate formation and gelation (Please see **Table 4.1-4.6** in Experimental Section). CO_2 was bubbled into the samples for 5-7 minutes to induce the exothermic carbamate formation. If the mixture appeared to be a gel, it was held upside down for twenty seconds: if no material flowed downward, the sample was considered a gel. Stability was tested by monitoring the gels for 2-4 weeks. Gels are defined as stable if they do not degrade or reverse within the observation period.

Stable gels with 5-17 weight % PEI-600, 7-18 weight % PEI-1200, and 4-15 weight % PEI-1800 in 1-octanol were observed (**Fig 4.7**). The molecular weight of PEI showed no significant effect on the stability of corresponding PEI/octanol/CO_2 gels at comparable molar concentration. However, PEI-1800 produced tougher gels due to longer polymer chain length. For all other combinations tested, instable gels (dissolved in 2-4 weeks), milky white precipitate, or no obvious physical change was observed.
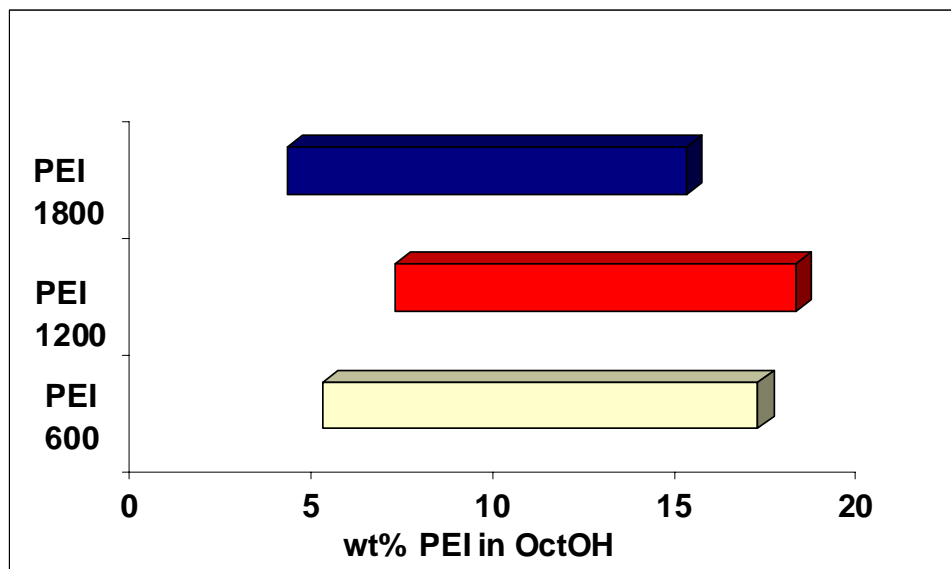
Fig 4.7: PEI/Octanol combinations that formed stable gels

All the PEI-CO_2 gels used for chemical and structural analysis were prepared with PEI-1200, unless otherwise stated.

4.2.2 Characterization of PEI-1200 CO_2 gels

4.2.2.1 IR analysis

Functional group information for PEI/1-octanol/CO_2 gel containing 7 weight % of PEI was obtained from FTIR experiments. FTIR data clearly indicated the presence of carbamate functional group in the gel: the FTIR spectra exhibited absorption bands at ~3300 cm^{-1} (N-H) and 2900 cm^{-1} (C-H). Absorptions in the lower energy region of the spectrum at 1432 and 1234 cm^{-1} were consistent with C-N and N-H stretching vibrations of carbamate and ammonium respectively.

4.2.2.2 Weight Analysis

The amount of carbon dioxide present in PEI/octanol/CO_2 gels was calculated by measuring weight before and after addition of carbon dioxide to solutions of PEI and 1-octanol mixtures. PEI was added to tared vials. Appropriate amounts of 1-ocatanol were added to create 7% PEI solutions. CO_2 was bubbled into the mixture until the weight was consistent. The weight of CO_2 was calculated from difference in weight of PEI-1200 and octanol compared to PEI/octanol/CO_2 gel. Theoretical calculations based on this data suggest that only 25% of the PEI amines react with CO_2.

4.2.2.3 NMR Studies

4.2.2.3.1 Neat PEI

$^{13}CO_2$ was bubbled into neat PEI (MW 600, 1200, 1800). Although gel formation is not observed, the ^{13}C NMR spectrum displayed a carbamate peak at 175.91ppm (carbamates usually found 150-170ppm), while no free CO_2 was observed (126 ppm) (**Fig 4.8B**). This experiment was done with PEI-600, -1200, and -1800, but only spectra of PEI-1200 are shown as they all displayed the same shifts.
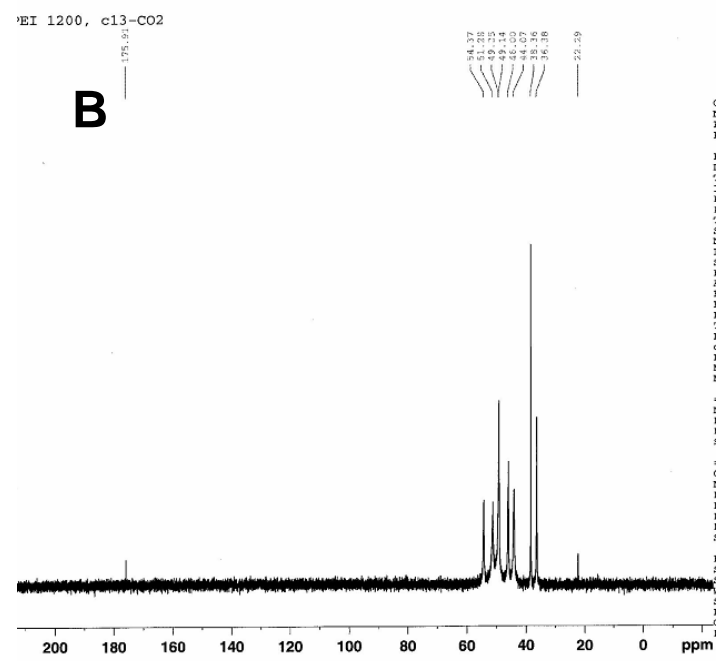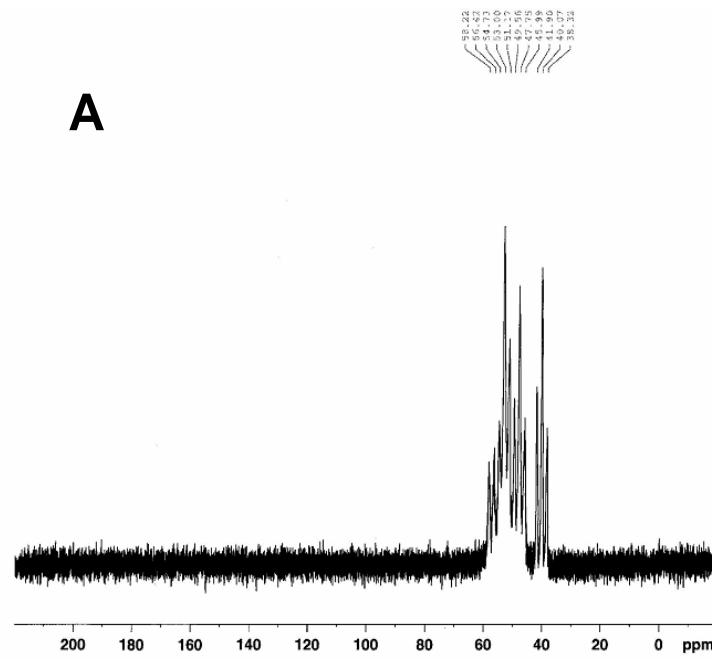
Fig 4.8: ^{13}C NMR of A) neat PEI-1200 B) bubbled with $^{13}CO_2$

124

Observation of the carbamate peak indicates the formation of ammonium-carbamate units, although it is not clear if the carbamates are formed inter- or intramolecularly (**Fig 4.9**).
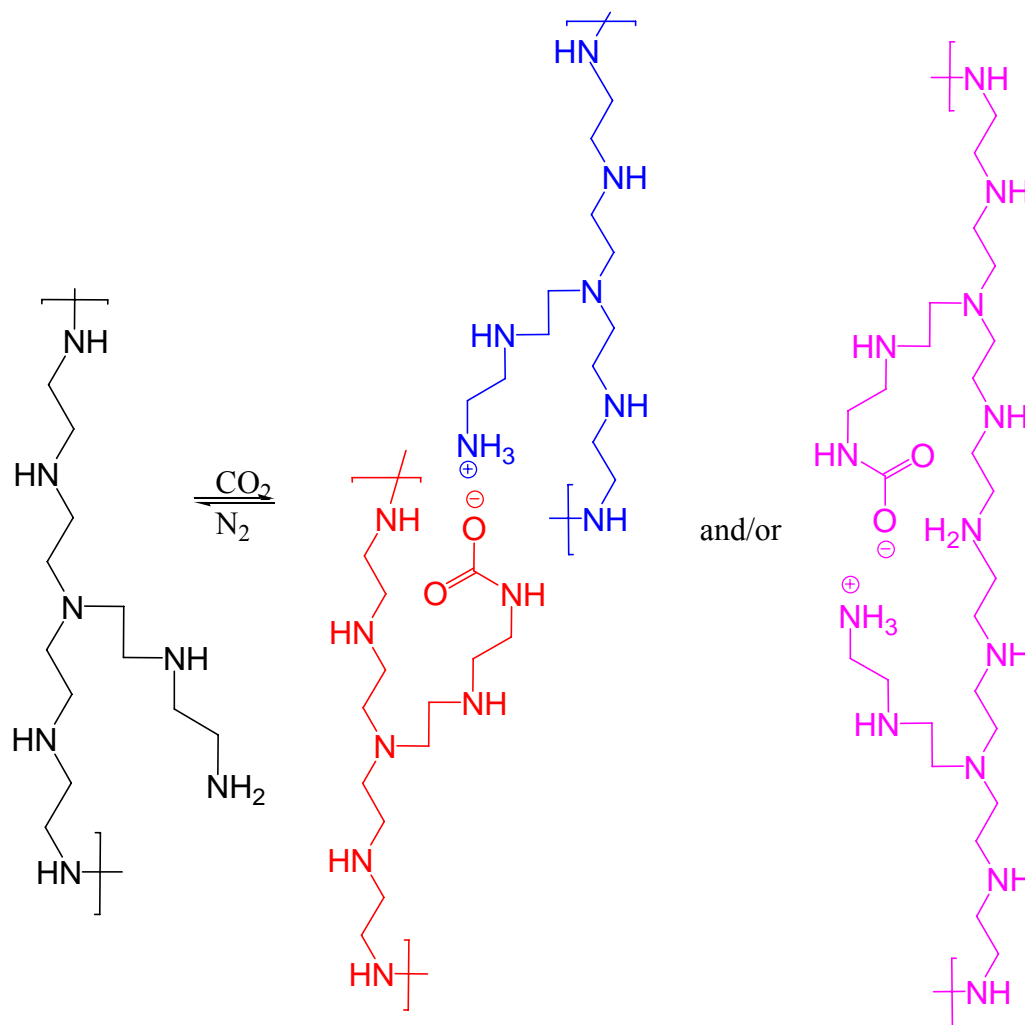
Fig 4.9: Formation of ammonium carbamate units in PEI

Although ^{15}N NMR was taken of neat PEI samples (MW 600, 1200, & 1800), only two types of nitrogen were ever observed. However, the signals were quite weak, and the third type of nitrogen may have been buried in the baseline (**Fig 4.10**). Again, only spectra of PEI-1200 are shown as all PEI MWs displayed the same shifts.

PEI 1200 with c13-CO2
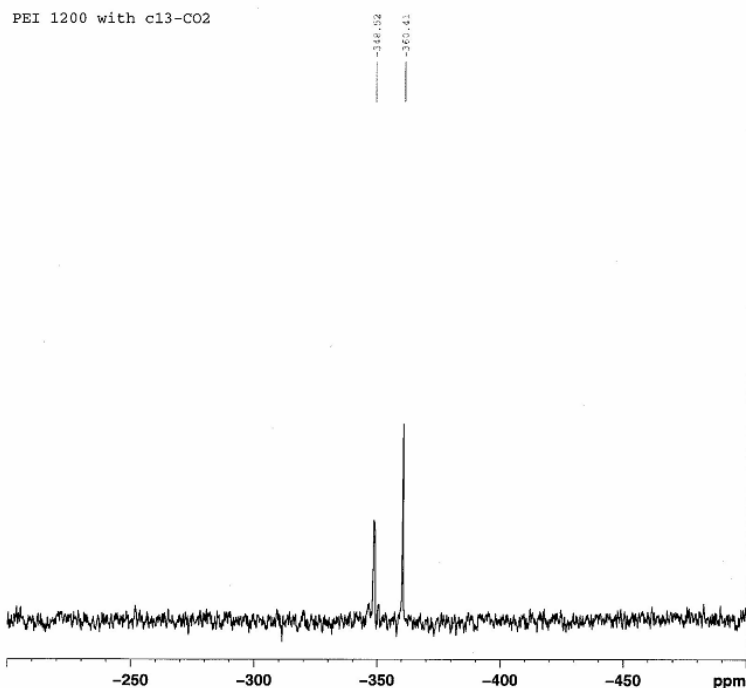
Fig 4.10: ^{15}N NMR of Neat PEI-1200

4.2.2.3.2 PEI/octanol/CO$_2$ gels

Because the carbon signals were somewhat weak in neat samples, we moved from using a 5mm probe to a 10mm probe to do NMR experiments that included 1-octanol. Unfortunately, the NMR spectrometer that is capable of using 10mm probes does not have the ability to run ^{15}N NMRs.

^{13}CO$_2$ was bubbled into a 20 weight % solution of PEI in 1-octanol to form a gel. Again, the ^{13}C NMR spectrum showed a carbamate peak (163.31ppm), while no free CO$_2$ was observed (**Fig 4.11B**). This experiment was done with PEI-600, -1200, and -1800, but only spectra of PEI-1200 are shown as they all displayed the same shifts.
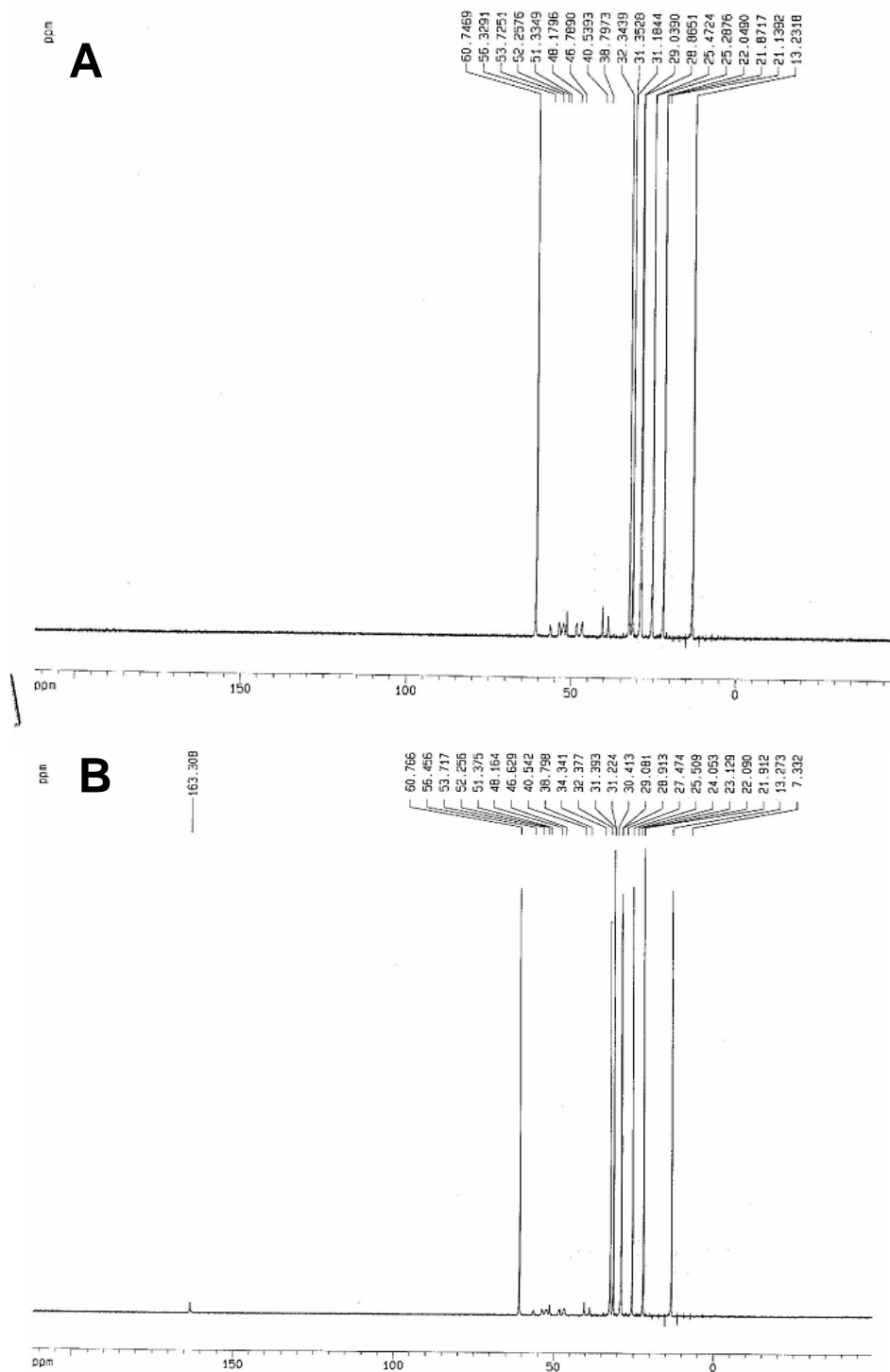
Fig 4.11: ^{13}C NMR of A) 20% PEI in octanol and B) sample A gelled with $^{13}CO_2$

4.2.3 Reversibility

5-18% PEI/Octanol/CO_2 gels were reversed to PEI and octanol by pulling vacuum and on the gel overnight. Furthermore, the gel could be reformed upon the introduction of fresh CO_2, and the cycle could be repeated twice more (three total cycles) (**Fig 4.12**).
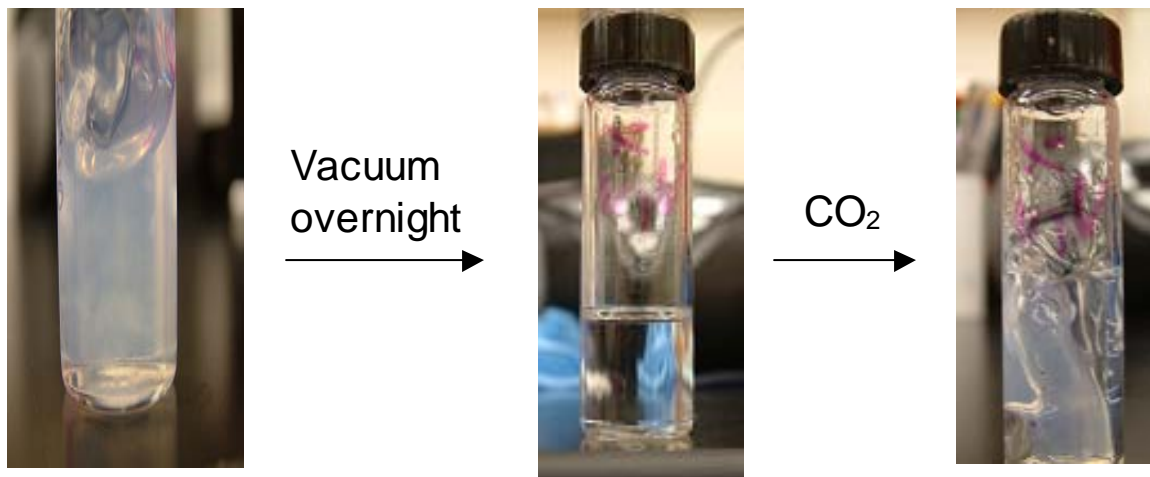
Fig 4.12: Formation, reversal, and reformation of PEI-based gel

Reversibility was also substantiated by NMR (**Fig 4.13**). Vacuum was pulled on a 20 weight % solution of PEI/octanol/$^{13}CO_2$ gel five hours with stirring. This time, the ^{13}C NMR spectra showed no carbamate peak nor free CO_2.
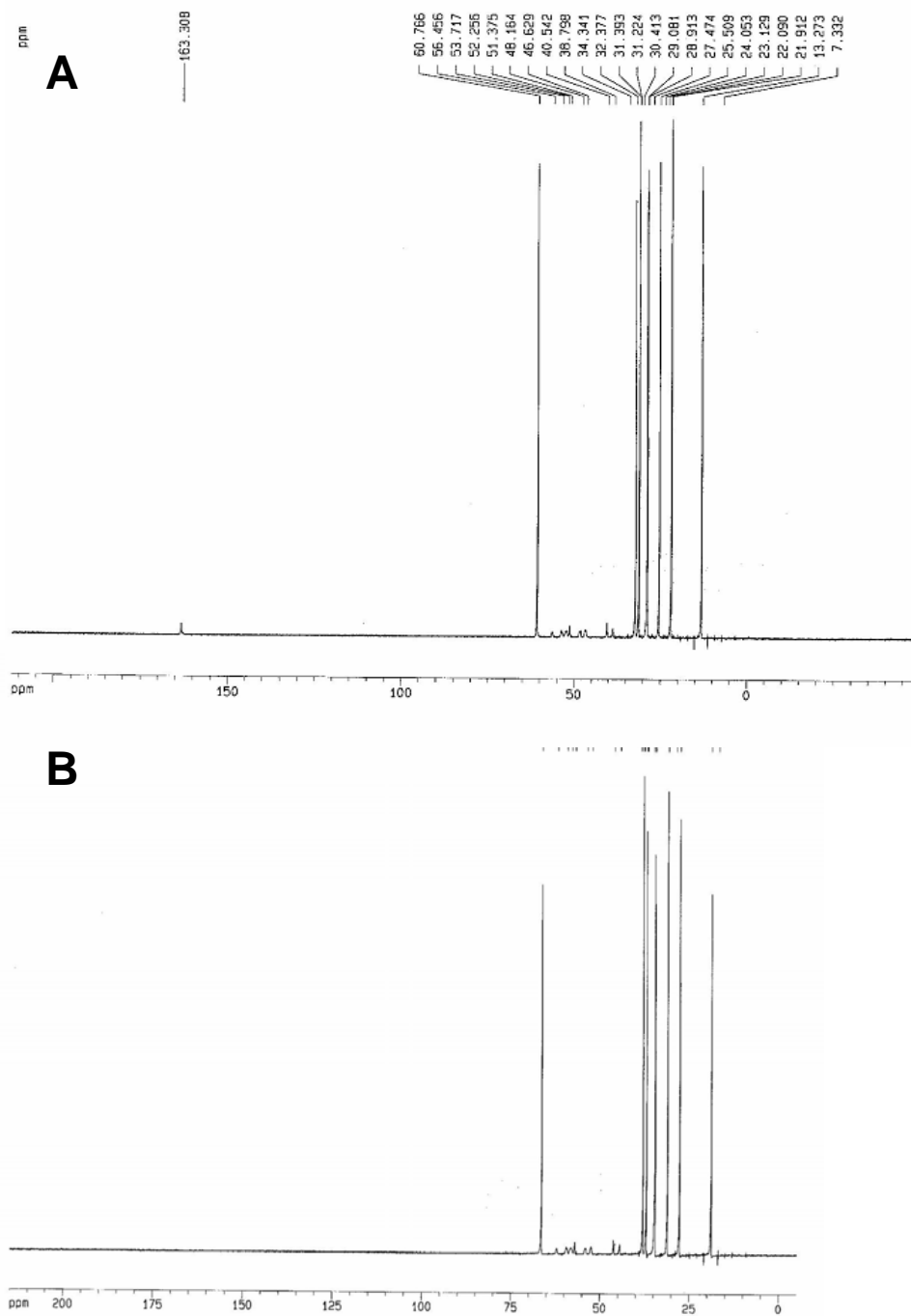
Fig 4.13: ^{13}C NMR of A) 20% PEI in octanol gelled with $^{13}CO_2$ and B) sample A reversed with vacuum

Thermoreversibility of the gels was also examined by DSC-TGA analysis. DSC-TGA data for PEI/octanol/CO_2 gel prepared with 10 weight % PEI-1200 is shown in **Figure 4.14**.
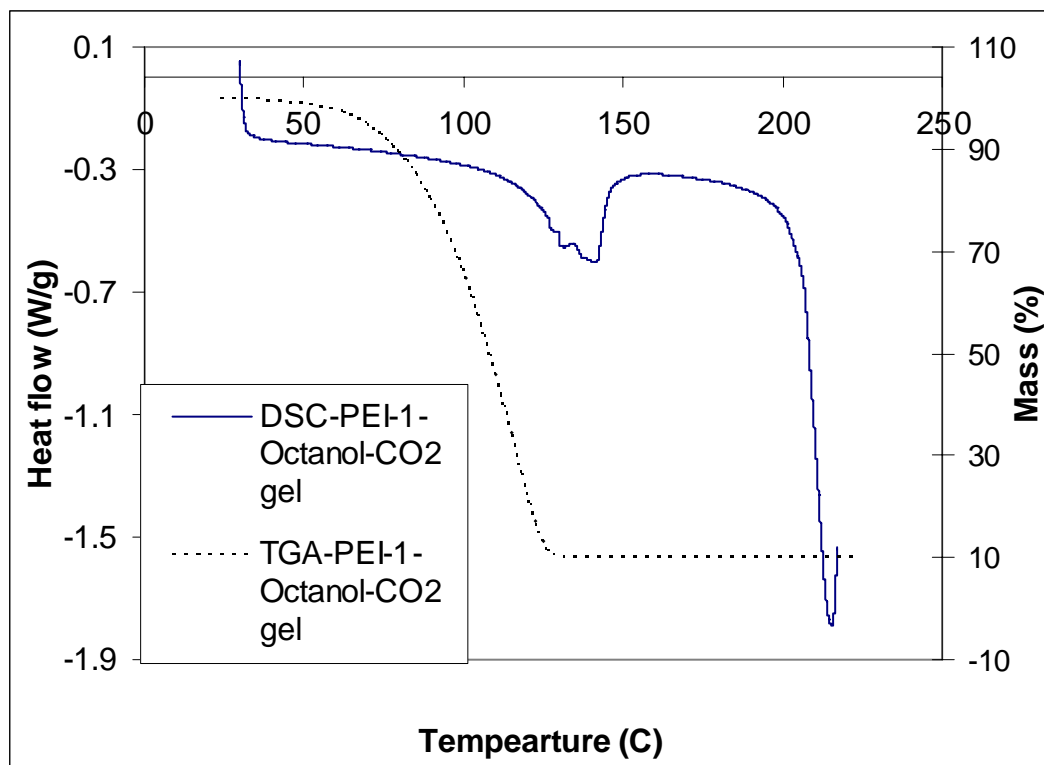
Fig 4.14: DSC-TGA of 10 %PEI-1200/CO_2/octanol gel

The DSC shows that reversal begins at 50°C. Two endothermic peaks at 130°C and 210°C (onset temperature) are also observed. The endotherm at 130°C indicates the reformation of original amine and carbon dioxide from ammonium carbamate species. This endotherm also shows a loss of mass of 27%, which is close to the amount of calculated CO_2 absorbed to form PEI/octanol/CO_2 gels. The peak at 210°C is due to the vaporization of 1-octanol (bpt 195°C) from the PEI-1-octanol solution. However, the TGA thermogram didn't exhibit two separate mass loss transitions because loss of CO_2 is obscured by the concurrent loss of 1-octanol present in the system through volatilization.

4.2.4 Conclusions from structural studies

By combining the NMR data and our weight analysis, we can postulate that PEI-octanol-CO_2 gels are formed by reaction of the primary amines in PEI with CO_2 to generate an ammonium carbamate salt matrix that traps octanol (**Fig 4.15**).
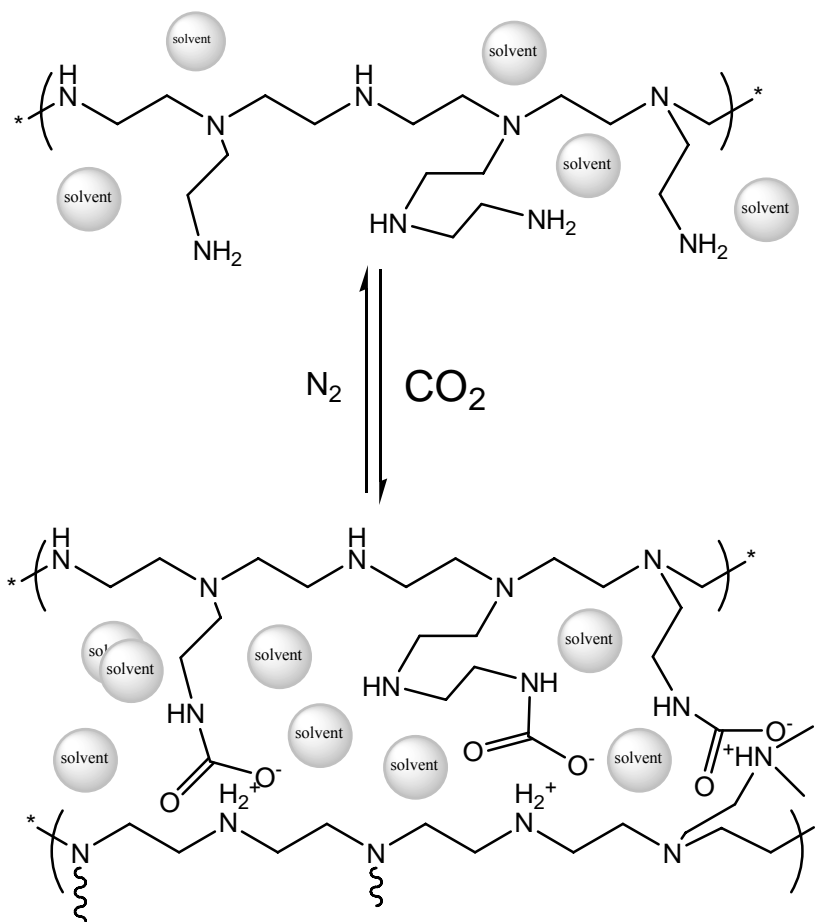
Fig 4.15: Structure of PEI/solvent/CO_2 gels

4.2.5 Morphology Studies

4.2.5.1 Cryo-HRSEM

Usually, preparation of HRSEM samples involves dehydration. This can change the morphology of samples since they can collapse or distort during dehydration. Cryo-HRSEM offers the opportunity of observation and microanalysis of samples under conditions that are closely related to their natural state. The preparation of the sample is a three-step process. The sample ($\sim$5μL) was first vitrified by rapidly submerging it in liquid ethane (-150°C). Cryo-immobilization is necessary to maintain the structural integrity of the gel samples under the extreme vacuum conditions (10^{-7} Torr) required for cryo-HRSEM. This ultra fast cooling process prevents any crystallization by nucleation in the sample and is preserved intact for observation. In the second step, the sample was cold-transferred into a cell to be chromium coated for high resolution. Finally, the cell was cold-transferred into the high vacuum atmosphere (10^{-7} Torr) of the electron microscope at low temperature (on the order of -180°C).[13] These data were obtained from IM&MF facilities at Emory University with the assistance of the late Dr. Robert Apkarian.

Cryo-HRSEM was used to study the morphology of the PEI-1200 gels. In a fresh sample of PEI/octanol/CO_2 gel, a bead-like arrangement is observed (**Fig 4.16**).
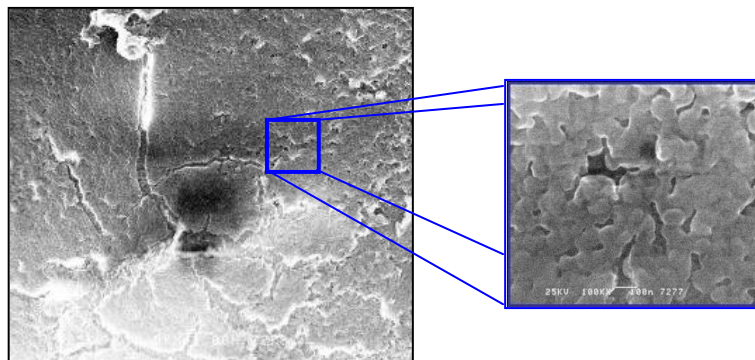
Fig 4.16: cryo-HRSEM of octanol/PEI/CO$_2$ gel

The average dimension of a single bead structure was around 100 nm. The PEI/octanol/CO$_2$ gel shows a "flooded" kind of structure, which was quite expected considering that PEI and CO$_2$ are minor components and octanol represents roughly 93 % of the sample. However, the observation of a two-week old sample shows amazing polymorphicity (**Fig 4.17**).
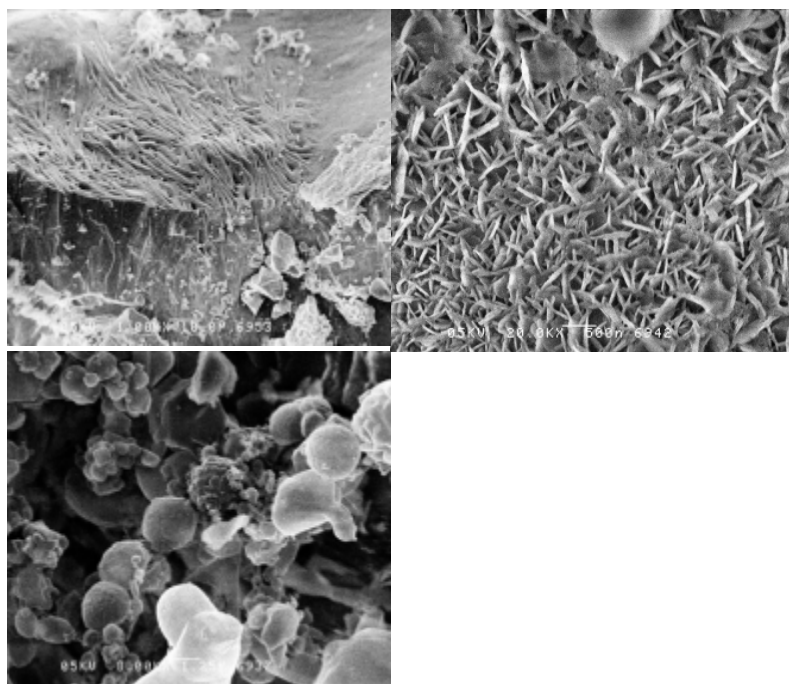
Fig 4.17: cryo-HRSEM of two-week old PEI/octanol/CO$_2$ gel

Indeed, thread, needles, and spheres were observed throughout the sample. The average dimension of the beads and needles were around 250 nm. It is believed that the gel is in a

metastable state, and crystallization starts to occur during the two weeks standing time, a common phenomenon with gels.

<u>4.2.5.2 SANS</u>

Neutron scattering techniques were also used to acquire information on the nanostructure of the gels. Small angle neutron scattering (SANS) spectroscopy can potentially provide critical information on the structure. It is typically used to measure size and shape of particles/aggregates in solution. It is a low energy non-invasive method which can penetrate the sample in depth, giving us clues about nuclear interactions, and is sensitive to small atoms (H, D, C, N). SANS also has the ability to contrast the neutron scattering length density of the gelled polymer and trapped 1-octanol because of the presence of hydrogen as a key component of the gel which has a strong scattering character.

Small Angle Neutron Scattering measurements of the PEI/octanol/CO_2 gels were performed on the NG-3 30 meter SANS at the NIST Center for Neutron Research (NCNR) in Gaithersburg, MD. A scattering vector, q, range of 0.003Å^{-1} to 0.43Å^{-1} was obtained using two sample to detector distances of 1.3m and 13m. A cold neutron source with an average wavelength of 6.0Å and a spread of 0.15 FWHM was used. The samples were contained in a demountable titanium cell with a sample path length of 1.0 mm and a circular cross section diameter of 19 mm. The samples were held between 2 quartz windows sealed with Teflon coated silicon o-rings. The sample cells were loaded into a 10 position heating/cooling block controlled using a circulating bath with a -15°C – 90°C temperature range. The scattering intensity data was collected using a mobile 2-

dimentional array detector and corrected for transmission, background and empty cell scattering. The 2-D data was radially averaged to give the scattering intensity, $I\,(q)$. The data reduction and analysis was performed using computer software and methods provided by NIST and run using IGOR Pro (Wavemetrics).[14] The common model, the Debye Function, was used to fit the data. In the Debye Function, the variables compared include: polymer volume fraction; scattering contrast; polymer volume; radius of gyration; and incoherent background. These variables are then compared to theoretical models of different shapes to indicate the morphology of the gel.

The gel samples were freshly prepared with varying weight percents (5, 7, 10, 15, and 20) of PEI-1200 solutions in 1-octanol. Gaseous CO_2 was then slowly bubbled through the solution at ambient temperature and pressure to form the gel. The gel could then be loaded into the sample cells. Reversal of the gel formation was achieved by slowly bubbling gaseous nitrogen through the gel to displace the CO_2, resulting in a liquid phase. The SANS data agreed with the cryo-HRSEM data, and indicated an observable structure (as opposed to an amorphous liquid) (**Fig 4.18**).
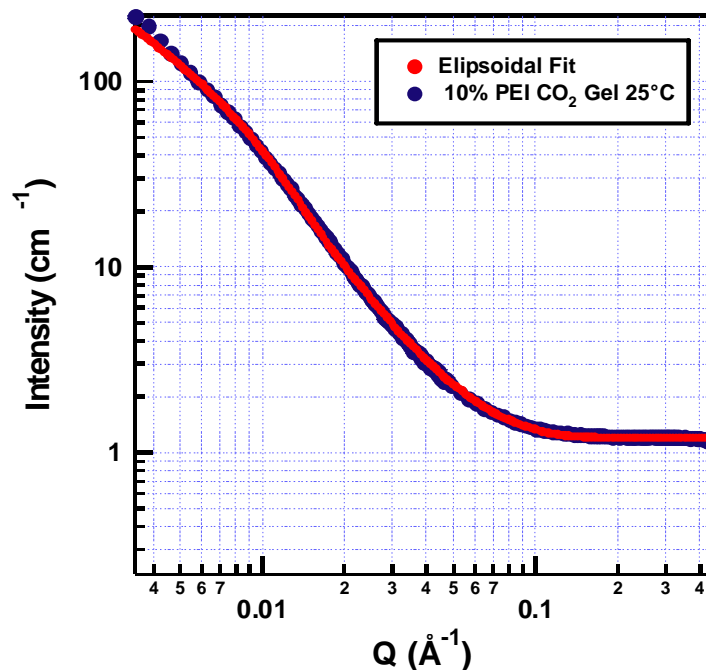
Fig 4.18: SANS data of PEI/octanol/CO₂ gel

Our PEI gels appear to have an ellipsoidal shape with half axis dimensions of 20.7 x 235x 1197 Å^3 (**Fig 4.19**).
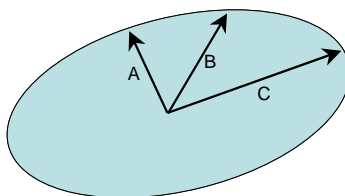
Fig 4.19: Ellipsoidal shape with dimensions A x B x C

The similarities in the scattering curves for the 7 and 10 wt % gels suggest a consistent structure fit by elliptical cylinders (**Fig 4.20**). At the higher 15 and 20 wt % gels, the scattering curves show slight differences and while the elliptical cylinder model provides an acceptable fit, the flexible elliptical cylinder seems to provide a better fit (not shown). This suggests that with increased polymer concentration, the elliptical cylinders become elongated and show contour along the length.
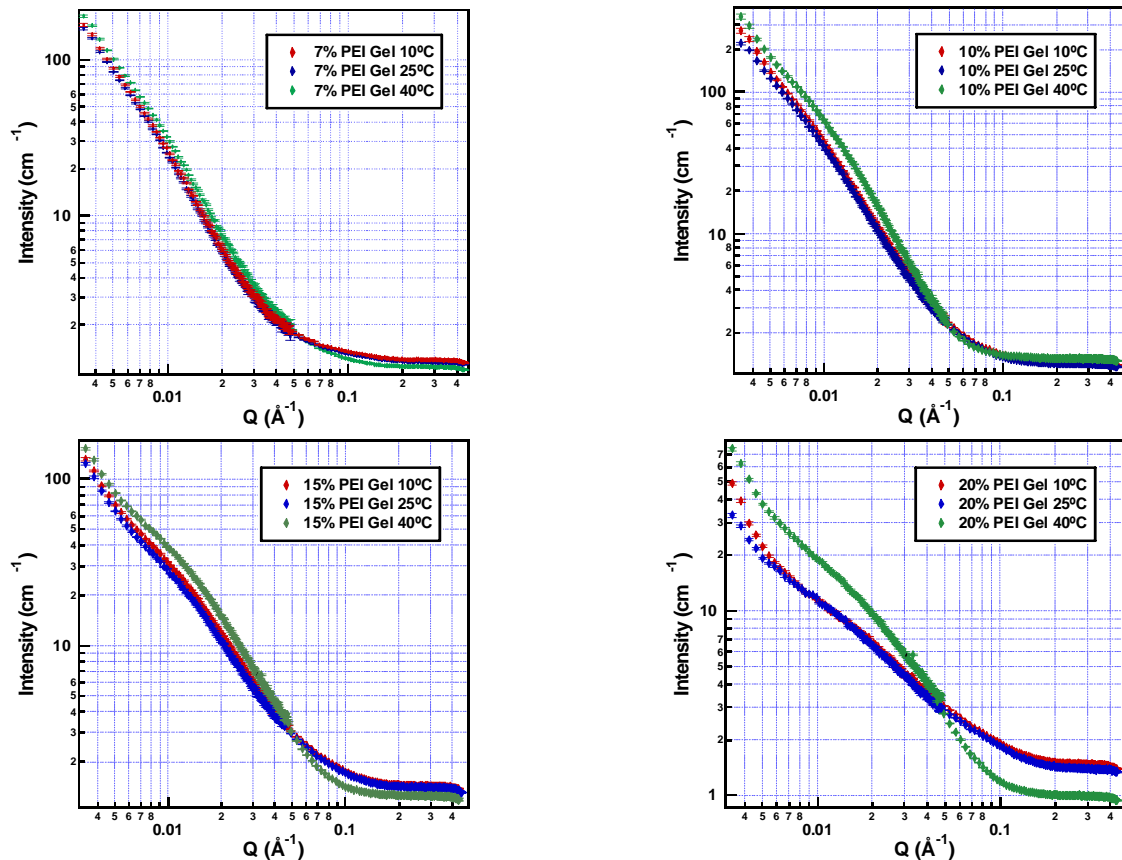
Fig 4.20: SANS of 7, 10, 15, 20% PEI-1200/octanol/CO2 gels at 10, 25, 40°C

Figure 4.20 also shows SANS results for the PEI gels over a temperature range from 10°C to 40°C. In most cases the scattering intensity was independent of temperature which suggests a lack of temperature induced structural changes within the gel. The exception is the 20 wt % PEI gel at 40°C, which shows an increase in the magnitude of the scattering curves slope. This change is indicative of some thermal structural transition that occurs in the gel at the higher PEI concentration.

The formation and reversal of a PEI/octanol/CO_2 gel was also further documented using SANS (**Fig 4.21**).
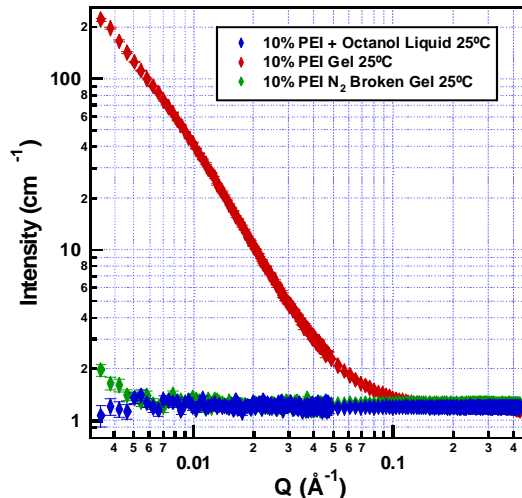
Fig 4.21: SANS of the formation and reversal of a PEI/octanol/CO_2 gel

The mixture of 10% PEI-1200 in octanol indicates that no scattering contrast was seen between the components of the polymer on the length scale probed by these measurements. This indicates a lack of structure. Upon addition of CO_2, the PEI-octanol-gel is formed, and structure is now seen. Finally, breaking the gel returns the amorphous liquid. This confirmed that a novel, reversible gel is formed from a solution of PEI-1200 and octanol upon the introduction of CO_2.

4.2.5.3 Conclusions of morphological studies

Cryo-HRSEM of fresh PEI/octanol/CO_2 gels revealed bead-like structures. The SANS results also suggest an elliptical structure. Similarly, both cryo-HRSEM and SANS data clearly indicate an ordered structure is created upon reaction with carbon dioxide. SANS results also demonstrate the reversibility of the gel, showing evidence of the formation of the gel structure and the absence of structure on gel reversal.

4.2.6 Potential for Drug Application

In the literature, it has already been proven that PEI could have possible drug delivery applications because of its interactions with DNA (encapsulation).[11, 12] Since PEI encapsulates DNA, we theorized that PEI would behave similarly in the presence of plain amino acids. Thus, we were interested in the behavior of a PEI/amino acid/octanol/ mixture with CO_2. As a proof of principle, the amino acid glutamic acid (1-2.2%) was added to solutions of octanol and PEI (5-15% of MW 1200). Upon the introduction of CO_2, gels were formed (**Table 4.7**).

Table 4.7: Combination and outcomes of PEI/amino acid/octanol/CO_2 mixtures

PEI-1200 (wt%)	Glutamic acid (wt%)	Solvent (wt%)	Physical state after adding CO_2
4.9%	1.6%	93.5%	Milk white gel
6.3%	2.2%	91.5%	Light white gel
7%	1%	92%	Milk white gel
15%	1%	84%	Milk white gel (not stable)

All gels formed were stable for two weeks, except for the 15 weight % PEI gel. The 15 weight % PEI gel dissolved overnight. The other gels were reversed in one hour at 80°C. This data indicates that amino acids (and possibly drug molecules) can be easily incorporated into PEI/octanol/CO_2 gels. Furthermore, this gel still degrades easily, which would allow straightforward release of potential drug molecules.

4.2.7 PEI/octanol/CO_2 gel Pellets

An alternative method of preparing the PEI/octanol/CO_2 gels was investigated. A solution of 10 weight % PEI-1200 in octanol was slowly pulsed into a pressurized chamber of liquid CO_2 at a rate of 0.15mL/min. As soon as the PEI/octanol mixture was in the presence of CO_2, cylinder-shaped pellets of PEI/octanol/CO_2 gel were immediately

formed. These pellets proved to be scoopable gel pellets that were easily collected (**Fig 4.22**).

Fig 4.22: Gel pellets of PEI/octanol/CO$_2$ gel

By modifying the flow of addition of solution or the shape of the tube feeding the solution into the chamber, the shapes of the gel pellets formed can be tuned to whatever shape or size pellets are desired.

4.3 Conclusions

Stable polyethyleimine-CO$_2$ gels have been synthesized with 1-octanol. PEI-1200 forms stable gels at 7-18 weight % with 1-octanol. Stable gels with 5-17 weight % PEI-600 and 4-15 weight % PEI-1800 in 1-octanol were also observed. All the PEI-1200/octanol/CO$_2$ gels were reversible. Carbamate formation by reaction between the primary amines in PEI and CO$_2$ was confirmed by ^{13}C NMR. c*ryo*-HRSEM studies show that freshly prepared PEI-1200 gels have an interconnected bead-like morphology which slowly changes with time to a polymorphic bead- and needle-like structure with average dimensions of 200 nm. Neutron scattering data for PEI-1200/octanol/CO$_2$ gels containing 10 weight % PEI-1200 suggests elongated ellipsoidal structure with a major axis dimension of 240 nm. The amino acid glutamic acid can successfully gel in mixtures of

PEI, 1-octanol, and CO_2. Together, these findings indicate that PEI-1200/octanol/CO_2

gels have potential as a possible drug carrier matrix for transdermal delivery applications.

4.4 Experimental

Materials

     The chemicals in these experiments were used without additional purification. The chemicals used in these experiments included: branched polyethyleneimine (PEI) (Polysciences Inc., 98%, molecular weights: 600, 1200 and 1800 containing 25 % primary amine, 50 % secondary amine and 25 % tertiary amine), 1-octanol (Aldrich, 99.9%), DMSO (Aldrich, 98%), silicon oil (Aldrich, 99.9%) and ^{13}C labeled CO_2 (Aldrich 99.99%, Isotech 99%).

Methods

     Synthesis of PEI/solvent/CO_2 gels. Mixtures of PEI (600, 1200, 1800) were made with various solvents. Gaseous CO_2 was then slowly bubbled through the solution at ambient temperature and pressure to form the gel. Any gels that formed were held upside down for twenty seconds. If the gel did flow to the bottom of the flask, this confirmed gel formation. Solutions that did not immediately gel were heated to 50°C and allowed to cool.

Results of PEI/solvent/CO_2 mixtures:

Table 4.1: PEI-1200 Combinations with alcohols and outcomes after reaction with CO_2

Weight% of PEI-1200	Weight % of solvent	Physical state after adding CO_2
5-15%	95-85% EtOH	Milky white precipitate
17-44%	83-56% EtOH	Opaque gel (not stable)
60-80%	40-20% EtOH	No change - clear liquid
5-44%	95-56% iPrOH	Milky white precipitate
60-80%	40-20% iPrOH	No change - clear liquid
5-44%	95-56% tBuOH	Milky white precipitate
60-80%	40-20% tBuOH	No change - clear liquid
1-5%	99-95% OctOH	Opaque liquid
7-18%	93-82% OctOH	Stable opaque gel
20-35%	80-65% OctOH	Opaque gel (not stable)
36-55%	64-45% OctOH	Milky white precipitate
60-100%	40-0% OctOH	No change - clear liquid

Table 4.2: PEI-600 Combinations with alcohols and outcomes after reaction with

CO$_2$

Weight% of PEI-600	Weight % of solvent	Physical state after adding CO$_2$
5-40%	95-60% EtOH	Milky white precipitate
60-80%	40-20% EtOH	No change - clear liquid
5-15%	95-85% iPrOH	Milky white precipitate
20%	80% iPrOH	Opaque gel (not stable)
40-80%	60-20% iPrOH	No change - clear liquid
5-15%	95-85% tBuOH	Milky white precipitate
20%	80% tBuOH	Opaque gel (not stable)
40-80%	60-20% tBuOH	No change - clear liquid
5-17%	95-83 OctOH	Stable opaque gel
20-40%	80-60% OctOH	Opaque gel (not stable)
60-80%	40-20% OctOH	No change - clear liquid

Table 4.3: PEI-1800 Combinations with alcohols and outcomes after reaction with CO$_2$

Weight% of PEI-1800	Weight % of solvent	Physical state after adding CO$_2$
5-40%	95-60% EtOH	Milky white precipitate
60-80%	40-20% EtOH	No change - clear liquid
5-15%	95-85% iPrOH	Milky white precipitate
20%	80% iPrOH	Opaque gel (not stable)
40-80%	60-20% iPrOH	No change - clear liquid
5-10%	95-90% tBuOH	Milky white precipitate
15-20%	85-80% tBuOH	Opaque gel (not stable)
40-80%	60-20% tBuOH	No change - clear liquid
4-15%	96-85% OctOH	Stable opaque gel
20-40%	80-60% OctOH	Opaque gel (not stable)
60-80%	40-20% OctOH	No change - clear liquid

Table 4.4: PEI-1200 Combinations with solvents and outcomes after reaction with CO_2

Weight% of PEI-1200	Weight % of solvent	Physical state after adding CO_2
5-44%	95-56% EtOAc	Milky white precipitate
60-80%	40-20% EtOAc	No change - clear liquid
5-44%	95-56% MEK	Milky white precipitate
60-80%	40-20% MEK	No change - clear liquid
5-15%	95-85% DMSO	Viscous clear liquid
17-25%	83-75% DMSO	Opaque gel (not stable)
29-80%	71-20% DMSO	Milky white precipitate

Table 4.5: PEI-600 Combinations with solvents and outcomes after reaction with

CO_2

Weight% of PEI-600	Weight % of solvent	Physical state after adding CO_2
5-15%	95-85% EtOAc	Milky white precipitate
20-40%	80-60% EtOAc	Opaque gel (not stable)
60-80%	40-20% EtOAc	Viscous clear liquid
5-15%	95-85% MEK	Milky white precipitate
20-40%	80-60% MEK	Opaque gel (not stable)
60-80%	40-20% MEK	No change - clear liquid
5-20%	95-80% DMSO	Milky white precipitate
40-80%	60-20% DMSO	No change - clear liquid

Table 4.6: PEI-1800 Combinations with solvents and outcomes after reaction with CO$_2$

Weight% of PEI-1800	Weight % of solvent	Physical state after adding CO$_2$
5-40%	95-60% EtOAc	Milky white precipitate
60-80%	40-20% EtOAc	Viscous clear liquid
5-15%	95-85% MEK	Milky white precipitate
20-40%	80-60% MEK	Opaque gel (not stable)
60-80%	40-20% MEK	No change - clear liquid
5-20%	95-80% DMSO	Milky white precipitate
40-80%	60-20% DMSO	No change - clear liquid

Reversal of PEI/solvent/CO$_2$ gels. Gels were heated in a sand bath (50°C, 80°C) with stirring under nitrogen, or stirred under vacuum (16h) to reverse them to PEI/solvent mixtures.   Results are reported in Tables.

NMR Study. NMR spectra were obtained from a Bruker DRX 500, Bruker AMX 400, and Varian-Mercury VX400 MHz spectrometer. ^{13}C spectra were collected at 100.58 MHz with a standard pulse sequence. The samples were run neat. We prepared the gel samples directly in the NMR tubes for analysis. The ^{13}C spectra were calibrated to external CDClB$_3$ at 77 ppm. The ^{15}N spectra were calibrated to external nitromethane. For the samples run in the Bruker AMX 400, a 10mm probe was used to enhance the size

of the peaks.   Neat mixtures of 20% PEI (MW 600, 1200, 1800) in 1-octanol were studied before addition of $^{13}CO_2$, after addition of $^{13}CO_2$, and after vacuum-induced gel reversal.

*Thermal Analysis. T*hermal analyses studies were performed on TA instruments Differential Scanning Calorimeter (DSC) Model Q20 and Thermogravimetric Analyzer (TGA) Model Q50. Gel samples were heated at 10°C/ min for both DSC and TGA analyses. DSC experiments were performed in hermetically sealed pans.

*Cryo-High Resolution Scanning Electron Microscopy (Cryo-HRSEM). C*ryo-HRSEM micrographs were taken on the Gatan CT-3500 cold stage used with In-Lens130F at IM&MF facilities at Emory University, Atlanta.   Electron microscopy requires extreme vacuum conditions (10^{-7} Torr). In order to maintain the structural integrity of the gel samples they were cryo-immobilized before observation.   The preparation of the sample is a three-step process. The sample (~5μL) was first vitrified by rapidly submerging it in liquid ethane (-150°C).   This ultra fast cooling process prevents any crystallization by nucleation in the sample and is preserved intact for observation. It is advisable to produce some shallow fractures, usually by just scraping the surface of the specimen with a cold-knife. In the second step, the sample was cold-transferred into a cell to be chromium coated for high resolution. The sample was sputtered with a 1-2 nm thick chromium film, without etching. Additionally, low accelerating voltage (5keV) may be utilized to limit deterioration of delicate samples. Finally, the cell was cold-transferred into the high vacuum atmosphere (10^{-7} Torr) of the electron microscope at low temperature (on the order of -180°C).[13]   These data were

obtained from IM&MF facilities at Emory University with the assistance of the late Dr. Robert Apkarian.

Small Angle Neutron Scattering (SANS). Small Angle Neutron Scattering measurements of the PEI/1-octanol/CO_2 gels were performed on the NG-3 30 meter SANS at the NIST Center for Neutron Research (NCNR) in Gaithersburg, MD. A scattering vector, q, range of 0.003Å^{-1} to 0.43Å^{-1} was obtained using two sample to detector distances of 1.3m and 13m. A cold neutron source with an average wavelength of 6.0Å and a spread of 0.15 FWHM was used. The samples were contained in a demountable titanium cell with a sample path length of 1.0 mm and a circular cross section diameter of 19 mm. The samples were held between 2 quartz windows sealed with Teflon coated silicon o-rings. The sample cells were loaded into a 10 position heating/cooling block controlled using a circulating bath with a -15°C – 90°C temperature range. The scattering intensity data was collected using a mobile 2-dimentional array detector and corrected for transmission, background and empty cell scattering. The 2-D data was radially averaged to give the scattering intensity, $I(q)$. The data reduction and analysis was performed using computer software and methods provided by NIST and run using IGOR Pro (Wavemetrics).[14]

The gel samples were freshly prepared with varying weight percents (5, 7, 10, 15, and 20) of PEI-1200 solutions in 1-octanol. Gaseous CO_2 was then slowly bubbled through the solution at ambient temperature and pressure to form the gel. The gel could then be loaded into the sample cells. Reversal of the gel formation was achieved by slowly bubbling gaseous nitrogen through the gel to displace the CO_2, resulting in a liquid phase. The SANS analysis includes the liquid PEI – 1-octanol solutions, the

corresponding gels and the liquid remaining following gel reversal. Temperature effects on the gels were also investigated at 10°C, 25°C, and 40°C.

Synthesis of PEI/amino acid/octanol/CO$_2$ gels.   The same procedure as the synthesis of PEI/solvent/CO$_2$ *gels* was followed; with the exception that glutamic acid was added before introduction of CO$_2$.

Reversal Synthesis of PEI/amino acid/octanol/CO$_2$ gels. The gels were reversed by stirring in a sand bath (80°C) under N$_2$.

Formation of PEI/octanol/CO$_2$ gel pellets. A 10 weight % mixture of PEI-1200 in octanol was premixed. Liquid CO$_2$ was added via an isco pump (973psi) to a windowed Jergenson cell and allowed to equilibrate. The 10% PEI-1200/octanol mixture was added at a rate of 0.15ml/min. Once in the presence of liquid CO$_2$, gel pellets immediately formed.

4.5 References

1.	Hoffmann, H., *Fascinating phenomena in surfactant chemistry.* Advances in Colloid and Interface Science, 1990 **32**(2-3): p. 123-150.

2.	Jordan, L.D., ed. *Colloid Chemistry.* The Chemical Catalog Co, ed. J. Alexander. Vol. 1, p767. 1926: New York.

3.	Pierre Terech and Richard G. Weiss, *Low Molecular Mass Gelators of Organic Liquids and the Properties of Their Gels.* Chemical Reviews, 1997. **97**: p. 3133-3159.

4.	David J. Abdallah, Richard G. Weiss, *Organogels and Low Molecular Mass Organic Gelators.* Advanced Materials, 2000. **12**(17): p. 1237-1247.

5.	Schroth, Werner; Andersch, Joerg, *Dimethylammonium dimethylcarbamate - a useful reagent for the Willgerodt-Kindler reaction.* Synthesis 1989 **3**: p. 202-4.

6.	Mathew George and Richard G. Weiss, *Chemically Reversible Organogels: Aliphatic Amines as "Latent" Gelators with Carbon Dioxide.* JACS, 2001. **123**: p. 10393-10394.

7.	Mattew George, Richard G. Weiss, *Primary Alkyl Amines as Latent Gelators and Their Organogel Adducts with Neutral Triatomic Molecules.* Langmuir, 2003. **19**: p. 1017-1025.

8.	Emiliano Carretti, Luigi Dei, Piero Baslioni, Richard G. Weiss, *Synthesis and Characterization of Gels from Polyallyamine and Carbon Dioxide as Gellant.* JACS, 2003. **125**: p. 5121-5129.

9.	G. V. Rama Rao, T. Konishi, N. Ise, *Ordering in Poly(allylamine hydrochloride) Gels.* Macromolecules, 1999. **32**: p. 7582-7586.

10.	Samanta, S., in *Dept of Chemistry.* 2007, Georgia Tech: Atlanta, GA.

11.	Senaratne, W., L. Andruzzi, et al, *Self-Assembled Monolayers and Polymer Brushes in Biotechnology: Current Applications and Future Perspectives.* Biomacromolecules, 2006. **6**(5): p. 2427-2448.

12.	Akin Akinc, Mini Thomas, Alexander M. Klibanov, Robert Langer, *Exploring polyethylenimine-mediated DNA transfection and the proton sponge hypothesis.* The Journal of Gene Medicine, 2005. **7**(5): p. 657-663.

13.	Dubochet, J., Adrian, M., Chang, J. J., Homo, J. C., Lepault, J., McDowall, A. W., Schultz, P., *Cryo-Electron Microscopy of Vitrified Specimens.* Quarterly Reviews of Biophysics, 1988. **21**(2): p. 129-228.

14.   Kline, S.R., *Reduction and analysis of SANS and USANS data using IGOR Pro.* Journal of Applied Crystallography, 2006. **39**: p. 895-900.

CHAPTER 5
RECOMMENDATIONS

5.1 Recommendations for Chapter 1: Switchable Room Temperature Ionic Liquids

Although we have not yet found an optimal application, our novel switchable room temperature ionic liquids are quite exciting (**Fig 5.1**).
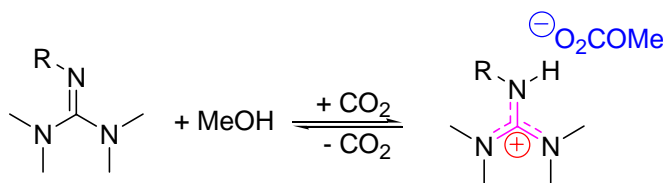
Fig 5.1: Formation of switchable ionic liquid 2-butyl-1,1,3,3-tetramethylguanidium methylcarbonate (TMBG MC IL) from 2-butyl-1,1,3,3-tetramethylguanidine (TMBG) and methanol

We have seen some excellent results in experiments involving bitumen and SO_2. It is in these two arenas that I believe our guanidine-based ILs will excel. Additionally, there are some other interesting areas of research that have yet to be explored that I will discuss.

5.1.1 Further investigation of purifying bitumen and oil shale

In Chapter **1**, initial experimental results indicated that TMBG MC IL was capable of separating alkanes from inorganic impurities. It was theorized that bitumen (a mixture of alkanes and inorganic impurities) could be dissolved in TMBG (**Fig 5.2**). After methanol and CO_2 were added to the mixture, the alkanes (insoluble in TMBG MC IL) would phase separate from the impurity-laden TMBG MC IL. The alkanes could then be further processed for fuel needs, and the TMBG MC IL could be reversed and purified for reuse.
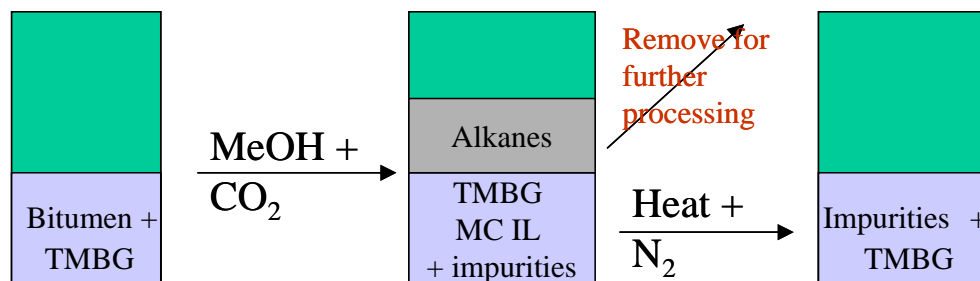
Fig 5.2: Separation of octane from bitumen

It was observed that when bitumen is dissolved in TMBG and phase separated with methanol and CO_2, the TMBG MC IL darkens in color while the bitumen is less viscous (**Fig 5.3**).
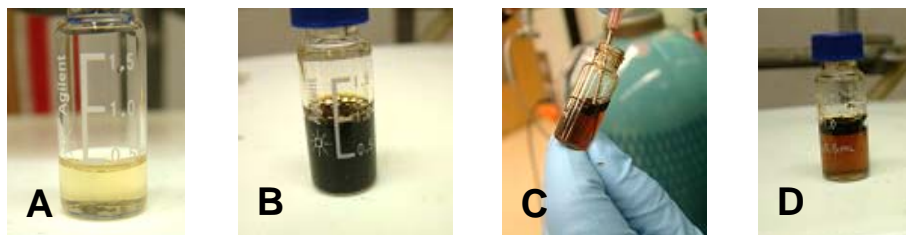
Fig 5.3: Separation of bitumen from TMBG via formation of TMBG MC IL, where A is TMBG; B is TMBG + bitumen mixture; C is CO_2 being bubbled into TMBG + bitumen mixture; and D is bitumen phase separated from TMBG MC IL

Because of the solubility characteristics of TMBG MC IL, and changes in color and viscosity, it is believed that the inorganic impurities in bitumen remain dissolved in the TMBG MC IL. To prove this, inorganic studies are necessary. Atomic absorption can be used to analyze the inorganic components of bitumen samples before and after treatment with our TMBG MC IL system. This would irrefutably show whether or not our TMBG MC IL system can be used to purify bitumen.

5.1.2 Further investigation of TMBG MS IL

We have shown with DSC-TGA data that an equimolar solution of methanol and TMBG can react with both CO_2 and SO_2 to form guanidinium methyl carbonates and sulfites, respectively (**Fig 5.4**).
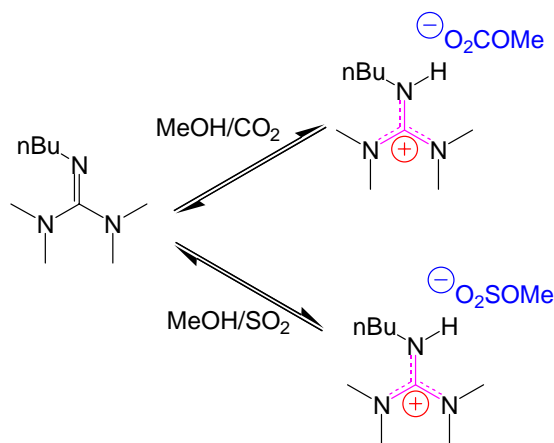
Fig 5.4: Formation of TMBG MS IL and TMBG MC IL

Although TMBG MS IL visually appears to be a RTIL, conductivity tests need to be done to prove that TMBG MS IL is indeed a switchable RTIL. Any conductivity meter that is used will need to withstand high temperatures (reversal takes place at $160^{\circ}C$) and the corrosive effects of free SO_2. Once the necessary equipment is found, it can be easily proven that TMBG MS IL is, indeed, an ionic liquid.

The absorption and release of SO_2 are commercially interesting,[1] yet the cost of TMBG deters its use commercially. Thus, a cheaper starting material needs to be found that undergoes the same reaction with SO_2 and methanol as TMBG. An easy way to cut costs would be to use a commercially available starting material such DBU and piperidine. Our group has previously shown that DBU reacts with alcohols and CO_2 to form switchable ILs,[2] so it is expected that DBU will react similarly with SO_2. While piperidine has never been tested with any alcohols and CO_2, it would still be interesting

to see if it reacts with SO_2 because the low cost of piperidine makes it a very attractive solvent (**Fig 5.5**).[3]
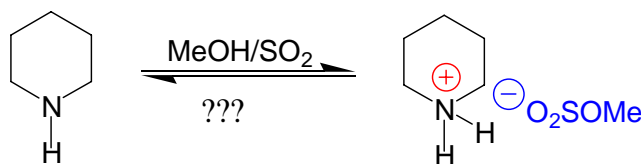
Fig 5.5: Possible synthesis of piperidine-based MS IL

5.1.3 Synthesis of biodiesel

In the synthesis of biodiesel, bioesters (bio-oils) undergo transesterification in the presence of methanol and sodium hydroxide (**Fig 5.6**).
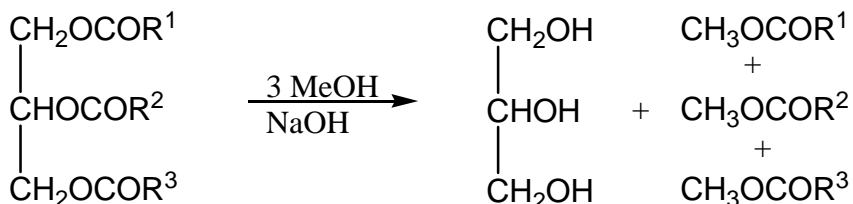
Fig 5.6: Formation of bioesters by base-catalyzed reaction with methanol

A high ratio of methanol to oil is required for transesterification.[4] The high ratio of methanol also helps the glycerol that is formed phase separate (**Fig 5.7**). Once the glycerol phase separates from the biodiesel, the biodiesel is purified via water washing, vacuum drying, and filtration. The energy intensive purification of the biodiesel is one of the many reasons its processing is not energy efficient.
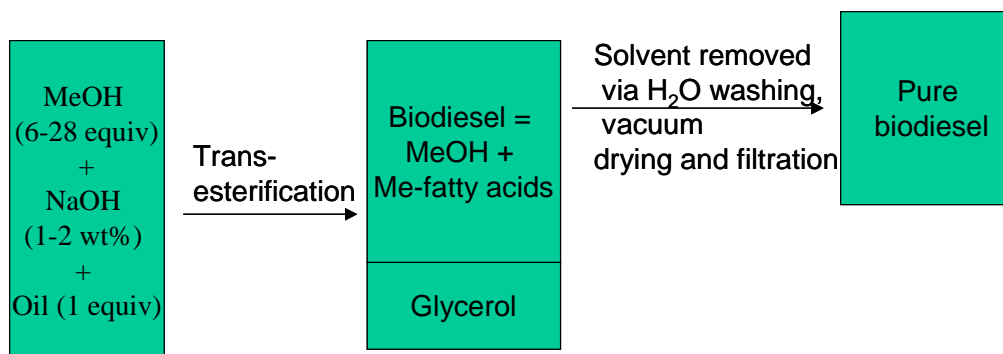
Fig 5.7: Synthesis of Biodiesel

One means to increase the efficiency of biodiesel processing is to make the isolation of pure biodiesel more straightforward. A way to achieve this would be to add TMBG and CO_2 to the biodiesel (**Fig 5.8**).
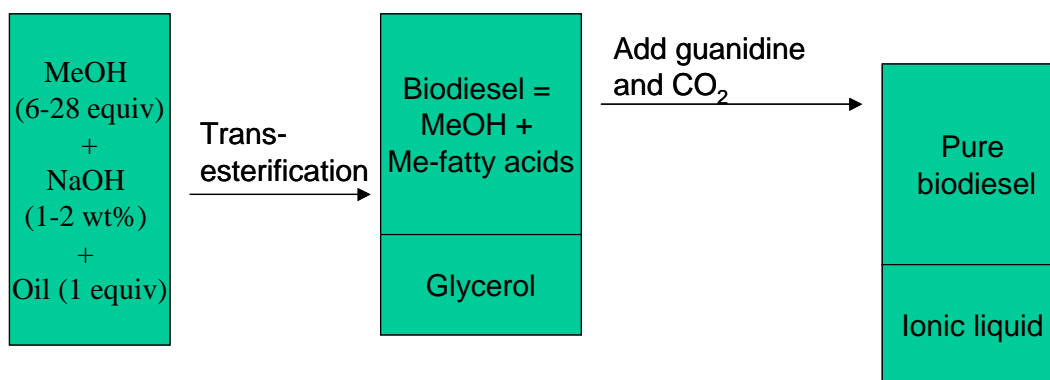
Fig 5.8: Synthesis of biodiesel using TMBG MC IL to ease separation/isolation of biodiesel

Upon formation of the TMBG MC IL, pure biodiesel can be easily separated from its contaminants. This method also leads to a reduction in water waste since washing and filtration are no longer necessary. Furthermore, other researchers have demonstrated that common biodiesel methyl esters [methyl oleate (olive oil) and methyl palmitate (palm oil)] are soluble in hexane.[5, 6] Since non-polar solvents such as hexane are insoluble in TMBG MC IL, it is expected that the biodiesel will easily phase separate from TMBG MC IL with little cross-contamination.

Another means to improve the efficiency of biodiesel processing would be to reduce the amount of methanol used. Since glycerol is a triol, it is expected to react with TMBG in the same manner as all alcohols: a guanidinium glycylcarbonate (TMBG GC IL) will be formed (**Fig 5.9**).
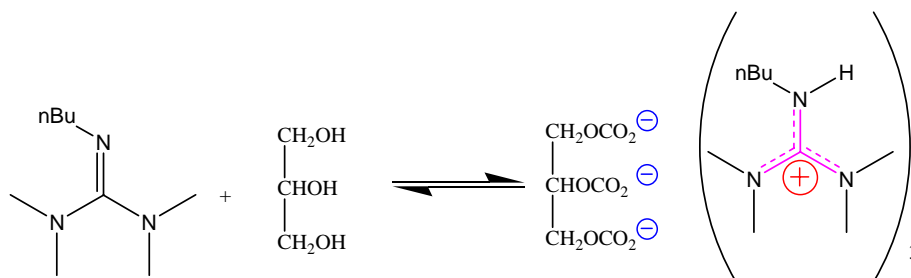
Fig 5.9: Generation of guanidinium glycylcarbonate IL

If TMBG GC IL can be formed, the amount of methanol used may be reduced. However, transesterification requires larges excesses of methanol in general.[7] The amount of methanol used will have to be balanced between using enough to ensure efficient transesterification while minimizing waste.

Previous research has also demonstrated that larger amounts of base increase the rate of transesterification,[4] but excessive amounts of sodium hydroxide precipitates out of methanol. TMBG is an excellent base that should dissolve bio-oils. Thus, TMBG can be potentially used as both the base and the solvent in the transesterification step of biodiesel processing. Upon completion of the reaction, CO_2 would be added to form TMBG MC IL and to phase separate the biodiesel (**Fig 5.10**).
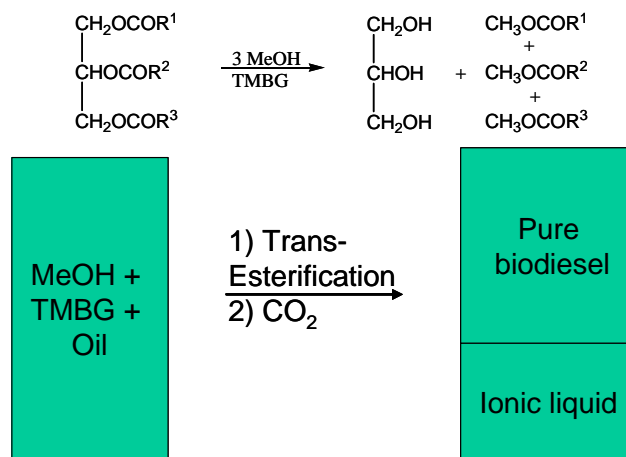
Fig 5.10: Generation of biodiesel using TMBG as both the reaction solvent and the base

Guanidine ($NH_2C(=NH)NH_2$) has already been demonstrated to be an effective base for the methanolysis of bioesters Peter and Weidner.[7] The addition of guanidine to a solution of methanol and a bioester (*e.g.*, grapeseed, soybean, and palm oils) under reflux resulted in high conversions (89.1 – 99%), but they were unable to recycle the guanidine catalyst. It was also necessary to degum the oils before use, an extra purification step. The TMBG MC IL would be a more efficient system because the basic catalyst is not only used as the solvent and base, it could also be recycled and reused. Furthermore, from our results with bitumen and crude oil, we know that gummy mixtures can be dissolved in TMBG, so degumming would not be necessary.

Finally, the most efficient means of biodiesel processing would generate pure biodiesel directly from the bio-oil source (*i.e.* soybeans for soybean oil). Haas and co-workers demonstrated that pulverized soy beans stirred in alkaline methanol removed 95% of soybean oil and transesterified 84% of that extracted oil in only eight hours.[8] Conventional purification methods were applied to yield pure biodiesel (water washing,

vacuum drying, and filtration). If our TMBG MC IL system were applied as the extraction solvent, base catalyst, and means of separation, the overall efficiency of biodiesel processing could be greatly improved (**Fig 5.11**).
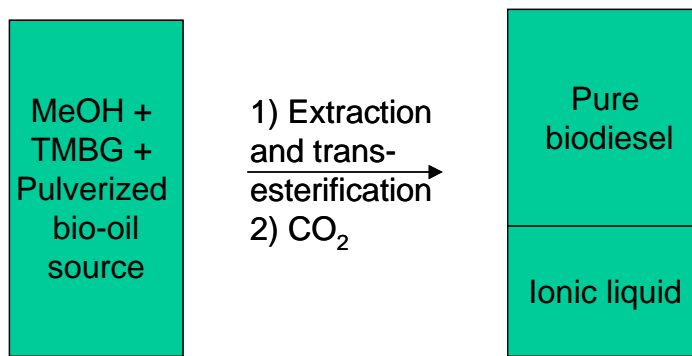
Fig 5.11: Generation of biodiesel using TMBG as both the reaction solvent and the base, but with a pulverized bio-oil source

5.1.4 Reaction with amines

Yamada *et al.* found that N,N-dimethyl-N'-hexyl ethanimidamide formed a reversible RTIL with n-butylamine and CO_2 (**Fig 5.12**).[9]
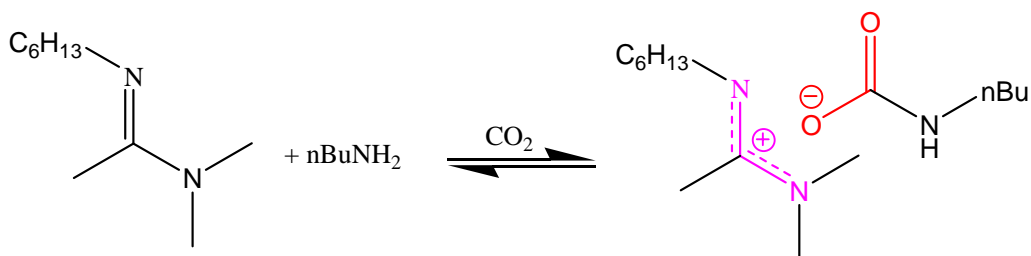
Fig 5.12: Reaction of N,N-dimethyl-N'-hexyl ethanimidamide, n-butylamine, and CO_2 to form RTIL

Furthermore, when 3wt% of water was added to this RTIL, the authors report never observing cloudiness. This cloudiness usually indicates the formation of amidinium carbonates from residual water. It would be of interest to investigate the reactivity of

161

TMBG with amines in the presence of CO_2 (**Fig 5.13**). If guanidinium amine-carbonates are more stable to water contamination, this would lead to more opportunities for reactions that generate or require water (*i.e.* Suzuki reactions, condensations).
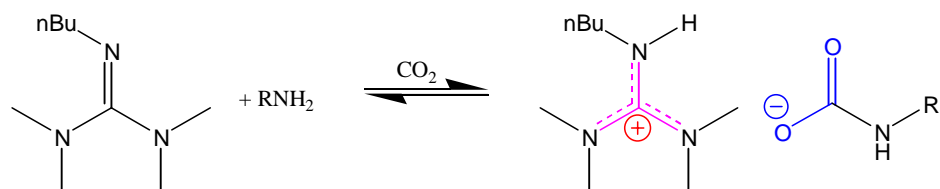
Fig 5.13: Formation of 2-butyl-1,1,3,3-tetramethylguanidium alkylcarbamate

5.2 Recommendations for Chapter 2: Piperylene Sulfone

Piperylene sulfone (PS) is a dipolar, aprotic solvent that can be switched to allow for an easy product recovery and solvent regeneration (**Fig 5.14**).
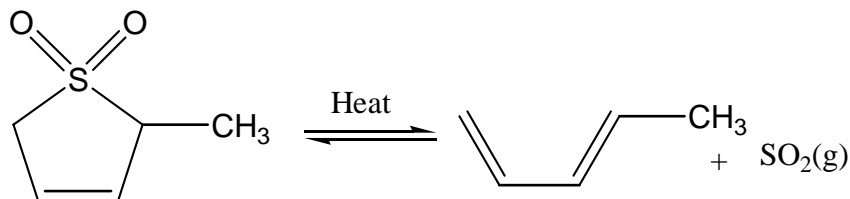
Fig 5.14: Reversal of PS to generate SO$_2$ and trans-piperylene

Anionic nucleophilic substitution reactions have been performed in PS. The products were isolated in high yields after decomposition of PS, and then the PS was reformed from recovered piperylene and SO$_2$ for reuse (**Fig 5.15**).
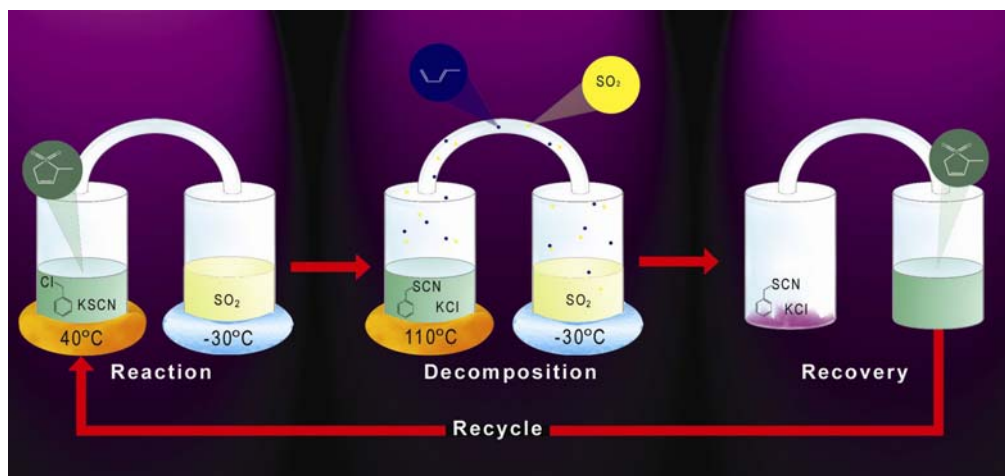
Fig 5.15: Illustration of complete process using PS

In the future, we can demonstrate the versatility of the piperylene sulfone process for a wide range of industrially important reaction types. Such a range of applications would be necessary for multistep processing. Examples of potential reactions that could demonstrate this use of a "smart solvent" with the separation "built-in" are shown in Figure **5.16**. The list includes an oxidation reaction, several reduction reactions, a

condensation reaction, and an addition reaction. In each case, we shall use the PS solvent for reaction, followed by decomposition of the piperylene sulfone for separation and product purification, with subsequent reformulation and reuse of the piperylene sulfone solvent.
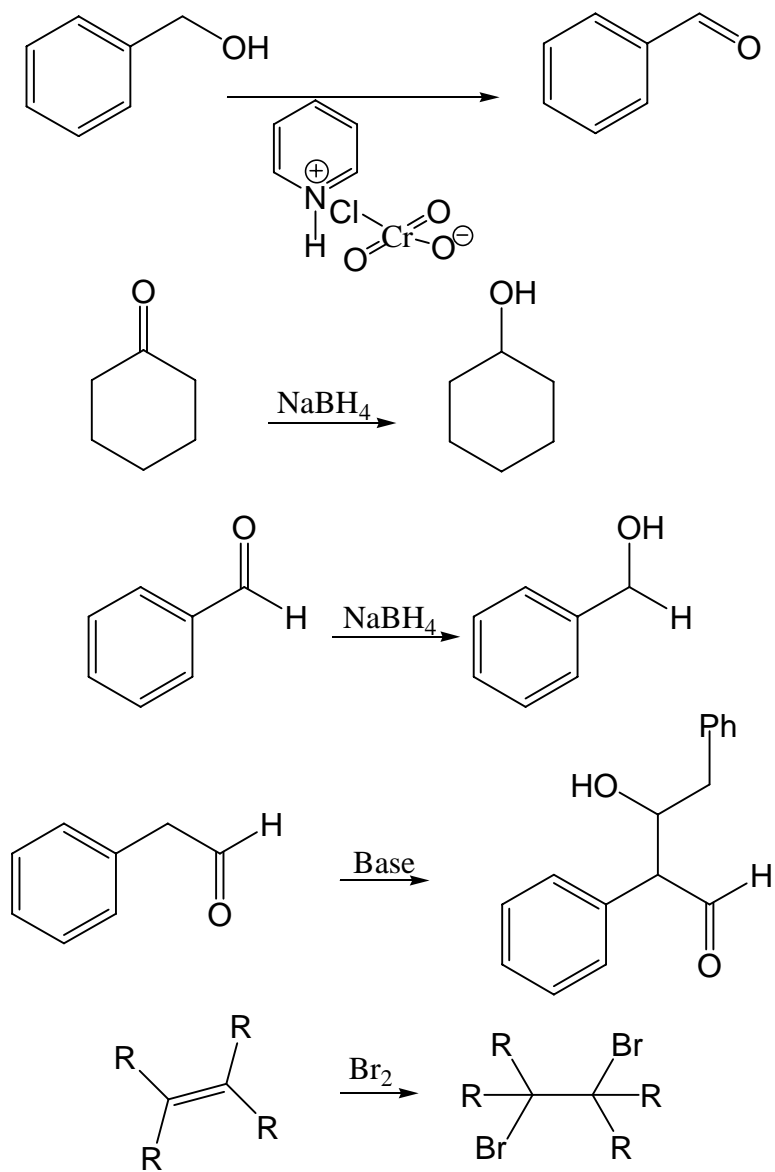
Fig 5.16: Possible reactions to test in PS

5.3 Recommendations for Chapter 3: Recycling homogeneous catalyst: Fluorous/GXL system

In Chapter **3**, we were able to develop a novel fluorous immobilized system based upon CO_2-gas-expanded liquid (GXL) chemistry. The fluorous immobilized phase consists of silica that has been fluorinated with perfluoropolyether tails (F-silica). It was demonstrated that our F-silica and a fluorinated catalyst could be used to achieve homogeneous catalysis even though we start with a heterogeneous system. In the absence of CO_2, the fluorophilic species congregate. It is believed that the fluorinated tails on the surface of the silica reversibly adsorb the perfluorinated catalyst species as shown in Figure **5.17**. Upon the addition of CO_2 and formation of the GXL, the fluorophilic nature of CO_2-expanded liquids causes the fluorinated tails on the silica to extend and release the fluorinated catalyst into the now fluorophilic solution.
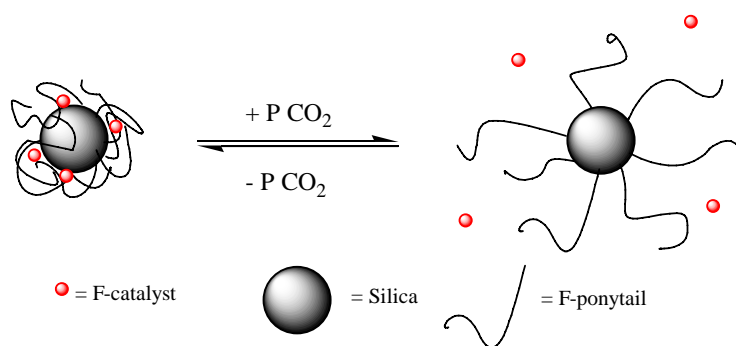
Fig 5.17: Behavior of immobilized fluorous phase with CO_2

The fluorous catalyst we used was F-MonoPhos (**8**) (**Fig 5.18**).
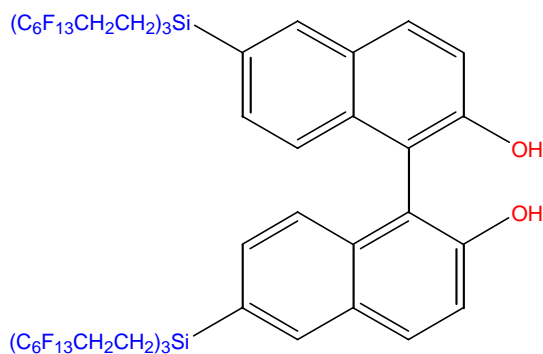
Fig 5.18: F-MonoPhos (8)

The fluorous immobilized system was tested on the asymmetric hydrogenation of α-acetamidocinnamic acid methyl ester (**Fig 5.19**).
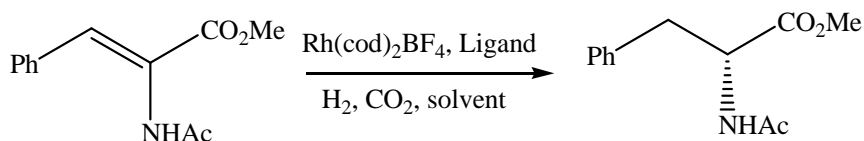
Ligand = F-Monophos (**8**) or Monophos
PCO_2 = 60 bar, PH_2 = 110 bar
Solvents = EtOAc, Hexane, Dioxane

Fig 5.19: Hydrogenation of α-acetamidocinnamic acid methyl ester using F-immobilized phase and GXL

Our results indicated that there was a problem with the combination of our F-MonoPhos (**8**) catalyst and F-silica; when combined we saw a complete loss of ee which was not observed when the F-MonoPhos and the F-silica were tested separately. One reason for this could be that the F-ligand is not strongly bound to the metal center, which decreases enantioselectivity. We theorize that a catalyst that has a strong bond between the metal center and the ligand may fare better in our fluorous immobilized system. A commercially relevant reaction that has a metal that strongly binds to its ligands is the asymmetric hydrogen transfer reaction, specifically hydrogen transfer with acetophenones for the formation of chiral secondary alcohols (**Fig 5.20**).[10]

166
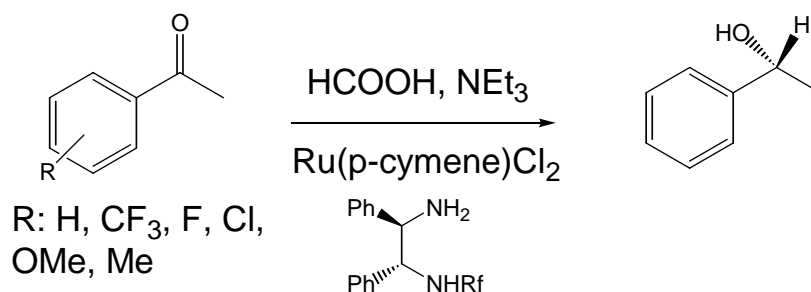
Fig 5.20: Asymmetric hydrogen transfer reaction

In this reaction, the Ru catalyst is formed *in-situ* by reacting the ligand with Ru precursor, Ru(p-cymene)Cl$_2$ (**Fig 5.21**).
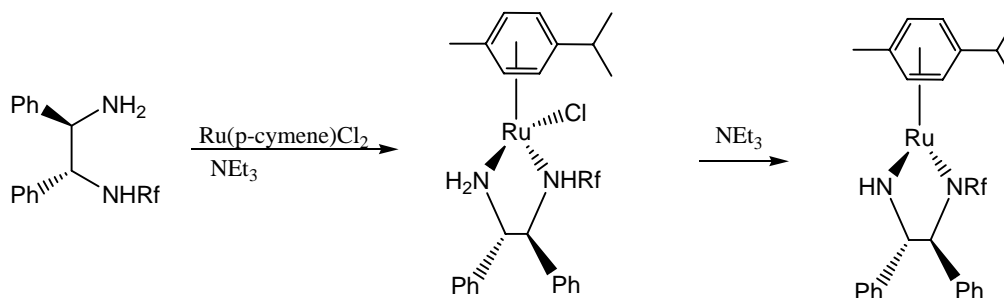
Fig 5.21: Ru catalyst formed in-situ in asymmetric hydrogen transfer reaction

This ruthenium catalyst has a strong bond between the Ru center and the ligand, making it a better candidate for recycling than F-MonoPhos (**8**). The asymmetric hydrogen transfer reaction is commercially relevant because pharmaceutical and advanced materials manufacturers often require optically active secondary alcohols for their synthetic schemes.

The fluorinated chiral amine we would investigate is (1,1,2,2,3,3,4,4,5,5,6,6,7,7,8,8,8-heptadecafluoro-octane-1-sulfonic acid (2-amino-1,2-diphenyl-ethyl)-amide) as shown in Figure **5.22**.
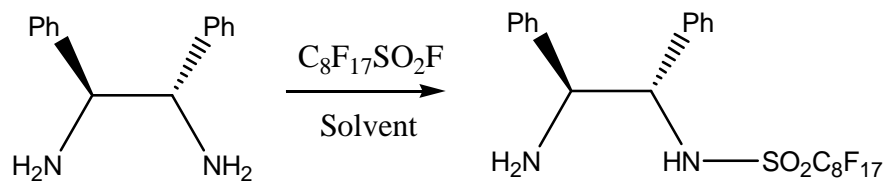
Fig 5.22: Synthesis of 1,1,2,2,3,3,4,4,5,5,6,6,7,7,8,8,8-Heptadecafluoro-octane-1-sulfonic acid (2-amino-1,2-diphenyl-ethyl)-amide

While this compound is not known in the literature, the non-fluorinated tosylate analog has been synthesized.[11, 12] Once the chiral F-diamine is synthesized, the hydrogen transfer reaction will be carried out in traditional fluorous biphasic conditions. At this stage, the recyclability of the catalyst should be evaluated. Once this has been done, a partitioning study of the catalyst with fluorous silica can be done. Finally, the hydrogenation of substituted acetophenone (conversion, enantiomeric excesses, etc.) with and without the fluorinated microphase system can be investigated. Positive results (high ee's sustained after recycle) would indicate that our F-MonoPhos (**8**) was not strongly bound to the metal center, which led to losses in enantioselectivity in our initial trials, and could indicate what kinds of reactions would be most suitable for our fluorous immobilized phase.

5.4 Recommendations for Chapter 4: PEI gels

In Chapter **4**, we demonstrated that amino acids could be gelled in our PEI 1200/octanol/CO_2 system (**Fig 5.23**). We tested amino acids because literature indicated that PEI has possible drug delivery applications.[13, 14]
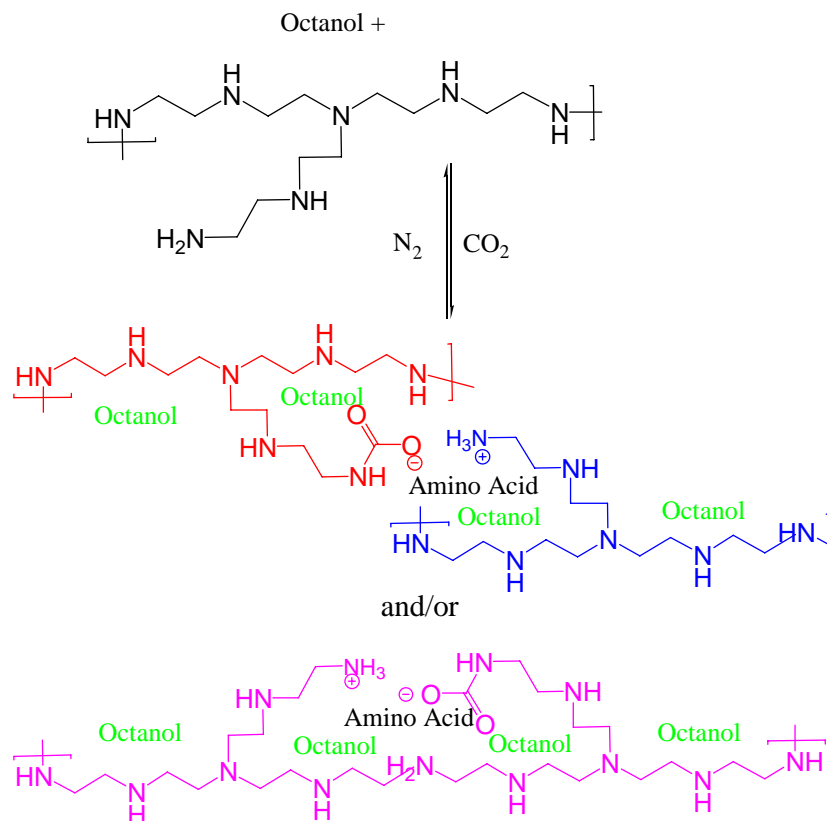
Fig 5.23: Amino Acid gelled in PEI/octanol/CO_2 gel

Two amino-acid based drugs, melphalan and acivicin, are anti-cancer agents that could be easily added to PEI and octanol mixtures (**Fig 5.24**).[15]
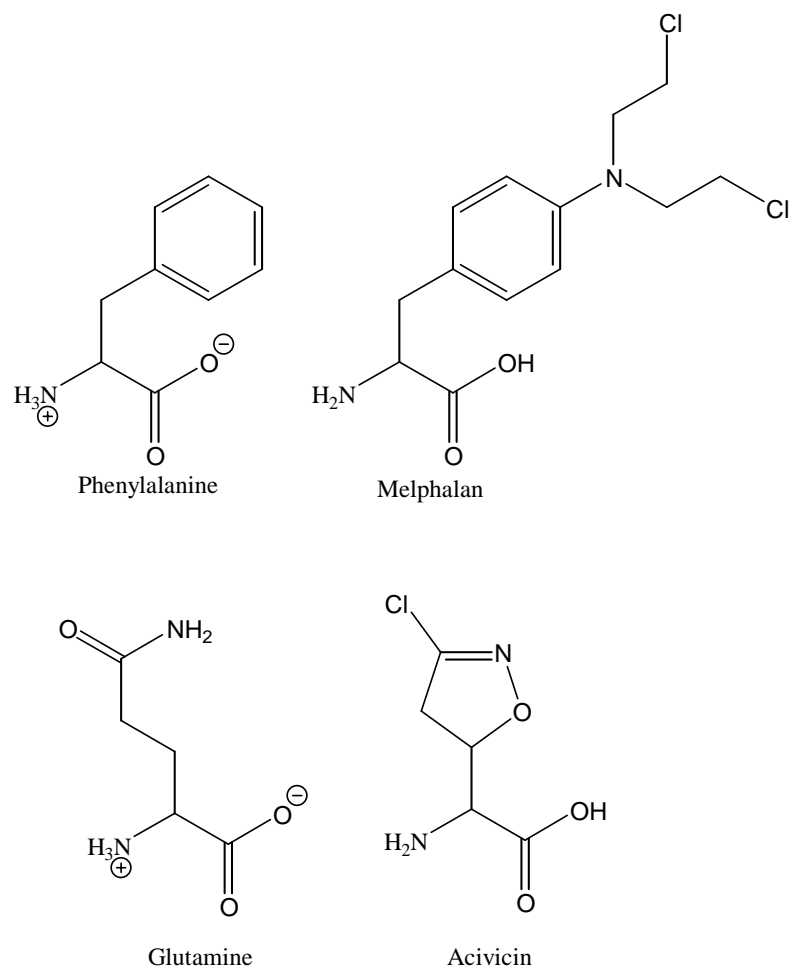
Fig 5.24: Amino-acid based anticancer agents Melphalan and Acivicin and their respective amino-acid parent structures

It is theorized that these drug molecules will be easily incorporated into PEI/octanol/CO_2 gels, and will still degrade easily. This would allow straightforward release of the drug molecules. By gelling actual pharmaceuticals in PEI/octanol/CO_2 based gels, we could provide an alternative means of administration (as opposed to tablets).

5.5 References Cited

1.   Jun Huang, A.R., Peter Wasserscheid, Rasmus Fehrmann, *Reversible physical absorption of SO2 by ionic liquids.* Chemical Communications, 2006: p. 4027-4029.

2.   Jessop, P.G., et al., *A Reversible Ionic/Non-Ionic Switchable Solvent.* Nature, 2005. **436**: p. 1102.

3.   www.aldrich.com, A.o.c., June 2007.

4.   David G.B. Boocock, Samir K. Konar, V. Mao, .Lee, Sonia Buligan, *Fast formation of High-Purity Methyl Esters from Vegetable Oils.* Journal of the American Oil Chemist Society, 1998. **75**(9): p. 1167-1172.

5.   J.F. Rusling, R.J. Bertsch, R.A. Barford, H.L. Rothbart, *Liquid Equilibria in the System Methyl Oleate - Methyl Palmitate - Acetonitrile - Hexane.* Journal of Chemical and Engineering Data, 1969. **14**: p. 169-173.

6.   August V.Bailey, James A. Harris, Evald L. Skau, *Solubilities of Some Normal Saturated and Unsaturated Long-Chain Fatty Acid Methyl Esters in Acetone, n-Hexane, Toluene, and 1,2-Dichloroethane.* Journal of Chemical and Engineering Data, 1970. **15**: p. 583-585.

7.   Weidner, S.P.E., *Methanolysis of triacylglycerols by organic basic catalysts.* European Journal of Lipid Science and Technology, 2007. **109**(1): p. 11-16.

8.   Michael J. Haas, Karen M. Scott, William N. Marmer, Thomas A. Foglia, *In situ Alkaline Transesterification: An Effective Method for the Production of Fatty Acid Esters from Vegetable Oils.* Journal of the American Oil Chemist Society, 2004. **81**(1): p. 83-89.

9.   Yamada, T., et al., *Reversible, Room-Temperature Ionic Liquids. Amidinium Carbamates Derived from Amidines and Aliphatic Primary Amines with Carbon Dioxide.* Chem. Mater., 2007. **19**(5): p. 967-969.

10.   Rahman, M.S.O., Marco; Hii, King Kuok (Mimi), *Mixed donor aminophosphine oxide ligands in ruthenium-catalysed asymmetric transfer hydrogenation reactions.* Tetrahedron: Asymmetry, 2004. **15**(12): p. 1835-1840.

11.   S. F. Hashiguchi, A., Jun Takehar, Takao Ikariya, Ryoji Noyori *Asymmetric Transfer Hydrogenation of Aromatic Ketones Catalyzed by Chiral Ruthenium (II) Complexes.* JACS, 1995. **117**: p. 7562-7563.

12. Wagner, A.M., Charles; Mohar, Barbara; Desmurs, Jean-roger; Le Guyader, Frederic; Schlama, Thierry, *Sulfonamides and carboxamides and their use in asymmetrical catalysis*. 2000.

13. Senaratne, W., L. Andruzzi, et al, *Self-Assembled Monolayers and Polymer Brushes in Biotechnology: Current Applications and Future Perspectives.* Biomacromolecules, 2006. **6**(5): p. 2427-2448.

14. Akin Akinc, Mini Thomas, Alexander M. Klibanov, Robert Langer, *Exploring polyethylenimine-mediated DNA transfection and the proton sponge hypothesis.* The Journal of Gene Medicine, 2005. **7**(5): p. 657-663.

15. Dennis M. Killian, L.G., and Prashant J. Chikhale, *Modulating blood-brain barrier interactions of amino-acid-based anticancer agents.* Drug Delivery, 2000. **7**: p. 21-25.

APPENDIX 1
NUCLEAR OVERHAUSER EFFECT IN MIXED SOLVENTS

A1.1 Introduction

Little is known about the gas-expanded liquid (GXL) microstructure surrounding solute molecules. The aim of this project is to develop a method to investigate GXLs on the molecular level and as a result learn more about the molecular environment around solutes. By compiling knowledge on the solvation shell surrounding solutes, we may be able to identify and exploit GXLs.

A1.2 Background

Previous investigations of the behavior of solutes in compressible fluids have indicated that local environments vary from that of the bulk. For instance, local density enhancements (or local density augmentation) for supercritical fluids have been investigated experimentally and validated by theory.[1-3] Similarly, ternary systems consisting of a two-component solvent (a polar organic and CO_2) and a solute have been investigated previously.[2,4,5] The Eckert-Liotta group investigated the solvatochromic parameters (α, β, π^*, and $E_T(30)$) of ternary systems consisting of acetone and methanol in CO_2, along with a solute [4-nitroaniline, 4-nitroanisole, 4-nitrophenol, N,N-dimethyl-4-nitroaniline, 4-(2,4,6-triphenylpyridinium)-2,6-diphenylphenoxide, and 2,6-dichloro-4-(2,4,6-triphenyl-1-pyridinio)phenolate]. It was found that the solvatochromic parameters displayed deviations from linear behavior with respect to mole fraction, clearly indicating that local environments vary from the bulk. DeGrazia *et al.* used spin-exchange reactions (monitored by EPR) to show solute-induced local density augmentations in super- and

subcritical CO_2.[5] The spin-exchange reaction rate of two paramagnetic species is highly sensitive to diffusion rate, which is inversely proportional to viscosity. Viscosity, in turn, is directly proportional to density. Thus, the lower than expected spin-exchange reaction rates indicate a higher local density than the density of the bulk. Clearly, local environments in compressible solvents can display different properties from that which would be expected based upon bulk composition.

A1.3 Previous Work

One technique that has quite recently been applied to studying mixed solvents or solutes in mixed solvents is nuclear Overhauser effect (NOE) NMR spectroscopy.[6] Several investigations using nuclear Overhauser effect NMR spectroscopy have shown interactions between solvent-solute pairs. For example, Diaz *et al*. examined the solvation of a tetrapeptide (NAc-Ser-Phe-Val-Gly-OMe) in water/alcohol mixtures using solvent-to-solute homo- and heteronuclear NOEs.[8, 9] Interestingly, trifluoroethanol showed preferential solvation of the peptide in mixed solvent systems with water or ethanol, and different protons on the peptide showed NOEs with different magnitudes. This showed that the peptide was not equally surrounded by water molecules, and by quantifying the NOE enhancements they were able to determine site specificity of solvation between the peptide and the solvent(s).

J. T. Gerig published results of solvent-to-solute NOEs shortly after the inception of this project.[10] He used the solute molecule 1,3-di-*tert*-butylbenzene (**Fig A1.1**) in tetramethylsilane, perfluoro-*tert*-butanol, and 50:50 mixtures of each with CCl_4. His study was aimed at developing a model for the prediction of solvent-to-solute NOEs, and

experiments were done to verify the validity of the model. The nearly spherical shape of the solvent molecules aided in the development of the model. Similar to Diaz *et al*. his results also showed that NOE intensity varied at different proton sites. He found that protons **H4**, **H5**, and **H6** showed larger NOE enhancements than did **H2**. He attributed this result to solvent exposure which was sterically hindered in the case of **H2**.
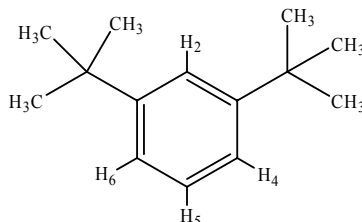
Figure A1.1: 1,3-di-*tert*-butylbenzene

These studies show that NOEs between solvent molecules and solute molecules can be detected and, with appropriate treatment, regional information (or solvation anisotropy[1]) can be observed in GXLs. The Eckert-Liotta group was interested in using NOEs to determine solvation structure around a solvent molecule in GXLs. We hoped to determine whether or not certain functional groups become preferentially solvated by one component of the GXL over the other (solvation anisotropy). This information would then give us unique insight into the approximate first solvation sphere (the cybotactic region) around a solute which could be used to refine our theoretical understanding of GXLs.

---

[1] Solvation anisotropy here is defined as the differences in the population of a solvent around a solute with changes to the environment.

A1.4 Results and Discussion

A1.4.1 Measurement of solvent-to-solute NOEs

Before we could start investigating GXLs by solvent-to-solute NOEs, we needed to establish that we had the capability of measuring liquid solvent-to-solute NOEs in a reproducible fashion.[11]   3,5-Dimethylanisole was chosen as the solute because the aromatic benzene ring is a rigid, planar scaffold for the pendant substituents: the aromatic protons, Ar*H*, the –OC*H₃*, and the two C*H₃* groups (**Fig A1.2**).
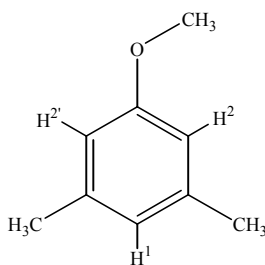
Figure A1.2: 3,5-dimethylanisole. Aromatic protons are differentiated by superscript number

This provides regional isolation of the groups from one another, so the NOEs observed from these different groups represent different regions of the cybotactic environment. Also, the protons have very different chemical shifts simplifying analysis of the NOE enhancement. Importantly, this molecule is also at least 1% soluble in the binary solvent mixtures typical of GXLs. This small amount of probe molecule is used to best simulate a binary solvent mixture, as there is not an appreciable amount of probe molecule. Finally, there are no exchangeable protons with protic solvents, and all protons are not sterically hindered.

Next, we assembled the hardware and techniques to study NOE signals for conventional binary systems (i.e. atmospheric pressure). The pulse sequence used herein, and in all the examples of solute-solvent NOEs previously mentioned, employed the

double pulsed field gradient with spin echo (DPFGSE) sequence which was developed by Stott *et al*.[12] This sequence has been used to see NOE enhancements as small as 0.1% of the unperturbed intensity, and it is believed to be capable of sensitivities as low as 0.01%.[6]

The probe molecule and the pulse sequence were examined on the liquid binary solvent MeOH and CCl_4 to demonstrate the viability of these selections. These solvent components were selected to represent similar conditions to which would be encountered when examining the GXLs; MeOH is a common GXL component and CCl_4 was used because it is similar to CO_2 in the respect that it is non-polar and has no ^{1}H NMR resonances. However, CO_2 is linear while CCl_4 is approximately spherical and larger in size. As the MeOH would provide the ^{1}H nuclei for excitation, no deuterium was incorporated in the sample; therefore, a sealed capillary of C_6D_6 was inserted into the NMR tube for purposes of lock and shimming. **Figure A1.3** shows the standard ^{1}H NMR spectrum of 1% 3,5-dimethylanisole in the mixture MeOH:CCl_4 (~20:80). The peaks are assigned as follows: 6.65 ppm (2H) and 6.73 ppm - the aromatic protons Ar*H;* (1H), 3.97 ppm (3H) - the –OC*H₃;* and 2.51 ppm (6H) - the C*H₃* protons.
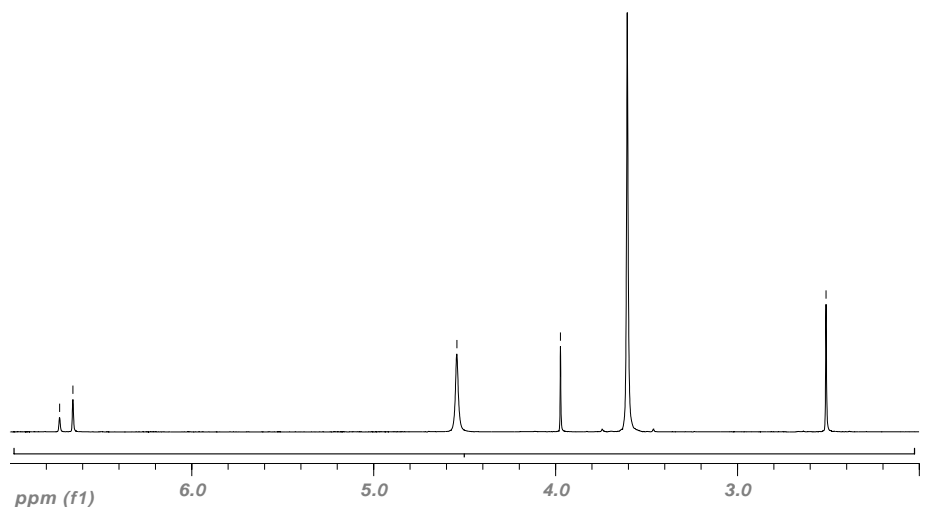
Figure A1.3: ^{1}H NMR of dimethylanisole in 20:80 MeOH:CCl$_4$

The peaks at 3.61 ppm and 4.54 ppm are due to methanol. The chemical shifts are well resolved and do not overlap, easing analysis.

A1.4.2 NOEs in liquid MeOH and CCl$_4$

The solvent-solute NOEs were obtained using the previously outlined pulse sequence (DPFGSE), with the selective 180° pulses centered on the methanol methyl resonance at 3.7 ppm. As molecular motions in solvents (10^{-12} sec)[14] are far faster than the observable time-scale for NMR (~ 10^0 sec),[6] the observed NOEs result from many different methanol molecules interacting with each site on the probe molecule. This also implies that distance values (often obtained in NOE spectroscopy) cannot be obtained. Instead the ratios of the NOEs arising from different sites are used to describe the extent to which one site is preferentially solvated by methanol over CCl$_4$ (NOE$_{siteA}$/NOE$_{siteB}$). Ratio values at or about 1 will indicate no preferential solvation, while values > 1 indicate preferential solvation of the group that appears in the numerator. Comparing the absolute intensities of the NOE enhancements could misrepresent the preferential solvation (the

anisotropy) as there is no way to scale the vertical intensity. In order to reference the vertical scale, some signal incapable of experiencing NOE's must be used. All peaks not experiencing NOE enhancements are cancelled out by the pulse sequence. Therefore only relative values (i.e. relative to one another) of NOEs obtained using the DPFGSE sequence have any physical significance. Average error for the ratios is 4.7%.

Figure A1.4 shows the relative NOEs versus percent carbon tetrachloride.
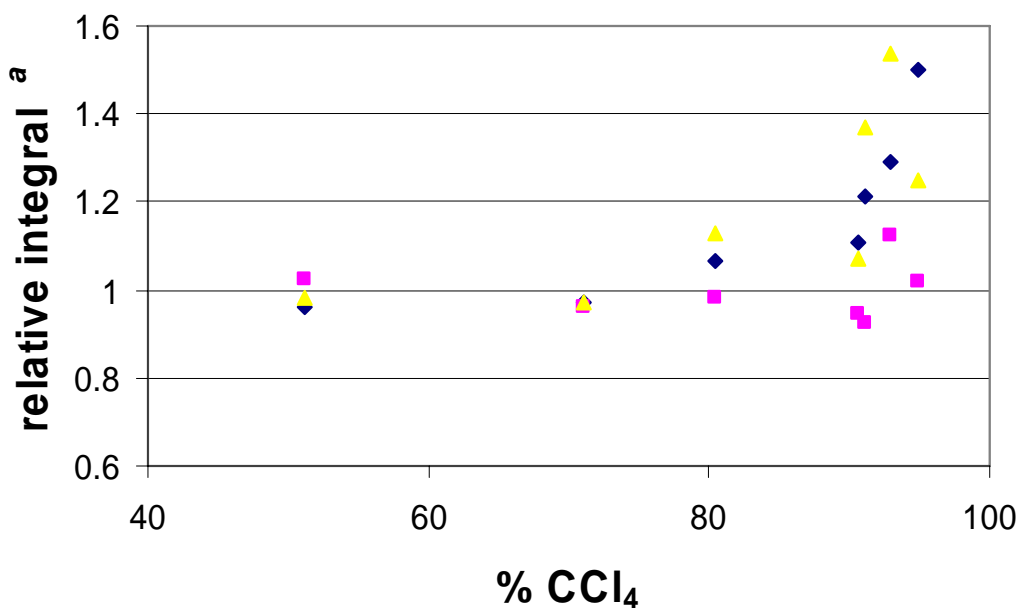
Figure A1.4: Relative NOE enhancements as a function of carbon tetrachloride concentration. ♦ = OCH_3/CH_3; △ = OCH_3/ArH^1; ■ = OCH_3/Ar$H^{2,3}$. – integrals normalized to equal numbers of protons

The diamond-shaped blue points (OCH_3 vs. CH_3, ♦) show that at low concentrations of methanol the methoxy group (the most polar region of the probe) shows more interactions with methanol versus the two methyl groups. At higher concentrations of methanol, all groups show similar interactions with methanol; this is indicated by the points approaching a value of one. This means that there is no preferential solvation of one group over the next at high concentrations of methanol. Similar behavior is observed when the methoxy group is compared to the aromatic protons (yellow triangles, △): the

results indicate that methanol interacts more strongly with the methoxy protons compared to the aromatic ones at low concentrations of methanol. The square-shaped purple points (■) compare the relative exposure of the aromatic protons to methanol versus the methyls. While the blue points display the same trend as seen in the other two cases at low concentrations of methanol, the values of the ratios are all less than one, indicating that the methanol solvates the methyl groups preferentially over the aromatic protons. This is likely due to steric reasons, rather than some effect of the regional polarity of the groups. Thus, our experiments indicated preferential solvation at the methoxy group of anisole by methanol (**Fig A1.5**).
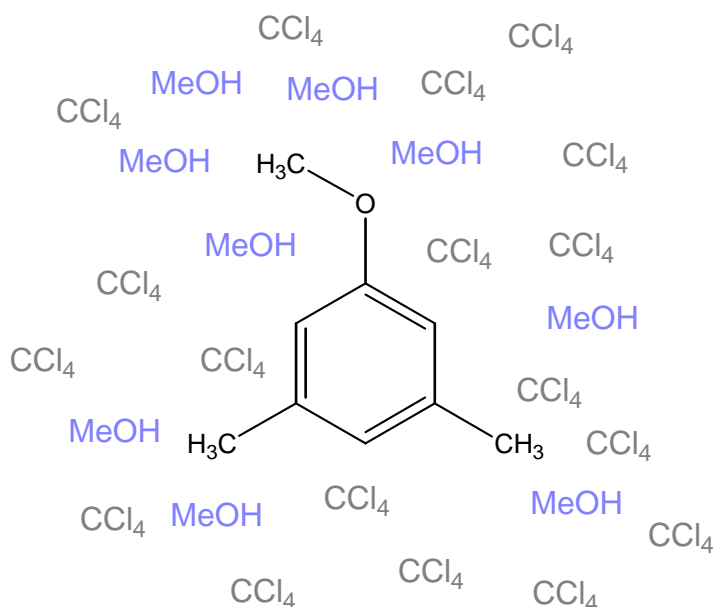
Fig A1.5: Solvation of anisole by methanol and CCl₄

As previously stated, the methoxy peak of the methanol was irradiated to observe NOEs. However, since the resonances were so close (3.58 - Me$_{MeOH}$, 3.7ppm − OMe$_{anisole}$), the NOEs were quite difficult to quantify. By testing a variety of other solvents (acetone, acetonitrile, DMF, DMSO), however, it was found that not only is an NOE seen between methanol and dimethylanisole in DMF, an internal NOE in the DMF

molecule itself is also seen which could be used as an internal standard to compare multiple sets of data (**Fig A1.6**). It is believed that DMF could replace methanol in future experiments.
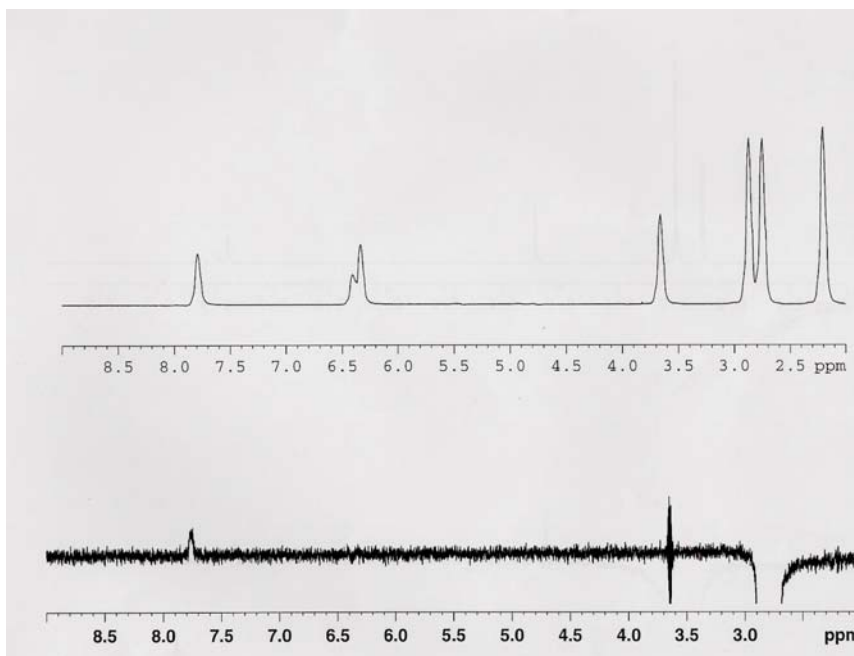
Fig A1.6: 1H NMR of DMF/anisole mixture (top) and NOE of mixture (bottom)

Because DMF has a slow exchange due to the rotation of the methyl groups, the internal NOE could actually be exchange instead of NOE.[16, 17] Thus, a ROESY experiment on the methanol/anisole/DMF system is necessary to differentiate between exchange peaks and NOE peaks.

A1.4.3 High Pressure NMR Tubes

With the pulse sequence and the analysis working on the chosen probe molecule the next step was to develop a high pressure NMR cell that could withstand the pressures, temperatures, and solvents to be used in the study of GXLs. The design we chose was

modified from the design of Wallen *et al.*,[15] and built in the School of Chemical and Biomolecular Engineering's machine shop.[11]

The cell body is constructed of poly(etheretherketone) (PEEK), which has high tensile strength (15,000 psi), a wide operable temperature range (-29 to 249 °C) and good chemical resistance. The cap is made from 30% carbon-filled PEEK. This material has a higher tensile strength (23,200 psi) and the same operating temperature and chemical resistance. This stronger material was incorporated to minimize the wall thickness of the threaded region (see **Fig A1.7**). Both 5 mm and 10 mm O.D. NMR tubes were made: ten of the 10 mm cells, and only one 5 mm cell.
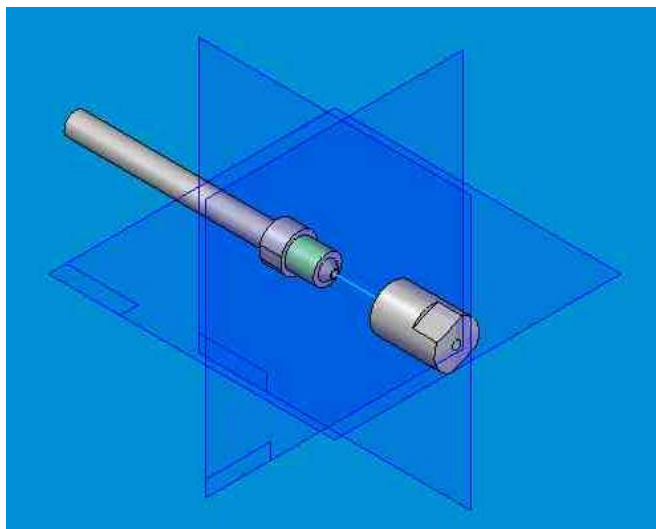
Figure A1.7: 10 mm PEEK high pressure NMR cell.

Our modifications to the design included: incorporation of "weep" holes to allow a path for depressurization should the seal fail, a more common swage-lock fitting for connection to plastic capillary tubing (Valco type 10-32 for 1/16" tubing), and a chamfered edge to ease insertion into the NMR probehead.

After construction of the cells, leak and pressure testing were done to ensure safety for users and for protection of the instrument. Pressure testing was done first by submerging a cell in a temperature controlled 50 °C water bath (the highest anticipated temperature of the GXL experiments). The cell was pressurized with water to 2551 psi (~176 bar). The cell was held at this temperature and pressure for 24 hour periods, after which it was depressurized and the outside diameter measured. This cycle was repeated 5 times. After the initial pressurization the outside diameter increased by .002 to .003 inches, and no subsequent increases in diameter were seen. The cell was then held at 50 °C and ~2500 psi for 10 days. No deformations or measurable changes were noticed in the cell. The cell was then leak tested. It was again submerged in 50 °C water and pressurized with increasing amounts of CO_2. The cell showed no indication of bubbles forming (indicating a gas leak) or a pressure drop at pressures > 170 bars. These two tests convinced us of the structural safety of these cells.

We next looked at some simple spectra in the 10 mm cell, first using liquids and then using pressurized samples. ^{1}H and ^{13}C measurements could be made in this cell with good resolution and little, if any, baseline distortions due to the PEEK cell.

A1.4.4 Future directions

Once an optimal system is found for measuring NOEs, we need to use 5 mm cells with the DPFGSE pulse sequence. The 5 mm high pressure cells are necessary as the only probe equipped with gradient coils is a 5mm probe. Then, we can finally study actual GXLs.

A1.5 Conclusions

This work has developed an analysis of preferential solvation that yields regional information (solvation anisotropy). While solvent-to-solute NOEs have been used previously, this work represents an application of NOE spectroscopy that looks for the first time to characterize the solvation environment around a solute molecule on a regional basis. Furthermore, the information gleaned from these experiments is planned for use in refining the theoretical understanding of solvation in binary solvents, and will be used in the ongoing simulation effort of solutes and reactions in GXLs.

Experimental

All chemicals were ordered from Aldrich and used as received. Carbon tetrachloride, 3,5-dimethyl anisole and anhydrous methanol (or acetone, acetonitrile, DMF, or DMSO) were mixed in appropriate proportions and introduced into Wilmad 528 series NMR tubes. A sealed capillary containing C_6D_6 was used to provide a lock signal and an external reference (7.15 ppm). Spectra were recorded on a Bruker DRX 500 MHz with an inverse triple resonance probehead with gradient coils. The DPFGSE pulse sequence[12] used a mixing time τ_m of 0.7 ms. The selective 180° pulses had a gaussian shape width with 1% truncation for a duration of 80 ms.

References

1. Hrnjez, B.J., et al., *Prediction of Supercritical Ethane Bulk Solvent Densities for Pyrazine Solvation Shell Average Occupancy by 1, 2, 3, and 4 Ethanes: Combined Experimental and ab Initio Approach.* Journal of Physical Chemistry A, 2005. **109**(45): p. 10222-10231.

2. Knutson, B.L., et al., *Local density augmentation in supercritical solutions. A comparison between fluorescence spectroscopy and molecular dynamics results.* ACS Symposium Series, 1992. **488**(Supercrit. Fluid Technol.): p. 60-72.

3. Rice, J.K., et al., *State-Dependent Solvation of Pyrene in Supercritical CO2.* Journal of the American Chemical Society, 1995. **117**(21): p. 5832-9.

4. Wyatt, V.T., et al., *Determination of solvatochromic solvent parameters for the characterization of gas-expanded liquids.* Journal of Supercritical Fluids, 2005. **36**(1): p. 16-22.

5. deGrazia, J.L., T.W. Randolph, and J.A. O'Brien, *Rotational relaxation in supercritical carbon dioxide revisited: a study of solute-induced local density augmentation.* Journal of Physical Chemistry A, 1998. **102**(10): p. 1674-1681.

6. Neuhaus, D. and M.P. Williamson, *The Nuclear Overhauser Effect in Structural and Conformational Analysis, Second Edition.* 2000. No pp given.

7. Bagno, A., F. Rastrelli, and G. Scorrano, *Detecting intermolecular NOEs by means of a novel DPFGSE pulse sequence. Application to the solvation of carbohydrates in binary mixtures.* Journal of Magnetic Resonance, 2004. **167**(1): p. 31-35.

8. Diaz, M.D. and S. Berger, *Preferential solvation of a tetrapeptide by trifluoroethanol as studied by intermolecular NOE.* Magnetic Resonance in Chemistry, 2001. **39**(7): p. 369-373.

9. Fioroni, M., et al., *Solvation Phenomena of a Tetrapeptide in Water/Trifluoroethanol and Water/Ethanol Mixtures: A Diffusion NMR, Intermolecular NOE, and Molecular Dynamics Study.* Journal of the American Chemical Society, 2002. **124**(26): p. 7737-7744.

10.   Gerig, J.T., *Selective Solvent Interactions in a Fluorous Reaction System.* Journal of the American Chemical Society, 2005. **127**(25): p. 9277-9284.

11.   Thomas, C.A., *Reactions and Separations in Tunable Solvents*, in *Chemistry and Biochemistry*. 2006, Georgia Institute of Technology: Atlanta.

12.   Stott, K., et al., *Excitation Sculpting in High-Resolution Nuclear Magnetic Resonance Spectroscopy: Application to Selective NOE Experiments.* Journal of the American Chemical Society, 1995. **117**(14): p. 4199-200.

13.   Wendt, M.A., et al., *Solvent and concentration dependence of the hydroxyl chemical shift of methanol.* Molecular Physics, 1998. **93**(1): p. 145-151.

14.   Ropp, J., et al., *Rotational Motion in Liquid Water Is Anisotropic: A Nuclear Magnetic Resonance and Molecular Dynamics Simulation Study.* Journal of the American Chemical Society, 2001. **123**(33): p. 8047-8052.

15.   Wallen, S.L., et al., *A polymer NMR cell for the study of high-pressure and supercritical fluid solutions.* Analytical Chemistry, 2000. **72**(17): p. 4230-4234.

16.   Gunther, H., *NMR Spectroscopy.* 2nd ed ed. 1996, Sussex, England.

17.   Friebolin, H., *Basic 1&2D NMR Spectoscopy.* 2nd ed. ed. 1993, Weinheim, Germany.

APPENDIX 2
POLYFOX – DEVELOPMENT FOR MARINE APPLICATIONS

A2.1 Introduction

Marine biofouling is an old problem (>2000 years) with many 'partners in crime' (> 2500 marine biofouling organisms exist). Because marine biofouling increases drag, it increases fuel consumption, which has detrimental environmental and economical implications. Past treatments have proved to be inadequate, or in the case of tributyltin (TBT), extremely damaging to the environment. An optimal antifouling agent would be effective, long-lasting, easy to apply, and have little-if any-long term environmental impact. One means to reach this goal is through the incorporation of natural defensive compounds within a coating with a low surface tension such as Polyfox. Capsaicin, zosteric acid, and eserine have all been shown to reduce biofouling in various studies (**Fig A2.1**).
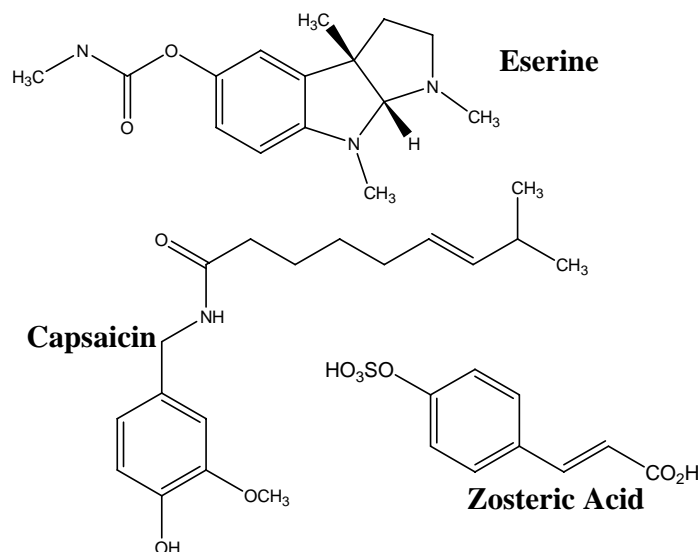
Fig A2.1: Structures of capsaicin, zosteric acid, and eserine

Either capsaicin, zosteric acid, or eserine can be directly mixed with Polyfox to create novel and potentially better antifoulant mixtures. Not only should these compounds increase and/or prolong the antifouling activity of Polyfox-coated materials, these molecules should not adversely affect the weight and surface properties of polyfox.

A2.2 Purpose

This is a project that I completely designed to revamp Polyfox—extending its potential markets. While I did not perform experimental work, I designed a proposal, which another group member may perform.

A2.3 Proof of Principle Plan

The literature has established that capsaicin, zosteric acid, and eserine are antifoulants. The combination of these molecules with Polyfox could potentially lead to a more potent antifouling coating material. Two options appear to be attractive approaches: (1) simply mixing the antifouling molecules with Polyfox; and (2) attaching the antifouling molecules onto an inert telemer or polymer backbone through a hydrolysable functional group and then mixing this with PolyFox.

The antifouling molecules can be easily attached to poly(acrylate chloride) through nucleophilic substitution. For example, the sodium salt of capsaicin could easily undergo the substitution reaction (**Fig A2.2**).
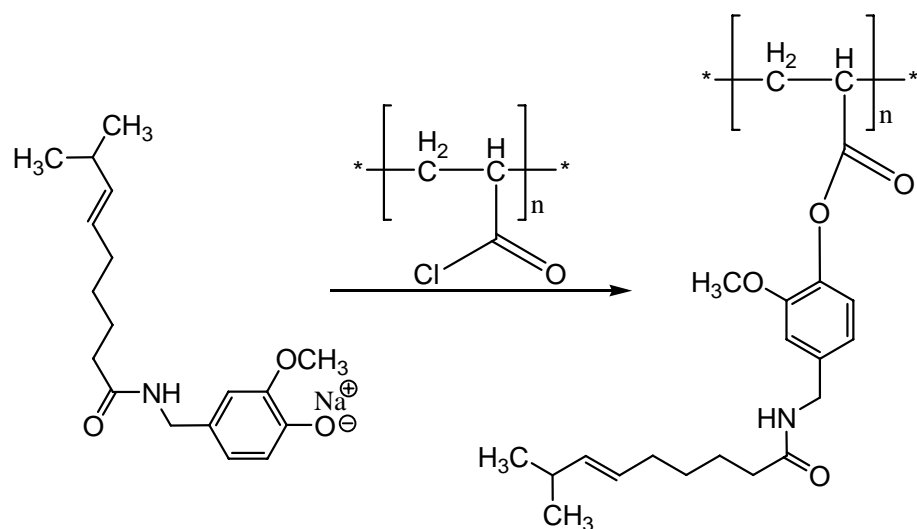
Fig A2.2: Substitution of sodium salt

In the literature, low amounts (1-10wt%) of the active compounds have demonstrated antifouling capabilities up to 98 %. In initial research, we would like to incorporate amounts from 1 to 20%. Using this range, we can test the range of efficacy of zosteric acid in PolyFox within reason.

A2.4 Characterization

The physical properties of the resulting polymer, level of incorporation, and the leaching of the active substance will be carefully studied via appropriate analytical methods. PolyFox has been fully characterized via ^{1}H and ^{13}C NMR, GPC, and IR. Furthermore, degree of polymerization is calculated using ^{1}H NMR spectroscopic end group analysis.[8] In this method, the α,ω-dihydroxy groups of polyfox are converted to trifluoroacetate derivatives by reaction with trifluoroacetic anhydride. The degree of polymerization is calculated by integrating the two methylene signals using **formula A2.1**:

Degree of polymerization $= 2I_{\text{-OCH2(CF2)nF}}/I_{\text{-CH2OC(=O)CF3}}$ (**Formula A2.1**)

where I is the integrated signal and the subscripts are the pendent fluorinated and terminal trifluoroacetate groups, respectively (**Fig A2.3**).
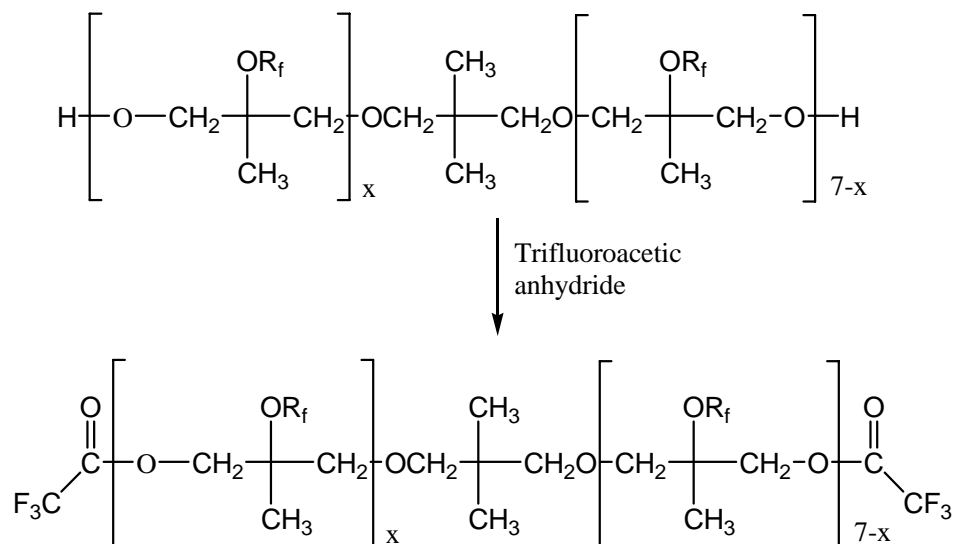
Fig A2.3: Fluorination of dihydroxy groups

We can use these same methods to characterize our novel polyfox mixtures. For lower wt%s of the polyfox/antifoulant mixtures where NMR spectroscopy may not be optimal, we can also use UV to further accurately quantify the host incorporation (all hosts have an aromatic ring that is easily detected by UV with both accuracy and sensibility).

A2.5 Lab Scale Testing

First we can use Petri dishes, or bottles with various aqueous mixtures including plates blanks (uncoated), PolyFox-coated, and PolyFox-antifoulant combinations-coated. In these containers, we can also add fouling organisms. Then, over time, we can physically measure biofilm as it is formed. By placing the containers at a slight angle, we can ensure that biofilm formation is not simply caused as a result of settling of species and organic matter. The most promising mixtures will be made into panels for small and (if these results are promising) large scale testing.

A2.6 Small and Large Scale Testing

AFC will arrange the testing of the panels.

References

1. Qingwei Xu, C. B., Teresa Cutright and Bi-min Zhang Newby (2005). "Assessment of Antifouling Effectiveness of two Natural Product Antifoulants by Attachment Study with Freshwater Bacteria " <u>Environmental Science and Pollution Research</u> 2005, **12**(5): 278-284.

2. Al-Juhni, A.N., B.Z., *Techniques for incorporating capsaicin into silicone coatings for enhanced antibacterial attachment.* Proceedings of the Annual Meeting of the Adhesion Society, 2004. **27**: p. 225-227.

3. Barrios, C. A., Q. Xu, et al. "Incorporating zosteric acid into silicone coatings to achieve its slow release while reducing fresh water bacterial attachment." <u>Colloids and Surfaces B: Biointerfaces</u> 2005, **41**(2-3): 83-93.

4. Qingwei Xu, C. A. B. T. C. B.-m. Z. N. "Evaluation of toxicity of capsaicin and zosteric acid and their potential application as antifoulants." <u>Environmental Toxicology</u> 2005, **20**(5): 467-474.

5. Alexandratos, S. D. (1999). Synthesis and purification of zosteric acid. U. S. P. Office, The University of Tennessee Research Corporation. **5990336**.

6. Faimali, M.F., C.; Gallus, L.; Piazzi, V.; Tagliafierro, G, *Involvement of acetyl choline in settlement of Balanus amphitrite.* Biofouling, 2003. **19(Suppl.)**: p. 213-220.

7. Simpson, L. S. and T. S. Widlanski. "A Comprehensive Approach to the Synthesis of Sulfate Esters." <u>J. Am. Chem. Soc.</u> 2006**128**(5): 1605-1610

8. Kausch, C. M., J. E. Leising, et al. "Synthesis, Characterization, and Unusual Surface Activity of a Series of Novel Architecture, Water-Dispersible Poly(fluorooxetane)s." <u>Langmuir</u> 2002, **18**(15): 5933-5938.

APPENDIX 3
SYNTHESIS AND ANTIFEEDANT EFFECT OF 2,3,4-TRIBROMOPYRROLE

A3.1 Abstract

2,3,4-Tribromopyrrole (**1**) and 2,3,5-tribromopyrrole (**2**) were synthesized from pyrrole. Spectral data and antifeedant effects for synthetic **1** and the anti-predatory chemical defense compound of the marine hemichordate *Saccoglossus kowalevskii* were in agreement, confirming the structure of the deterrent natural product as **1**. Spectral data for **2** differed from synthetic and natural **1**.

A3.2 Background

Recently, the anti-predator chemical defense of a marine hemichordate worm, *Saccoglossus kowalevskii*, was identified as 2,3,4-tribromopyrrole (**1**) (**Fig A3.1**).[1]
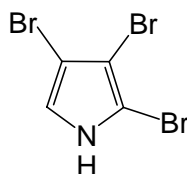
(1)

Fig A3.1: 2,3,4-tribromopyrrole

At its natural concentration of 0.20 % of dry mass, this natural product deterred feeding by two species of predatory fish, *Fundulus heteroclitus* and *Leiostomus xanthurus*, but had no effect on the feeding behavior of a predatory crab, *Callinectes similis*.[1] Although **1** was previously reported from this and other worm species,[2-5] it remained possible that the natural product was in fact 2,3,5-tribromopyrrole (**2**), because of ambiguities in the published spectral data (**Fig A3.2**).

194
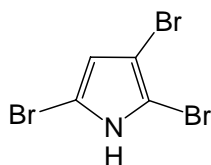
(2)

Fig A3.2: 2,3,5-tribromopyrrole

Specifically, the chemical shift of the aromatic proton was previously reported using different solvents for **1** and **2**, no ^{13}C NMR data were available for **2**, and mass spectral data were identical for both compounds.[3-4,6] Although the syntheses of **1** and **2** had been achieved from pyrrole as a complex mixture,[3] the uncertainties above made it difficult to exclude either structure for the natural product. In this study, we performed a regioselective synthesis of **1**, and compared spectral data and feeding assay results for synthetic **1** with data for the tribromopyrrole natural product from *S. kowalevskii*. We also synthesized **2** for comparison of spectral data with **1**.

A3.3 Results and Discussion

A3.3.1 Synthesis of 2,3,4-tribromopyrrole

The synthesis of 2,3,4-tribromopyrrole (**1**) was accomplished in three steps from pyrrole (**3**) (**Figure A3.3**).
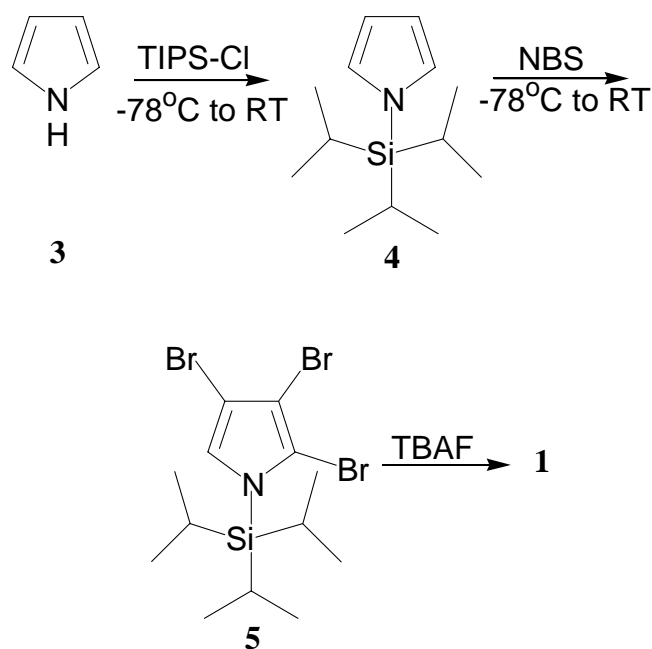
Figure A3.3: Synthesis of 2,3,4-tribromo-pyrrole (1)

We hypothesized that the steric bulk of a silyl protecting group would lead to selective bromination at sites more distant from the protected nitrogen, such that positions 2, 3, and 4 on the pyrrole ring would be brominated, rather than positions 2, 3, and 5. Protection of **3** afforded the silyl ether **4**,[6] which was then treated with two successive batches of *N*-bromosuccinimide (NBS) at low temperature. Conversion under kinetic control to 2,3,4-tribromo-1-(triisopropylsilyl)pyrrole (**5**) was followed by an assessment of high purity of the product using LC-MS, so purification was achieved simply by filtration through silica gel. Although the bromination step was previously reported to require only one addition of between three and five equivalents of NBS,[6] in our hands, two separate additions provided higher yield (97 %) of tribrominated product, and tetrabromination was never observed. Intermediate **5** was deprotected using tetrabutylammonium fluoride (TBAF) under ambient conditions to produce 2,3,4-tribromopyrrole (**1**), for a deprotection yield of 90 %, and an overall yield of the three-step sequence of 87 %.

A3.3.2 Synthesis of 2,3,5-tribromopyrrole

2,3,5-Tribromopyrrole (**2**) was synthesized directly from pyrrole using three equivalents of NBS.[6] We expected that this reaction would lead to the electronically favored product **2** over **1**. The multiple products decomposed rapidly upon storage and handling, so only a preliminary separation was achieved with silica gel without drying the product **2** (thus, without quantitation of yield). Tetrabromopyrrole and other minor products were detected in the mixture but, from ^{1}H and ^{13}C NMR spectral data for the crude reaction mixture, **2** appeared to be the major product, and no chemical shift data consistent with **1** were observed.

A3.3.3 Comparison of 2,3,4- and 2,3,5- tribromopyrrole

^{1}H and ^{13}C NMR spectral data for synthetic **1** acquired in $CDCl_3$ and also in deuterioacetone (see Experimental Section) were in close agreement with published data for **1** isolated from the hemichordate worm *Saccoglossus kowalevskii*.[1,4] In contrast, NMR spectral data for our synthetic **2** in were clearly different than for synthetic and natural **1**. For example, the carbon chemical shift of the only CH (confirmed by DEPT) was 121.9 ppm (in acetone-d_6) and 119.5 (in $CDCl_3$) for natural[1] and synthetic **1**; whereas, the methine carbon in synthetic **2** resonated at 114.1 ppm in acetone-d_6. The methine proton chemical shift was also consistent for natural[1] (δ 6.83) and synthetic **1** (δ 6.81) whereas the methine proton of synthetic **2** resonated at δ 6.04 (all in $CDCl_3$).

Since synthetic isomer **1** proved to be the more robust of the two synthetic isomers, it was extensively studied spectroscopically. In the HMBC spectra of **1**, we

expected to see only one instance of ^{1}H-^{13}C coupling: the aromatic proton in four points with its only carbon neighbor. Isomer **2** would display two instances of ^{1}H-^{13}C coupling, the aromatic proton with each of its two carbon neighbors. HMBC was performed on synthetic **1** in deuterated acetone and displayed only one instance of coupling: 7.13ppm (pyrrole H) with 101.7ppm (aromatic carbon, with bromine connected). This is in accordance with isomer **1**. In the HMQC spectra, we expected to see the aromatic proton coupling to the most downfield carbon in the ^{13}C spectra. When HMQC was performed on synthetic **1** in deuterated acetone, the spectra of **1** displayed only one instance of coupling: pyrrole H (7.13ppm) with the carbon it is bonded to (121.9ppm). Unfortunately, aromatic systems can sometimes display three and four bond coupling, so HMQC data does not conclusively tell us that the aromatic hydrogen is definitely bonded to C-5 of the pyrrole. Furthermore, literature values for long-range coupling in pyrroles are very close[8], so those values were inconclusive.

Since the previously mentioned analysis of synthetic **1** did not generate unequivocal evidence that we have, indeed, synthesized isomer **1**, we turned our attentions to their precursors: 2,3,4-tribromo-1-(triisopropylsilyl)pyrrole (**5**), and the protected version of **2**: 2,3,5-tribromo-1-(triisopropylsilyl)pyrrole (**6**). Since isomerization upon deprotection of **5** and **6** to **1** and **2** is not expected, the structure of the precursor can be fully investigated as well. Because of the differences in synthetic routes, however, only **5** could actually be tested. Theoretical *ab initio* calculations using Hartree-Fock database was used to calculate the distance between the CH and CH$_3$ of iPr groups and the respective aromatic hydrogens of **5** and **6**. According to our calculations for isomer **5**, the distance between the pyrrole hydrogen and the CH group of iPr is 2.060

angstroms, and the distance between the pyrrole hydrogen and the CH3 group of iPr is 2.543 angstroms. In the case of isomer **5**, the distance between the pyrrole hydrogen and the CH group of iPr is 5.240 angstroms, and the distance between the pyrrole hydrogen and the CH3 group of iPr is 4.762 angstroms. Since NOE does not occur past distances of 5 angstroms, we believed it would be appropriate to differentiate between isomers **5** and **6**. Isomer **5** was expected to show two strong incidences of NOE, whereas isomer **6** would only display one weak incidence, if any at all. An NOE experiment was performed on synthetic **5** in deuterated chloroform. Two strong incidences of NOE were found: the aromatic proton (6.87ppm) coupled to both the CH (1.68ppm) and CH$_3$ (1.14ppm) of the i-Pr group. Furthermore, varied mixing times continued to display this phenomenon, verifying the robustness of this correlation. This coupling could have only been generated by isomer **5**, and thus unequivocally proves that our three step synthetic procedure exclusively generated isomer **1**. It is also apparent that a silyl protecting group did indeed provide the steric bulk to overcome the electronic factors involved in determining the regioselectivity of bromination by electrophilic substitution (resulting in bromination at positions 2, 3, and 4), whereas unprotected pyrrole subjected to bromination selectively yielded the electronically favored product **2**.

A3.3.4 Biological testing

When predatory fish (*Fundulus heteroclitus*) were offered squid-based food pellets containing synthetic **1** at the concentration at which it is found in *S. kowalevskii*, eight out of 14 fish rejected pellets containing synthetic **1**, whereas all fish consumed control pellets (squid pellets without **1**), indicating a significantly deterrent effect of **1**

(p=0.002), similar to the deterrence of natural **1**.[1] The six fish that consumed the treated pellets appeared to be larger than the other eight, raising the possibility that larger individuals who generally eat more may be less sensitive to deterrent compounds. Thus, these six fish were fed control pellets to near-satiation, and then were offered treated pellets a second time. Although three of these fish were too satiated to eat control or treated pellets in the second experiment, the remaining three fish rejected pellets treated with **1** and then consumed a control pellet, suggesting that chemical defense effectiveness is dependent on hunger status.

Compared to the deterrent properties of **1**, pyrrole (**3**) at the same concentration was found to be palatable to *F. heteroclitus*, as all 12 fish offered pellets containing **3** consumed both treated and control pellets. This indicates that bromination plays a crucial role in the deterrence of **1**, although Kicklighter *et al*.[1] showed that many brominated aromatic compounds from marine worms do not deter predators at natural and greater than natural concentrations. Unfortunately, we were unable to test **2** due to its extreme lability. However, our data (both spectral and experimental) does support our hypothesis that the tribrominated pyrrole natural product of *S. kowalevskii* is indeed 2,3,4-tribromopyrrole (**1**) and not 2,3,5-tribromopyrrole (**2**).

Conclusions

In conclusion, for the first time 2,3,4-tribromopyrrole (**1**) has been unambiguously and regioselectively synthesized. The NMR spectral data for synthetic **1** agree with previously reported data for **1** isolated from the marine worm *Saccoglossus kowalevskii*, whereas these data differ from that of synthetic **2**. Additionally, synthetic **1** was found to

deter feeding by predatory fish. Thus, this published work indicates that 2,3,4-tribromopyrrole is indeed the anti-predator chemical defense of the marine hemichordate worm, *Saccoglossus kowalevskii*.[8]

<center>**Experimental**</center>

General Experimental Procedures. Melting points were measured with a Mettler Toledo FP62 melting point apparatus. NMR spectra were acquired using a Bruker Avance DRX 500, a Bruker AMX 400, or a Varian Mercury Vx 300 spectrometer, in $CDCl_3$, deteurioacetone, or in deuteriodiethyl ether, and referenced to the residual light solvent. Low and high resolution mass spectra were acquired on a Micromass 70SE instrument with FAB and EI ionization. LC-MS data were generated using a HP Series 1100 system with electrospray ionization, using a Symmetry C_{18} column with a gradient mobile phase of acetonitrile and water. HPLC purification was performed with a Waters 515 pump and 2487 UV detector, using a Zorbax RX-SIL normal phase column (10 x 250 mm). Molecular modeling was achieved by *ab initio* calculations with a Hartree-Fock database using a Spartan 2004 system. Solvents and other chemicals were purchased from Fisher Scientific and Sigma-Aldrich Corporation.

Bioassays. Feeding assays with the predatory fish *Fundulus heteroclitus* were performed in aquaria at the Georgia Institute of Technology's marine facility on Skidaway Island, Georgia, as previously described.[1] Consumption of treated and control foods were compared using a Fisher's exact test with an alpha value of 0.05.

N-**(Triisopropylsilyl)pyrrole (4).**
n-Butyllithium in hexane (19.3 mL of a 1.6 M solution, 30.8 mmol) was added dropwise to argon-dried pyrrole (1.94 mL, 28.0 mmol) in distilled THF at $-78\ ^oC$. Triisopropylsilyl chloride (6.00 mL, 28.0 mmol) was added after 10 minutes and the

<center>202</center>

reaction warmed to room temperature. The solvent was then removed, water was added, and the resulting residue was extracted with diethyl ether. The organic phase was then dried over anhydrous magnesium sulfate and concentrated by rotary evaporation. *N*-(Triisopropylsilyl)pyrrole (**4**) was isolated as a colorless oil (6.26 g, 28.0 mmol), in 100 % yield: ^{1}H NMR (CDCl$_3$, 400 MHz) δ 6.79 (2H, t, *J*=1.8), 6.31 (2H, t, *J*=2.0), 1.44 (3H, septet, *J*=7.6), 1.09 (18H, d, *J*=7.2); ^{13}C NMR (100 MHz): δ 124.0, 110.0, 17.8, 11.7; FABMS *m/z* 224.2 (15), 223.2 (20), 180.2 (11), 153.2 (25), 154.2 (100), 137 (29), 136 (57), 138 (65), 106.6 (19); HRFABMS [M]$^+$ *m/z* 223.1765 (calc for C$_{13}$H$_{25}$NSi 223.1756).

2,3,4-Tribromo-1-(triisopropylsilyl)pyrrole (5).

N-(Triisopropylsilyl)pyrrole (**4**) (2.00 g, 9.00 mmol) was dissolved in distilled THF (5.0 mL) and cooled to –78 ^{o}C. NBS (4.78 g, 26.9 mmol) in THF (35 mL) was then added over 10 minutes and the reaction was warmed to room temperature overnight under argon. Cold hexane was then added to the reaction mixture to precipitate unreacted NBS and succinimide by-product, and the slurry was filtered through neutral alumina. The partially brominated intermediate was dissolved in distilled THF (5.0 mL) and cooled to –78 ^{o}C. NBS (2.40 g, 13.5 mmol) in THF (20 mL) was added as before and the product recovered as above. Solvent was removed by rotary evaporation, and the product was filtered through silica gel and recrystallized in pentane at –78 ^{o}C to produce **5** as a pale yellow solid (4.00 g, 8.69 mmol) in 97 % yield: mp 50 ^{o}C; ^{1}H NMR (CDCl$_3$, 400 MHz) δ 6.85 (1H, s), 1.66 (3H, septet, *J*= 7.6), 1.12 (18H, d, *J*= 7.6); ^{13}C NMR (100 MHz): δ 125.7, 105.6, 104.6, 100.8, 34.1, 18.0; EIMS *m/z* 464.9 (32), 462.9 (88), 460.9 (87),

458.9 (30), 419.9 (9), 417.9 (24), 415.9 (25), 413.9 (9), 382 (26), 380 (47), 378 (25),

204.9 (9), 202.9 (22), 200.9 (9), 157.1 (95), 138.0 (39), 136.0 (38), 115.1 (100), 87.1

(52), 73.0 (47), 59.0 (58); HREIMS [M]$^+$ m/z 458.9055 (calc for $C_{13}H_{22}Br_3NSi$

458.9051).

2,3,4-Tribromopyrrole (1).

2,3,4-Tribromo-1-(isopropylsilyl)pyrrole (**5**) (100 mg, 0.217 mmol) was dissolved in

THF (3.0 mL) at room temperature. TBAF (0.543 mL, 0.543 mmol) as a solution in THF

was slowly added, and the mixture stirred for approximately one hour. The mixture was

then washed with water (3x), sodium bicarbonate (3x), and brine (3x). The organic

materials were concentrated in an ice bath with a stream of nitrogen gas to yield **1** as a

pale yellow oil (59.3 mg; 0.195 mmol) in 90 % yield. ^{1}H NMR: (CDCl$_3$, 300 MHz) δ

8.81 (1H, br s), 6.81 (1H, d, J=3.2); ^{1}H NMR: (acetone-d$_6$, 400 MHz) δ 11.23 (1H, br s),

7.11 (1H, d, J=3.2); ^{1}H NMR: (diethyl ether-d$_{10}$, 500 MHz): δ 11.05 (1H, br s), 6.87 (1H,

s); ^{13}C NMR (CDCl$_3$, 75 MHz): δ 119.5 (CH), 101.9 (C), 100.2 (C), 99.8 (C); ^{13}C NMR

(acetone-d$_6$, 100 MHz): δ 121.9 (CH), 101.7 (C), 101.2 (C), 99.5 (C); EIMS m/z 306.8

(34), 304.8 (98), 302.8 (99), 300.8 (37), 225.9 (14), 223.9 (28), 221.9 (15), 198.9 (9),

196.9 (20), 194.9 (10); HREIMS [M]$^+$ m/z 300.7749 (calc for $C_4H_4Br_3N$ 300.7737).

2,3,5-Tribromopyrrole (2).

NBS (1.92 g, 10.8 mmol) in THF (10 mL) was added by canula over a period of 10

minutes to a solution of pyrrole (242 mg, 3.60 mmol) stirring in THF (10 mL) at –78 °C.

After 10 more minutes, the reaction flask was warmed to -10 °C for two hours, then

warmed to room temperature and most of the THF was removed by rotary evaporation. An aliquot of crude product mixture was separated on silica gel using a gradient of hexane and diethyl ether. Gradual removal of solvent and addition of NMR solvent using a gentle N_2 stream enabled spectral analysis of mixtures before and after silica gel separation (without ever drying or weighing the product). Further attempts to purify or handle the product resulted in rapid decomposition. ^{1}H NMR: (CDCl$_3$, 500 MHz) δ 6.04 (d, J=2.9); ^{1}H NMR: (acetone-d$_6$, 500 MHz) δ 11.55 (1H, br s), 6.24 (1H, d, J=2.8); ^{13}C NMR (acetone-d$_6$, 100 MHz): δ 114.1 (CH), 100.3 (C), 99.1 (C), 99.0 (C); EIMS m/z 306.8 (38), 304.8 (99), 302.8 (100), 300.8 (36), 225.9 (13), 223.9 (26), 221.9 (13), 198.7 (11), 196.9 (21), 194.9 (10); HREIMS [M]$^+$ m/z 300.7763 (calc for C$_4$H$_4$Br$_3$N 300.7737).

References

(1) Kicklighter, C.E.; Kubanek, J.; Hay, M.E. *Limnol. Oceanogr*. **2004**, *49*, 430-441.

(2) Woodin, S.A.; Walla, M.D.; Lincoln, D.E. *J. Exp. Mar. Biol. Ecol*. **1987**, *107*, 209-217.

(3) Emrich, R; Weyland, H.; Weber, K. *J. Nat. Prod*. **1990**, *53*, 703-705.

(4) Fielman, K.T.; Targett, N.M. *Mar. Ecol. Prog. Ser*. **1995**, *116*, 125-136.

(5) Fielman, K. T.; Woodin, S.A.; Walla, M.D.; Lincoln, D.E. *Mar. Ecol. Prog. Ser*. **1999**, *181*, 1-12.

(6) Gilow, H.M.; Burton, D.E. *J. Org. Chem*. **1981**, *46*, 2221-2225.

(7) Bray, B.L.; Mathies, P.H.; Naef, R.; Solas, D.R.; Tidwell, T.T.; Artis, D.R.; Muchowski, J.M. *J. Org. Chem*. **1990**, *55*, 6317-6328.

(8) John, E.A., Pollet, P., Gelbaum, G., Kubanek, J. J. Nat. Prod. **2004**, *67*, 1929-1931.